Design of Experiments Approach for Optimizing a Chitosan-Polyphosphate-Copper Based Material for Trauma Wound Treatment

By

Jonah Glazebrook

Submitted in partial fulfilment of the requirements

for the degree of Master of Applied Science

at

Dalhousie University

Halifax, Nova Scotia

October 2023

Table of Contents

List of Tables

List of Figures

Abstract

The primary focus when treating traumatic wounds is to control bleeding. Once hemostasis is achieved, the priority shifts to preventing infection. Wound dressings, predominantly gauze, are used for initial on-site treatment but typically lack additional hemostatic or antibacterial effects. This thesis aims to create a material with enhanced hemostatic and antibacterial effects for trauma wound dressing through polyelectrolyte complexation of chitosan (CS), polyphosphate (PP) and copper followed by lyophilization. A consistent production protocol for synthesizing the CS-PP-Cu mesh-like material was developed. A design of experiments (DoE) approach with predictive modelling was subsequently undertaken to optimize key process variables (factors) according to relevant outcome measures (responses) crucial to wound dressing performance. Along with validating the DoE models, these optimized material formulations were used to verify the potential effectiveness of the CS-PP-Cu material as a trauma wound dressing relative to commercial wound dressing (Celox™) and CS-only mesh. Although the material demonstrates promising characteristics for trauma wound treatment, additional studies to refine these materials are warranted.

List of Abbreviations

CS   Chitosan

PP   Polyphosphate

DoE   Design of Experiments

DDA   Degree of Deacetylation

ICP-OES   Inductively Coupled Plasma Optical Emission Spectroscopy

D_p Degree of Polymerization

NaPP   Sodium Polyphosphate

aPTT   Activated Partial Thromboplastin Time

CFU   Colony Forming Units

OD   Optical Density

Acknowledgements

I would first like to express my deepest appreciation to my supervisor, Dr. Mark Filiaggi. He took me in when I was fresh out of undergrad a little unsure of what I wanted to do and gave me the guidance and space I needed to develop not only as a researcher but as a young man as well. Despite his somewhat hands-off approach when it came to lab instruction, he always made himself available to meet or edit my work, even if admittedly it was a little last minute. Without him not only would I not have been able to complete this work, but I likely would not have even realized my passion for biomedical engineering. You're not so bad for an Eagles fan, I hope I can continue to come to you as a mentor for the rest of my career.

I'm extremely grateful to my committee Dr. Daniel Boyd and Dr. Brendan Leung. They both went above and beyond in helping whenever I came to them regardless of their own busy schedules. It always felt as though they cared about my research and success just as much as they did their own students. I would like to extend the thanks to many of my peers in the Boyd and Leung lab including Christine, Brenna, Sarah and Andrew who were a great help with areas of design of experiments and biological lab work that I had yet to master.

This endeavor would not have been possible without the help of Dr. Alicia Oickle, Sajjad Fanae and Hanan Moussa. As a researcher with very limited experience in a wet chemistry lab, Alicia taught me everything I needed to know in the lab and was always there to help despite her own busy schedule. Without Sajjad I would never have even known where to begin with polyphosphates and chitosan, so I appreciate his imparting of expertise. Without Hanan and Sajjad there to collaborate and share the workload, the lab would have been pretty lonely.

Finally, I would like to give a very special thanks to my family and friends who supported me along the way. When work weeks dragged on and lab work wasn't going as planned, the men of Bolf and Scott Hanson kept me motivated to make it to the weekend.

To Jazzy, you were there to support me throughout this whole process, whether it was the delicious meals you prepared or simply having you by my side, your presence in my life made all the difference. Without you, I might have never mastered the art of getting out of bed before 10 on weekdays, a crucial factor in completing my thesis. Thank you from the bottom of my heart.

To Mom and Dad who have loved and supported me unconditionally throughout my entire education and life. You provided every opportunity and instilled in me the necessary values to achieve my goals, I am forever grateful.

Chapter 1: Introduction

When treating traumatic wounds, blood loss poses a major immediate threat to the patient's life. Once bleeding and other immediate threats have been controlled, the concern shifts to mitigating complications from the wound becoming infected [1]. The initial treatment most trauma patients receive is some form of wound dressing that is applied on site, well before they reach a hospital. Although active wound dressings intended for trauma are more effective at stopping bleeding, gauze remains the most common wound dressing used in these scenarios [2]. Even when these active wound dressings are used, their hemostatic effects could be improved. Further, these more traditional dressings lack antibacterial properties to mitigate the threat of infection.

This project proposes the development of a chitosan (CS) and polyphosphate (PP) based material with added copper ions to treat trauma wounds more effectively. PP is a polyanionic polymer that has been shown to accelerate coagulation and stabilize blood clots [3, 4]. CS will be included to make use of its polycationic nature, hemostatic effects and antimicrobial properties that will work in tandem with copper ions to provide an antibacterial environment [5-7]. This approach utilizes polyelectrolyte complexation of CS-Cu and PP solutions, followed by freeze drying to create a mesh like material that can easily be applied to wounds in the field.

The first objective is to identify a consistent and reproducible production protocol for creating a freeze-dried mesh-like material using CS, PP, and copper. The second objective will utilize a DoE approach to build a design space that considers process variable factors such as CS, PP and copper concentration, and PP degree of polymerization (D_p). The third and final objective involves selecting an optimal material formulation using the predictive models generated from this design space. This formulation will be used to validate the model by characterizing the same responses used in the DoE and to verify the material's potential effectiveness as a trauma wound dressing in comparison to a commercial competitor and a CS-only material.

1.1 Trauma Treatment

The current standard of care for pre-hospital treatment in trauma situations triages the most immediate threats to the patient's life. This is done by following a systematic approach to check the patient's airway, breathing and circulation, in this order [8, 9]. Once an airway and breathing have been established, the circulation step involves controlling hemorrhaging, which is the leading cause of preventable death in military settings and second leading cause in civilian settings [10, 11]. At this stage it is also important to take as many precautions as possible to diminish the risk of infection, as patients who develop infections have increased mortality or morbidity leading to a more difficult recovery period [12].

The standard method for treating hemorrhaging is to apply pressure by packing the wound using sterile gauze until the bleeding is controlled. Once the bleeding is controlled, the wound is wrapped with gauze to create a mechanical barrier, protecting the wound from contamination. More advanced wound care treatments may then be utilized at hospital including methods such as surgery, vacuum assisted closure and medication [1, 13, 14]. Treatment can also involve the use of tourniquets, although this is always done in conjunction with proper wound packing and pressure [15]. To improve this treatment, an emphasis should be placed on accelerating blood clotting to achieve more timely hemostasis.

1.1.1 Clotting and Hemostasis

When treating traumatic open wounds, especially those with profuse bleeding, stopping or minimizing bleeding is the highest priority. This can be achieved through mechanical means with methods like clamping arteries or occluding the defects in the vascular wall. It can also be achieved through the body's own natural coagulation process [16]. This process is under the control of several inhibitors to prevent detrimental clot formation and maintain normal function. A complex balance of thrombogenic and antithrombogenic components is required to allow blood to flow freely under normal circumstances and coagulate properly when necessary [17]. When this balance is compromised due to events such as trauma to the endothelium, the coagulation process will initiate with primary hemostasis that is followed by the coagulation cascade. To better understand the role of wound dressings in hemostasis, these clotting mechanisms will be briefly described.

1.1.2 Primary Hemostasis

Primary hemostasis is the first step of the coagulation process that occurs between platelets, the vessel wall, and adhesive proteins. Normally, platelets do not adhere to endothelium. However, once the endothelium layer is breached to expose subendothelial tissue, platelets begin adhering to collagen and Von Willebrand factor [18]. Von Willebrand factor acts as a bridge connecting the platelets and collagen by attaching to the platelet glycoprotein complex I receptor. This triggers platelet degranulation, changing their morphology to lose their disc shape and subsequently to release various factors [17]. Calcium is also released and binds to phospholipids, providing a surface for assembly of the coagulation factors. These activated platelets then stimulate further platelet aggregation through the production of thromboxane A2, leading to the formation of the platelet plug that can temporarily seal the endothelial defect [17]. The formation of this platelet plug is then followed by secondary hemostasis, or the coagulation cascade, where thrombin converts fibrinogen into fibrin allowing for the creation of more stable fibrin clots.

1.1.3 Coagulation Cascade

The coagulation cascade is the second step and has traditionally been classified as having extrinsic and intrinsic (or contact) pathways that both converge to a common pathway. Although this model remains useful conceptually, it does not perfectly describe what is happening and, as such, the consensus model is a cascade seen in Figure 1 that involves initiation, amplification and propagation [19]. The initiation phase begins when tissue factor is released upon cell damage and forms a complex with factor VII to activate it. Subsequently, this complexed factor VII activates factor X which generates a small amount of thrombin, although not enough to induce a fibrin clot [19, 20]. The amplification phase follows, where the thrombin generated in the initial phase acts as positive feedback to accelerate platelet activation and activate factors XI, IX, VIII and V. The increase in activated platelets and positive feedback factors results in large quantities of factor X being activated, forming prothrombinase in the propagation phase. In this final phase, the prothrombinase converts prothrombin into larger quantities of thrombin that can convert enough fibrinogen into fibrin to form a fully developed fibrin clot. All the processes described in the amplification and propagation phase always occur

on the surface of platelets, which localizes the coagulation cascade [20]. Primary hemostasis and the coagulation cascade will happen on their own when damage to the endothelium occurs. However, certain compounds such as CS or PP can accelerate and promote these mechanisms.
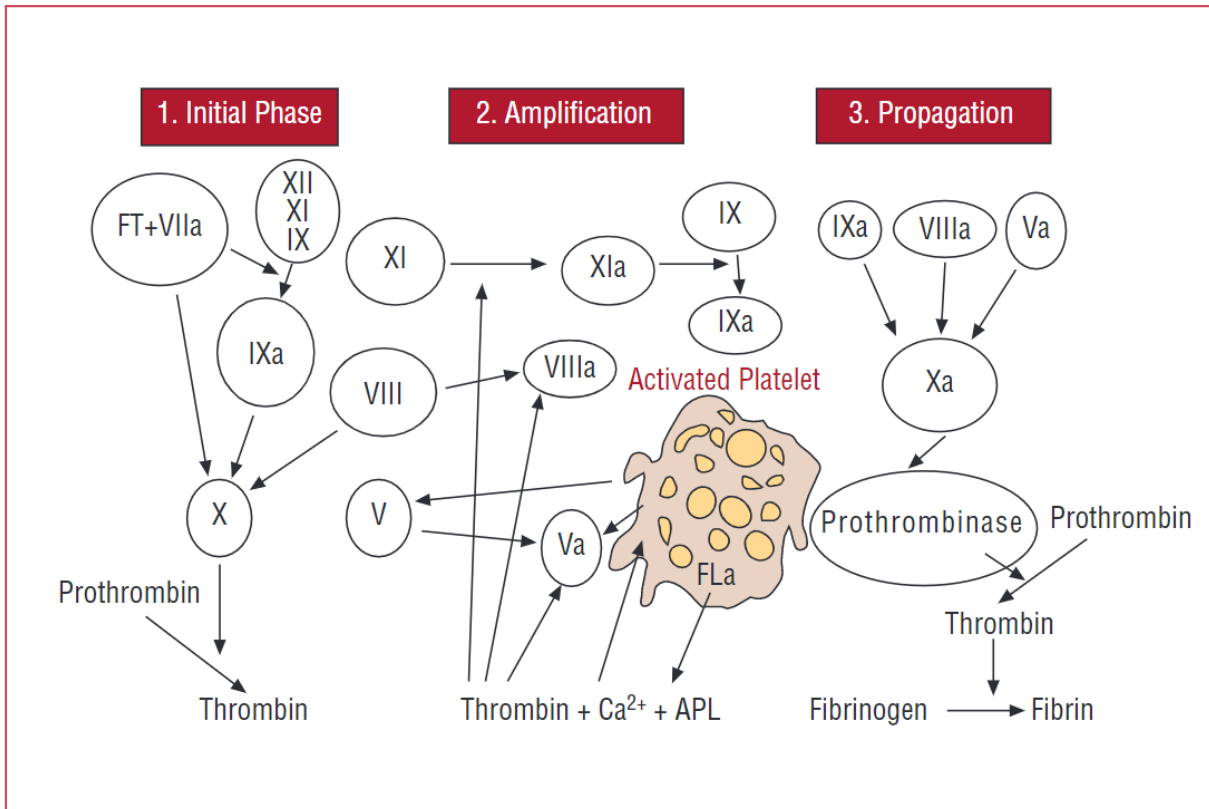
Figure 1 – Phases of the coagulation cascade depicting how each component interacts to culminate in the activation of fibrin [20].

1.2 Chitosan

CS is a polycationic biomaterial derived from a natural polysaccharide, chitin. CS is composed of N-acetyl D-glucosamine and D-glucosamine units linked through glycosidic bonding in a randomly distributed pattern to form the polymer chain. The glucosamine unit is an amino sugar with the chemical formula $C_6H_{13}NO_5$. The acetylated version is the same with an added acetyl group attached to the amino group [21, 22]; the structure of CS is depicted in Figure 2. CS can vary in molecular weight, with the majority of commercially available CS falling between 50-2000 kDa. The chains can also vary in the percentage of glucosamine units that are

deacetylated (DDA). For the polymer to be considered CS, consensus in the literature indicates that the DDA must be at least 50%; typically it is in the 70%-90% range [23].

Molecular weight and DDA largely influence key properties of CS such as its polycationic nature, hydrophobicity, immunogenicity, and biocompatibility [21, 22]. A lower molecular weight will result in lower density, higher water solubility, lower viscosity, lower surface tension and more significant biological activity. In contrast, lower DDA will result in less water solubility and reduced bioactivity [21]. With higher DDA, there are more functional amino groups that can be protonated, which is vital for water solubility and biological interactions. Protonation is so important for water solubility that, in order for CS with a molecular weight of over ~30 kDa to be water soluble, it must be in an acidic environment to protonate the amino groups (often using acetic acid, though other solvents such as HCl, lactic acid, and citric acid can be used as well) [6].

CS is polymorphic with a semicrystalline morphology due to the intra- and intermolecular hydrogen bonds formed by its hydroxyl and amino groups [24]. There are three different allomorphs of CS (α, β and γ) that can form based on the parent chitin used to produce the CS. Each of these allomorphs refer to how the polymer chains are oriented in relation to one another and also influence water solubility and bioactivity of the CS [25].
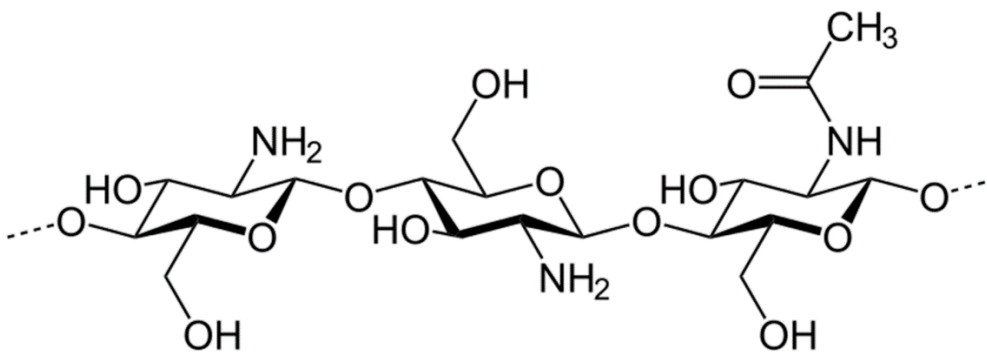
Figure 2 - Segment of the CS chain structure containing two deacetylated units and one acetylated unit [26].

1.2.1 Biomedical Applications

CS has become an extremely popular material choice for biomedical applications due to its unique set of properties and relative abundance. Because of its polycationic nature,

biocompatibility, biodegradability and tunability, CS is extremely versatile and can be used in a wide range of applications. Some applications include cosmetics and drug/gene delivery, but it has especially garnered attention in tissue engineering and wound healing applications. This is largely due to CS having demonstrated inherent antimicrobial, antioxidative, hemostatic and immunomodulatory properties under specific conditions [5, 6].

Practical considerations also contribute to the increasing use of CS for wound healing applications. CS has already been well established as a safe and biocompatible material that has been approved for a wide range of biomedical applications [27]. This means that wound dressings that use CS could be more likely to achieve faster regulatory approval as there is a precedent for their use. Another practical consideration supporting the use of CS is its low environmental impact and relative abundance through natural sources [5].

1.2.2 Antibacterial Properties

Most wound dressings using CS focus on its antimicrobial properties as the main reason for its inclusion given the increasing threat of drug-resistant bacteria such as Methicillin-resistant Staphylococcus Aureus [28]. When using CS as an antibacterial agent it is important to define molecular weight and DDA, as both can have a large impact on antimicrobial activity.

There is much debate within the literature regarding its antibacterial effectiveness against gram-negative bacteria compared to gram-positive bacteria, with conflicting reports on which bacteria CS is more effective against. Additionally, the antibacterial mechanisms by which CS acts are also not fully understood [29]. It is believed that the cationic reactive groups of CS interact with the anionic teichoic acids in the cell walls of gram-positive bacteria, causing alterations in the cell wall and disrupting the cell membrane, eventually resulting in cell death. Gram-negative bacteria on the other hand have negatively charged outer lipid bilayers due to the lipopolysaccharides. It is believed that the CS interacts with the lipopolysaccharides and prevents the exchange of nutrients into the bacteria by forming a polymer layer around the surface, leading to cell death [29]. It is likely that CS is effective against both gram-positive and negative bacteria to different extents under different conditions. To improve the antibacterial effectiveness of CS these conditions could be controlled based on the target bacteria.

1.2.3 Hemostatic Properties

CS has been widely proposed as a hemostatic agent throughout literature with multiple possible mechanisms of action reported. One such mechanism by which CS is suggested to expedite hemostasis is through promotion of platelet and erythrocyte aggregation due to interactions between the positively charged CS and negative charges on the surface of platelets and erythrocytes [5, 30, 31]. Platelet aggregation plays a key role to achieve primary hemostasis by plugging the defect independently of the coagulation cascade. After primary hemostasis, platelet aggregation contributes to amplifying the coagulation cascade as activated platelets generate and stimulate activation of various coagulation factors. It is also suggested that CS promotes clot retraction along with platelet aggregation which together results in more dense and stable clots [32]. More recent research suggests that CS may have the ability to absorb and reduce antithrombin levels through electrostatic interactions. Reduced antithrombin would induce the activation of more Factor X to Factor Xa, resulting in more thrombin generation that acts as a positive feedback for the coagulation cascade and leads to eventual fibrinogen to fibrin conversion [33]. All this suggests the presence of CS has the potential to induce more stable fully developed fibrin clots.

1.3 Polyphosphate

PP is an inorganic anionic polymer that exists extensively throughout biology. PP has been proposed for many biomedical uses due to its bioactive properties such as accelerating bone formation and proinflammatory/procoagulant effects [34]. The structure of PP can be seen in Figure 3. It is a relatively simple linear polymer that consists of phosphates linked together through phosphoanhydride bonds. At physiological pH, each monomer unit of the PP carries a negative charge, making PP an intensely anionic polymer [3]. PP can vary greatly in its D_p, reaching upwards of 25,000 phosphate units long; PP that have an average of less than 100 units are generally considered short chain PP [35]. The D_p has been shown to have a substantial effect on the bioactive properties of PP. Many studies suggest that longer chain PP has a greater hemostatic and proinflammatory effect that could be valuable for many biomedical applications [35-39].
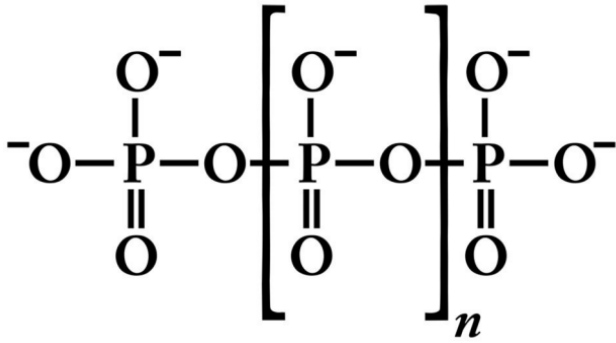
Figure 3 - Diagram of the PP structure at physiological pH [3].

1.3.1 Hemostatic Properties

Several studies support the ability of PP to accelerate clotting, with most indicating that this is achieved through activation of what has been traditionally referred to as the contact pathway [40-42]. For this route, initiation of the coagulation cascade occurs when factor XII and other coagulation components assemble on anionic polymers, which activates the factor XII leading to the propagation of the coagulation cascade [3, 41]. Although this is the most reported way in which PP accelerates clotting, there is evidence of many other interactions that likely play a role in accelerating coagulation. It was shown that PP can accelerate the generation of thrombin by accelerating the proteolytic conversion of factor V to factor Va. This quick burst of thrombin allows the amplification and propagation stages of coagulation to work more quickly and effectively [3, 4, 43]. PP is also reported to reduce and delay fibrinolysis, resulting in more stable clots, by preventing tissue factor pathway inhibitor, a natural anticoagulant, from executing its function [3, 4, 42]. Finally, it is worth mentioning that platelets naturally release PP when activated and PP is a known proinflammatory. This suggests that PP could play a role in recruiting more platelets to the clot site, perpetuating a higher concentration of activated platelets [3, 41].

1.4 Polyelectrolyte Interactions and Copper Additions

The polycationic and polyanionic natures of CS and PP, respectively, are key characteristics being exploited in this research to create a new material. Electrostatic interactions driven by these opposite charges are what allow the two components to combine through a process called polyelectrolyte complexation. Polyelectrolyte complexation affords

8

many advantages over other methods of linking polymers that will be described in the following sections along with a more detailed description of polyelectrolyte complexation.

1.4.1 Complex Coacervation vs. Polyelectrolyte Complexation

Mixing oppositely charged polyelectrolytes in aqueous solution can result in the formation of complex coacervates or polyelectrolyte complexes due to electrostatic interactions between the charged polymers [44, 45]. Although the difference between complex coacervates and polyelectrolyte complexes is not entirely clear, a prevailing distinction lies in what form the mixture takes on when combined. Complex coacervates refer to systems where there are two separate liquid phases, one containing a high colloidal concentration and the other effectively consisting of only the solvent. Polyelectrolyte complexes are similar with respect to this two-phase separation; however, in this case the colloid phase resembles that of a solid precipitate rather than a liquid phase. It is believed that many parameters effect the formation of these systems, including charge density, pH, ionic strength, solvents, temperature and perhaps most importantly polyelectrolyte concentration [46, 47]. Mixing CS and PP can result in complex coacervates or polyelectrolyte complexes being formed depending on what polyelectrolyte concentrations are used [48]. During preliminary lab work it was determined that polyelectrolyte complexes were more effective than coacervates for synthesizing freeze-dried CS-PP-Cu materials, so they will be the focus moving forward.

1.4.2 Specific Mechanisms

When CS and PP solutions are mixed, CS acts as the polycation and PP acts as the polyanion to create a polyelectrolyte complex. This happens when the negatively charged oxygen groups of the PP undergo Coulomb interaction with the positively charged amine groups of the CS to create primary complexes. The primary complexes then become entangled and aggregate through inter-complex interactions resulting in a polyelectrolyte complex [46, 47]. This is a spontaneous process that occurs without the addition of any chemical cross-linkers, avoiding the possibility of added toxic/undesirable effects and keeping the production process simple [44, 47, 49]. A potential pitfall of CS-PP polyelectrolyte complexes is the speed in which this interaction occurs, which appears to reduce the overall interaction between the polymers. This likely occurs because these instantaneous interactions create a barrier of polyelectrolyte

complex, separating the CS solution from the PP solution and preventing the PP from interacting throughout the bulk of the CS. In order to circumvent this, salts can be added to the PP solution for a charge shielding effect to slow down the reaction rate and allow for more thorough interactions [48].

1.4.3 Copper interactions

Ensuring any copper that may be included in the material is bound within an existing CS-PP structure is important for maintaining a sustained release of copper to the wound site. If the copper were to be simply dispersed throughout the structure with no interactions, one would expect a burst of copper release as soon as the material is applied to the wound, creating a cytotoxic environment without any sustained antibacterial effects [50]. When incorporated in solution as a copper chloride, copper ions assume a positive charge of +2. It is well known that PP is capable of chelating copper through the electrostatic interactions between the positive charge of the copper and negative charge of the PP [51-53]. Intuitively, it stands to reason that the copper would be retained within the structure through these interactions with PP rather than CS since copper and CS are similarly charged. Although this seems to be the most likely outcome, copper has also been observed to form interactions with CS as well. There does not seem to be a consensus in the literature on exactly how this occurs. However, it is suggested that these interactions arise due to coordinate bonding between the copper and the amino groups on the CS [54, 55]. In either case it is likely that the presence of copper impacts complexation interactions between CS and PP, which could have an impact on the resulting characteristics of the material.

1.4.4 Antimicrobial Mechanisms of Copper

With copper being included as a key antibacterial component of the proposed material, it is important to understand the basic mechanisms by which copper kills microbes, specifically bacteria. The exact mechanism of bacterial death via copper is not entirely understood. However, the prevailing notion is that many mechanisms act in tandem to achieve microbial death with the relative importance of each depending on the microorganism [56]. The most widely accepted mechanisms include disruption of the plasma membrane, generation of reactive oxygen species and disruption of metalloprotein function. It is believed that sufficient

copper levels will lead to the breakdown of bacteria plasma membrane through direct interaction with copper ions, leading to eventual cell death [56]. Sufficient copper will also catalyze the production of hydroxyl radicals leading to oxidative stress and cell death. More recent discoveries suggest that copper binding with the native metalloprotein cofactors inhibits key metabolic processes of the bacteria leading to cell death as well [57, 58]. It is also important to note that copper is an essential trace element for humans and microorganisms. At the right concentrations, it can be completely harmless or even beneficial to humans yet toxic to microorganisms such as bacteria [50, 58].

1.5 Wound Dressings

Wound healing is a dynamic and complex process consisting of four phases: the coagulation/hemostasis phase, the inflammatory phase, the proliferation phase and the maturation phase [59]. A wound dressing can be defined as a device that is meant to promote any or multiple phases of the healing process. To be considered a wound dressing and not an engineered scaffold of some sort, the device must be applied externally to the wound rather than implanted with the intention of regenerated tissue replacing it slowly over time. Wound dressings can be meant for acute wound treatment or chronic wound treatment provided they meet the above requirements [59, 60].

Many types of wound dressings with different applications are frequently used in practice. The most basic and well known of these wound dressings is gauze. The main purpose of gauze is to absorb blood/exudate from the wound and act as a barrier to prevent foreign substances from infiltrating the wound. Because gauze is so inexpensive, easy to use, readily available and biocompatible, it is the most frequently used wound dressing [2]. The limitations of gauze lie in its lack of active benefits to promote any of the healing phases, with its only functions being to absorb fluid and act as a mechanical barrier. Treatment of wounds could be greatly improved by choosing enhanced wound dressings suited for specific applications.

1.5.1 Types of Wound Dressings

Enhanced wound dressings can be categorized into the following groups: hydrogels, films, freeze-dried and composites. Hydrogel wound dressings are hydrated polymeric gel

masses meant mainly to promote healing in dry wounds. Film wound dressings are thin transparent films, commonly made of polyurethane, that cover the wound to maintain a moist environment and protect the wound from foreign body contamination. Composite wound dressings are any platform that consist of a combination of the other dressing types [61, 62].

The most common type of commercial wound dressing is obtained through a freeze-drying route. This is especially true for wound dressings meant for trauma treatment [59]. These dressings are made by taking solutions, coacervates or complexes of polymers and dehydrating them through lyophilization (freeze drying). This leaves behind a porous sponge or mesh-like mass in the shape it was molded in prior to freeze drying. The main benefit of freeze-dried dressings is their ability to absorb large amounts of wound exudate or blood, creating a favourable environment for wound healing. They also have the added benefit of increased structural integrity, making them easier to store and handle compared to hydrogels and films [62].

1.5.2 Commercial Hemostatic and Antibacterial Wound Dressings

Trauma specific wound dressings are dressings that are meant to be applied in the field by Emergency Medical Technicians (EMTs) or field medics as urgent pre-hospital treatment. Their purpose is to promote the first two phases of wound healing over an intended application period of only a few hours. During this period the main goal of wound care is not to accelerate healing but rather to keep the patient alive and minimize complications down the road [1]. To achieve this, the two most important properties a wound dressing must possess are the ability to quickly stop the bleeding and prevent the wound from becoming infected. Historically, this was done using gauze or any other fabric material available. However, this approach uses only mechanical means of stopping the bleeding and preventing infection. Now there is the possibility for enhanced wound dressings with additional bioactive properties to accelerate clotting time and kill bacteria that have infiltrated the wound site. Currently, three brands of commercial wound dressings dominate the trauma wound market: Celox™, HemCon® and QuikClot® [63, 64].

Celox™

Celox™ is a CS based composite hemostatic dressing that is composed of gauze and CS granules on one side and a polyurethane foam film as the other side. When the dressing comes in contact with a wound, the CS granules absorb the water from the blood creating a gel plug and concentrating the coagulation factors. According to the literature, Celox™ is much more effective than gauze in stopping initial bleeding and preventing rebleed. Much of the data also suggests it is the most effective of the trauma dressings on the market [63-67]. There is no explicit mention of Celox™ providing any antibacterial benefits, but the presence of CS indicates Celox™ can likely help prevent infections. Additionally, Celox™ Medical makes an antibacterial dressing containing silver called Silvapro. However, this dressing is intended for the treatment of burn wounds rather than hemostatic applications.

HemCon®

HemCon® is another CS based wound dressing. Here, normal gauze is coated in CS. Like Celox™, it seeks to make use of the hemostatic properties of CS in order to accelerate clotting. The literature has consistently demonstrated that HemCon® is more effective than plain gauze at controlling bleeding. However, there are conflicting reports on how it performs compared to other hemostatic dressings on the market [63, 64, 66-68]. HemCon® does not claim to provide any active bactericidal effects, although it does claim to provide an antibacterial barrier.

QuikClot®

QuikClot® is likely the most widely adopted hemostatic wound dressing due to its widespread use in the military. QuikClot® is not a CS based wound dressing but rather gauze that is coated in an inorganic mineral called kaolin that acts as the hemostatic agent, which is said to activate Factor XII to accelerate the coagulation cascade. Once again there is consensus in the literature that QuikClot® is superior to regular gauze for trauma treatment [63, 64, 66, 67, 69]. QuikClot® does not make any claims related to antibacterial activity and no aspect of the product suggests there would be any antimicrobial benefits. Of the three hemostatic wound dressings, QuikClot® was the only one to appear on the Manufacturer and User Facility Device Experience (MAUDE) database, an FDA database of adverse event reports involving medical devices. Five adverse events were reported, all related to the QuikClot® dressing being left in

the patient after surgery. All three of these dressings are non-absorbable dressings and are only intended for an application period of less than 24 hours. Although QuikClot® is the only one with adverse events reports, this might be a common issue among all three dressings that has only been reported for QuikClot® because it is the most widely used.

Axiostat®

Axiostat® is another CS based wound dressing that was developed in India and as such is much less commonly used in north America. Unlike the other CS based wound dressings, Axiostat® is made from CS only in freeze dried form. Like HemCon®, Axiostat® does not claim to have any bactericidal benefits but does claim to provide a barrier to bacterial penetration and rapid control of moderate to severe bleeding [70]. Evidence suggests Axiostat® is a much more effective hemorrhage control dressing than standard gauze, although no comparisons have been made versus other hemostatic wound dressings [71].

Antibacterial Wound Dressings

Although there is currently no commercial hemostatic trauma wound dressing with specified antibacterial effects available, many commercial antibacterial wound dressings intended for burns, ulcers, surgical wounds, and chronic wounds exist. These include wound dressings that incorporate iodine or antibiotics among other antimicrobial agents. However, the most relevant antibacterial wound dressings are those that make use of silver [72]. Silver ions kill bacteria by the binding to DNA to prevent cell division and interrupting the respiratory system leading to eventual cell death. Commercial antibacterial wound dressings like Actisorb® Silver, Contreet Foam and Silverlon® make use of a slow sustained release of silver ions to maintain an antibacterial environment while minimizing cytotoxicity [72]. Although silver wound dressings have seen a lot of success for burns and ulcers, there has been no attempt to incorporate silver into trauma wound dressings where the main goal is to achieve hemostasis faster.

1.5.3 CS and PP Based Wound Dressings

Aside from commercially available wound dressings, there is a large body of literature surrounding the use of CS in wound dressings and some literature that has examined PP as a

material for wound dressings. Although CS-based wound dressings have been proposed for many different wound applications, this section will focus on hemostatic wound dressings to narrow the scope.

A study from M. Buriuli, et al. looked at a freeze-dried wound dressing made from a polyelectrolyte complex of CS and alginate [73]. Polygalacturonic acid was also incorporated as an anti-inflammatory agent, but the main hemostatic agent was CS. To achieve a homogenous material before freeze drying, the complexes were ultrasonicated, resulting in light flexible meshes. To evaluate the hemostatic performances of their wound dressings, their sample were compared to HemCon® dressings in whole blood clotting time, plasma recalcification time, prothrombin time, activated partial thromboplastin time and platelet adhesion tests. The results showed faster whole blood clotting time, though the other tests were not as conclusive.

X. Fan, et al. produced a wound dressing by taking a cellulose sponge, submerging it in a CS solution, then freeze drying [74]. They reported that the addition of CS improved the mechanical properties of the freeze-dried mesh compared to cellulose alone. This study validated performance using a whole blood clotting assay, an antibacterial assay and conducted animal testing using a mouse tail amputation model, rat leg artery trauma model and rat liver trauma model. The cellulose-CS wound dressing showed improved performance over the gauze control group in these tests. However, there was no comparison to any currently used trauma wound dressings. This same lab group released another study, this one involving a CS only structured wound dressing [75]. This study used the same validation methods as their previous study and came to similar conclusions that the dressing could be effective as a trauma wound dressing. Once again there was no comparison to any currently used and proven wound dressings.

A wound dressing made by mixing solutions of polyacrylate, CS and collagen followed by freeze drying was produced by W. Liu et al. [76]. This study measured the mechanical properties of the mesh using compressive strength, ultimate tensile stress and Young's modulus. They reported a range of 0.1-0.8 MPa for compressive, 0.002-0.01 Mpa for tensile and 0.81-1.83 for Young's modulus. No conclusion was made on whether these values were acceptable for the

intended application. This study validated not only the hemostatic and antimicrobial properties of the mesh, but also its regenerative capabilities as well, surprising given that most hemostatic dressings are only intended for short term use to manage trauma and would not benefit much from regenerative properties.

A study from S. Biranje, et al. used centrifuged CS-tripolyphosphate (TPP) nanoparticles that are then freeze dried to create a wound dressing [77]. The resulting wound dressing was characterized for morphology, porosity, pore volume, surface area and biodegradability and claimed that higher surface area/porosity facilitated biodegradation. In-vitro testing suggests the wound dressing is safe for wound dressing applications and succeeded in enhancing thrombin generation.

To improve the hemostatic properties further, a study by S. Ong, et al. attempted using longer chain PP rather than TPPs. To do this CS solution was mixed with PP solution having chain lengths of either 45 or 65 to form a hydrogel complex that was then freeze dried [78]. The wound dressing also used silver nanoparticle additions to provide a more pronounced antimicrobial effect. This wound dressing showed significant improvements over a CS only control group in accelerating blood clotting, platelet adhesion and thrombin generation. It also exhibited a much stronger antimicrobial effect due to the silver nanoparticles; however, this did come at the cost of some cytotoxicity. Although this study provided a good initial basis for research involving CS-PP based wound dressings, it did not attempt any production optimization or characterization prior to validating performance *in vitro* and *in vivo*. Further, no additional follow-up to this study could be found.

1.5.4 Ideal Trauma Wound Dressing

To create the ideal trauma wound dressing it is important to define the design inputs that are desired. Firstly, the wound dressing must have appropriate physical properties and accessibility so it can be implemented in trauma situations. This considers the material having sufficient compressive and tensile properties to allow for adequate manipulations of the material in the wound space. Additionally, the material must be inexpensive, shelf stable and portable so it can be available for widespread implementation. Provided these basic

requirements are met, a more critical design input of a trauma dressing is to maximize hemostatic effects. This should be done by maximizing absorbency to mechanically plug the defect and through active biological effects to promote the coagulation cascade locally without inducing disseminated hemostasis [17, 18]. The wound dressing should also be able to maintain an antimicrobial wound environment for 24 hours. The most common complication after a traumatic wound is infection caused by bacteria that contaminated the wound during the traumatic event [12, 79]. Therefore, it is important for a trauma dressing to provide an antimicrobial environment that eliminates bacteria before it has a chance to colonize spread through the circulatory/digestive systems. The final design input that must be considered is biocompatibility when applied to an open wound. This remains a highly important criteria for any medical device to be effective and approved for use [80, 81]. Specifically, this means the material should not have a cytotoxic effect on the patient's wound tissue.

Although the current commercially available trauma wound dressings partially address some of these design inputs, there is much room for improvement. These commercial dressings meet the physical property requirements; however, their hemostatic effects could be improved, and the issue of infection could be more adequately addressed [63, 82]. These dressings could incorporate components to stimulate biological activity that promote the coagulation cascade and clot stability alongside mechanical clotting. Antibacterial agents could also be incorporated to create the antibacterial environment for the 24-hour application period. To achieve this and create a wound dressing that better meets the design inputs of an ideal trauma dressing, a freeze-dried copper-loaded CS-PP polyelectrolyte complex is proposed in this project as a material for traumatic wound dressings.

Chapter 2: Motivation and Objectives

2.1 Project Motivation

The leading cause of preventable death in military settings and the second leading cause in civilian settings is uncontrolled hemorrhage due to trauma [10, 11]. In cases where the bleeding is able to be controlled, patients that develop infections from the trauma have a greatly increased in-hospital mortality rate and a much more difficult recovery period [12]. Widespread implementation of a wound dressing that can more effectively control bleeding and actively prevent infections would greatly reduce mortality rates and post treatment quality of life in trauma situations. This will likely also result in financial benefits to health care delivery due to shorter hospital stays and a conservation of other expensive resources.

Previous unpublished work in the Filiaggi lab group and preliminary work for this project has shown that combining solutions of CS and PP produces a polyelectrolyte complex that, when freeze-dried, exhibits desirable qualities of a wound dressing. These qualities include strength and elasticity properties that a wound dressing would require to be applied in trauma situations as well as a high absorption capacity. It is also reasonable to assume that a material made of CS and PP with copper additions will have added biological effects based on what is understood about these components.

CS has been investigated extensively as a biomaterial in wound dressings and has proven antimicrobial properties [29]. Additionally, it is well established that copper ions at appropriate concentrations kill bacteria [7]. Although the dressing is only intended for use within the first 24 hours of injury, it is generally accepted that the bacteria responsible for acute infections after trauma contaminate the wound before initial care is administered [12, 79]. With CS and copper acting as antibacterial agents shortly after the bacteria enters the wound, it is likely that the resulting material would be very effective at preventing infections. PP, although not studied as extensively as CS, has also been investigated for the role it can play in accelerating coagulation [36]. It is believed that PP eluted from the wound dressing will accelerate the body's own coagulation cascade to stop the bleeding biologically [3]. In concert, the wound dressing will also work to stop the bleeding by plugging the defect mechanically as the device swells. Several

CS-based wound dressings use this latter approach to achieve hemostasis without the added benefit of the accelerated coagulation [82]. Using both these effects in tandem will not only allow hemostasis to be achieved more quickly, but also increase the stability of the clot until secondary care is reached.

Additional justification for why a wound dressing made with CS and PP could be extremely valuable and effective is because of their proven utility in biomedical applications and accessibility. CS is a well-known biocompatible material and PP is a ubiquitous biological molecule; both have been used for various other medical applications [6, 34]. Copper, while toxic to the body at high concentrations, has been proven safe and effective as an antimicrobial agent when administered in the appropriate dosage [83]. This precedent, while supporting the anticipated safety and efficacy of the proposed wound dressing, will also likely facilitate regulatory approval. Since the material is made of CS, PP and copper using basic production methods, the material will be relatively inexpensive while freeze-drying makes it highly portable and shelf stable.

2.2 Research Aim

The primary aim of this research is to create a material using CS, PP and copper that has superior hemostatic and antibacterial properties for traumatic injury wound dressing care compared to what is currently available commercially. To optimize the material, a DoE approach will be taken. This includes thoroughly characterizing the material to demonstrate its clinical potential as a trauma wound dressing. In addition, this project seeks to provide a better understanding of the interactions between CS, PP and copper, which are not yet entirely understood in the context of a polyelectrolyte complex. To achieve these aims, the project was parsed into three main objectives.

2.3 Objective 1

Determine a consistent and reproducible method to create a mesh-like material suitable for wound dressing using CS, PP and copper.

2.3.1 Goals

Each objective can be broken down into 3 main goals that once achieved, will enable the next objective. The first goal of objective 1 is to create a standard operating procedure to produce a freeze-dried mesh-like material from CS, PP and copper. Any refinement of this protocol should improve material characteristics for all relevant sample formulations. Once an effective standard operating procedure is made the next goal is to identify which processing variables have the most impact on resulting material characteristics. These variables can then be included as factors in a DoE approach to support optimization studies. The final goal of objective 1 is to test the consistency and reproducibility of the standard operating procedure by comparing samples made by two different operators. This will ensure the production method is consistent enough to execute a DoE.

2.3.2 Hypotheses

- CS, PP and Copper solution concentrations will have the biggest impact on material properties while other process variables will have little to no impact.
- The product arising from the standard operating procedure will display consistent appearance, handling properties, absorption capacity, chemical composition and elution profiles for samples produced using the same formulation, independent of the operator.

2.4 Objective 2

Using a DoE approach, build a design space for the predictive modeling of a freeze-dried CS, PP and copper material.

2.4.1 Goals

The first goal of objective 2 is to build a design space with a manageable number of samples using the factors identified in objective 1, such that all generated samples can be made using the standard operating procedure. In practical terms, a design space with 3 to 5 factors will keep the samples at a manageable number (~ 16-30 samples), while setting appropriate upper and lower limits for these factors based on preliminary work will ensure all generated samples can be made using the standard operating procedure. Subsequently, all samples as designated in the design space need to be synthesized and characterized for the selected

responses. These responses should be relevant to the trauma wound dressing design criteria, while allowing for a better understanding of CS, PP, and copper interactions in this polyelectrolyte complex. Once the design space is complete, the final goal is to generate predictive models for each of the characterized responses such that the properties of a material made using any sample formulation within the design space can be predicted.

2.4.2 Hypotheses

- Predictive models will be statistically robust enough to allow for optimization of response levels within the design space.

2.5 Objective 3

Select an optimal material formulation or formulations using the predictive models, then validate the models and verify the effectiveness of the material as a trauma wound dressing.

2.5.1 Goals

The first goal of objective 3 is to generate an optimal material formulation using the predictive models with optimization criteria selected based on the ideal trauma wound dressing design considerations. The next goal is to validate the predictive models by producing the optimized material formulation, then characterizing this formulation for the designated responses to ensure these responses fall within prediction tolerances. The final goal of the project is to verify the effectiveness of the optimized material formulation as a potential trauma wound dressing by evaluating its antibacterial and hemostatic properties and overall cytocompatibility relative to a commercial wound dressing.

2.5.2 Hypotheses

- The measured response levels for the optimized material formulations will fall within the accepted prediction tolerances thereby validating the predictive models.
- Due to the inclusion of CS and copper for antibacterial effects and PP and CS for hemostatic effects, an optimized material formulation comprised of CS, PP and Cu will demonstrate greater antibacterial and hemostatic capacity when compared to a commercial trauma wound dressing *in vitro*. This material formulation will also demonstrate comparable cytotoxicity.

Chapter 3: Production Protocol

3.1 Introduction

The first objective of this research was to develop a production protocol to make a material using CS, PP and copper that is suitable for trauma wound dressing. For the purposes of this research project, the most important design criteria to satisfy at this stage for successful implementation are the physical properties of the material. In this context, physical properties refer to the material composition, handling properties and absorption capacity of the material. Biological properties such as cytotoxicity, antibacterial effects and hemostatic effects should be optimized only after a production protocol that yields adequate chemical composition, handling properties and absorption capacity for a wide range of sample formulations is determined. In terms of this research, adequate chemical composition means the material includes sufficient CS, PP and copper to extract their proposed benefits. The relative amount of each component should also be tunable by adjusting the variables selected as factors. Adequate handling properties means users can handle the material with minimal care without the material falling apart or disintegrating. The material also needs to have a degree of flexibility since if it is too brittle it will be difficult to apply to wounds. Absorption capacity should always be maximized for this application and thus samples with significantly reduced absorption capacity cannot be considered adequate.

Once a production method that satisfies these criteria is found, the potential variables involved in the process must be identified. The goal is to determine the process variables that can be precisely controlled and have a significant impact on physical properties so they can be included as factors in the DoE. Variables that show little impact on these properties or cannot be controlled with precision are instead held constant at a set-point that produced the most consistent resulting material during preliminary work. Controlling the variables and constants can be difficult so all reasonable measures must be taken to ensure the protocol is consistent and reproducible. This is especially important when utilizing a DoE approach. If samples of the same material formulation were to vary significantly across each production run, then the

resulting model would have statistically weak prediction power. Because of this, much of the preliminary work focused on refining the production protocol as much as possible.

3.2 Production Protocol Development

3.2.1 Starting Point

Prior to this thesis project, research conducted by others in the Filiaggi lab group identified a protocol for producing a mesh-like material from CS and PP. This production protocol was used as the starting point for the research conducted in this thesis project. The material was synthesized by combining a 15 mg/mL solution of CS with a 15 mg/mL solution of PP and mixing on a magnetic stirrer, leading to a gel-like polyelectrolyte complex that forms a spongy mesh-like material upon freeze drying (Figure 4). While meeting some of the design criteria, this material lacked thorough PP interaction throughout the bulk of the material. This was apparent during production, as the gel complex produced using this method appeared to be a bubble of CS-PP complex with a CS-only gel core. This was supported by compositional data measured with Inductively Coupled Plasma Optical Emission Spectroscopy (ICP-OES) analysis that showed only roughly 3% of the material was phosphorous. The first step in refining this protocol, therefore, was to increase PP inclusion and interaction in the bulk of the material.
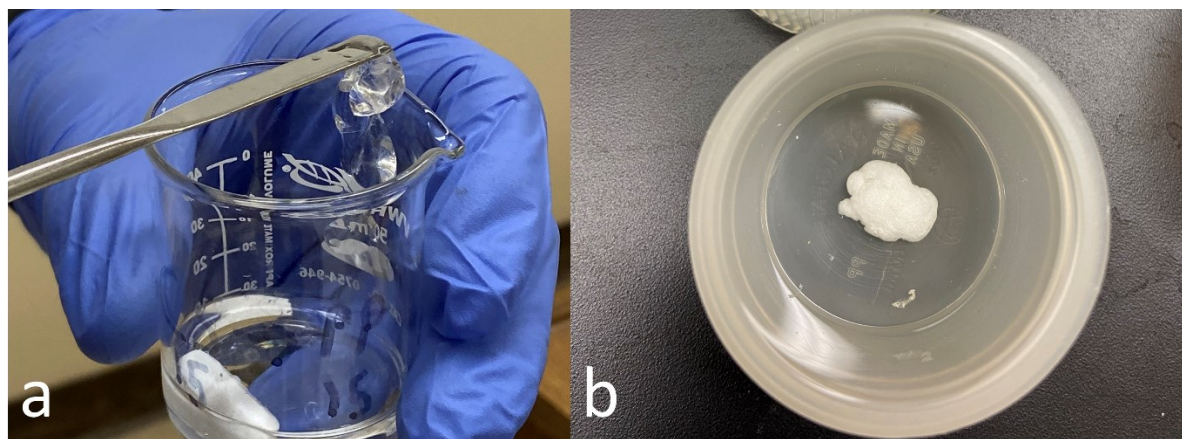
Figure 4 – The gel-like polyelectrolyte complex made from mixing solutions with magnetic stirrer (a) and the resulting freeze-dried spongy mesh-like material (b).

3.2.2 Increasing PP Content

The first attempt to improve PP inclusion was to vary CS and PP solution concentrations, with samples made from combinations of 0.5-50 mg/mL CS and 0.5-500 mg/mL PP using the established production protocol. These tests revealed that changing the solution concentrations had a major impact on the physical properties of the material. PP inclusion was increased for samples made using very high concentrations of PP and low concentrations of CS. However, these samples exhibited very little water absorption capacity and were extremely brittle, indicating that changing the solution concentrations alone would not produce adequate material properties.

Subsequent experiments involved the addition of salt to the PP solution to act as a charge shield to slow down the CS-PP interactions and facilitate PP penetration into the bulk of the CS [48]. Samples were made with salt concentrations ranging from 0.1-2 M NaCl added to the PP solutions. The salt appeared to have the expected result; gel complexes made with higher salt concentrations had a more translucent white appearance indicating more polyelectrolyte interaction; higher levels of PP inclusion were confirmed with ICP-OES. However, after freeze-drying the samples were very brittle with almost ceramic-like properties at the highest concentrations. Lower concentrations reduced this effect but did not provide enough of a charge shield effect to increase PP levels significantly. After trying a few other salts in place of NaCl such as KBr that yielded very similar results, the idea of using salt as a charge shield was abandoned.

After the first few attempts to include more PP impaired the physical properties of the samples, changes to the method of mixing the solutions were pursued. The approach taken was to use more aggressive mixing methods to compromise the integrity of the polyelectrolyte complex bubble and mechanically force more interaction between CS and PP. This was first done using vortexing, with solutions added to a falcon tube and vortexed at high speeds. Rather than one large polyelectrolyte complex bubble, the vortexing resulted in many small bubbles exhibiting slightly increased PP content following freeze drying, suggesting that increasing the mixing aggressiveness even further would yield the desired result.

To this end, a homogenizer was used at high speeds to essentially blend the solutions together. CS solution was added to PP solution in a 250 mL Nalgene then homogenized using an impellor attachment for 30 seconds at 1400 RPM, three times, stopping after each mix to remove any material stuck in the impellor. More extensive mixing using the homogenizer did not appear to have any effect on the chemical composition, handling properties and absorption capacity, thus going beyond three 30 second mixes was unnecessary. The homogenization resulted in paste-like gel complexes having many advantages over the complexes produced using the original mixing method. ICP-OES analysis indicated 8-12% phosphorous in these homogenized samples, depending on the solution concentrations used, indicating a relatively high PP inclusion. The paste-like nature of the complexes allowed for the samples to be cast in convenient shapes before freeze-drying. This method also seemed to universally improve the handling properties of the samples, especially for formulations that yielded a very brittle material in prior studies as they were now able to retain more sponge-like characteristics. An example of the paste-like gel complex and resulting freeze-dried material can be seen in Figure 5.

Figure 5 – The paste-like gel polyelectrolyte complex made using the homogenizer (a) and the resulting freeze-dried material (b).

3.2.3 Other Considerations

Although the use of a homogenizer solved many of the issues with the original production protocol and produced samples with superior physical properties across a wide

range of solution concentrations, some challenges remained. The first involved how the material would be loaded with copper. To determine which approach produced better results, a stock solution of copper was added to either the CS solution or the PP solution before homogenizing. Testing revealed that adding the copper to the CS solution resulted in more consistent copper levels and a more homogeneous gel complex, making it clear that the copper should be added to the CS solution. The duration that the copper was in the CS solution before homogenizing was also tested. When copper was left in the solutions for 1 hour, 6 hours or 24 hours there was no impact on the resulting material.

Another challenge that needed to be addressed was the presence of residual acetic acid in the material arising from the CS solution that could cause cytotoxicity. A rinsing step was required in the production protocol to remove the acetic acid so that the resulting freeze-dried material would not cause a significant drop in pH when applied to a wound. The first attempt at rinsing involved carefully pouring the supernatant off the top of the gel complex and then refilling with Tris buffer and inverting to mix. The mixture was then left for one hour to allow the complex to settle so the Tris buffer could be poured off the top and the process was repeated until the pH reached 7. This required many rinses to reach a pH of 7, and substantial amounts of gel complex were lost each time the supernatant was removed. To improve efficiency and retain as much of the sample as possible, a vacuum filter was used to remove the supernatant. This method ensured that the supernatant could be removed entirely each time without losing any gel complex, greatly reducing the number of rinses that were needed to reach a pH of 7. Testing concluded that only 3 rinses using this method were necessary regardless of the sample formulation.

3.3 Process Variables

With the general production protocol refined, the next step was to determine which process variables would be included as factors in the DoE. To do this, a list of process variables seen in Table 1 was made. The relative impact each variable had on the material was determined throughout preliminary testing. To be selected as a factor for the DoE, the variable must have a high impact on material properties, otherwise there is very little benefit from in depth optimization. Variables with little to no impact were fixed as constants at the conditions

that appeared most consistent during preliminary work (Glentham CS, room temperature mixing, solutions pH of ~3 for CS and ~7 PP, three 30 second mixes and overnight solution preparation). CS molecular weight and DDA were not tested due to time and supplier limitations so medium molecular weight and >90% DDA were chosen as constants based on what is reported as most effective for wound dressing application in literature [21, 22, 84].

Table 1 - Process variables and their impact on the resulting materials physical properties.

Variable	Impact
CS solution concentration	Major effect on chemical composition, handling properties, absorption capacity and apparent density.
PP solution concentration	Major effect on chemical composition, handling properties, absorption capacity and apparent density.
Copper solution concentration	Major effect on material copper level.
CS-PP ratio	Major effect on chemical composition, handling properties, absorption capacity and apparent density.
Solution volume	No effect on material properties provided the ratio of volumes remained the same.
CS molecular weight	Only medium molecular weight CS was tested.
CS DDA	Only >90% DDA CS was tested.
CS supplier	CS from Sigma and Glentham Life Sciences were tested; CS from Glentham was more consistent and easier to work with.
PP D_p	Minimal effect on chemical composition only.
Mixing temperature	No discernible effect on material properties.
Mixing pH	No discernible effect on material properties.
Mixing time	Mixing time had no effect on material properties provided mixing was sufficiently thorough.
Solution preparation time	Solution prep time had no effect on material properties provided solutes had sufficient time to fully dissolve.

CS, PP and copper solution concentration and PP D_p were the variables selected as factors for the DoE. CS and PP solution concentration were chosen because they had major effects on all the measured properties and optimal levels were completely unknown. Copper solution concentration was included as a factor because it was the only variable that appeared to influence sample copper levels during preliminary work and optimal copper levels were unknown. Although the impact PP D_p had on physical properties during preliminary work was minimal, this variable was chosen as it was hypothesized that it would have a significant impact on biological properties. Although CS-PP ratio appeared to be the best indicator of sample properties, it was not selected as a factor because it is dependant on CS and PP solution concentration. Instead, solution volumes were fixed so that the CS-PP ratio could be included as a response, thereby reducing the number of factors while maintaining the ability to investigate the effect CS-PP ratio has on the material.

After selecting the process variables that would be included as factors, a standard operating procedure was developed. The standard operating procedure carefully detailed the protocol for making freeze-dried CS-PP materials with varying concentrations of CS, PP, and copper and PP D_p of 20 or 180. Following this protocol should allow any experimenter to make consistent and reproducible samples by controlling all the process variables.

3.4 Standard Operating Procedure

3.4.1 Materials

1. Dry medium molecular weight CS (300-1000 cps, DDA of ~90%; Glentham Life Sciences)
2. Sodium phosphate monobasic monohydrate ($NaH_2PO_4 \cdot H_2O$; Sigma Aldrich)
3. Sodium carbonate (Na_2CO_3; Sigma Aldrich)
4. 20000 PPM copper chloride stock solution
5. 1% glacial acetic acid
6. Ultrapure water

3.4.2 Sodium Polyphosphate Synthesis

Before any samples were made, sodium polyphosphate (NaPP) with an approximate mean D_p of 20 or 180 was synthesized following a protocol developed by previous researchers in

the Filiaggi lab group [35]. Synthesis of each D_p NaPP follows the same protocol with the only difference being the starting powder. D_p180 was made using 120g sodium phosphate monobasic monohydrate ($NaH_2PO_4 \cdot H_2O$; Sigma Aldrich) only, while D_p20 required the addition of 3.28g sodium carbonate (Na_2CO_3; Sigma Aldrich) to 120g sodium phosphate monobasic monohydrate ($NaH_2PO_4 \cdot H_2O$; Sigma Aldrich), followed by thorough mixing. The powders were then heated in a Thermolyne Type 46200 High Temperature Furnace in a platinum-5% gold crucible from 25°C to 900°C over a 90-minute period, maintained at 900°C for 4 hours, then subsequently quenched on a copper plate. The copper plate was cleaned prior to use with a combination of sodium chloride salt and acetic acid. The NaPP glass was then manually crushed using a custom machined tool, transferred into sintered corundum aluminum oxide grinding bowls, and ground into a powder using a Planetary Micro Mill Pulverisette 7 (Laval LabInc.) to improve dissolution in water. The D_p at the time of DoE sample production was evaluated using liquid ^{31}P nuclear magnetic resonance (NMR), with the D_p20 and D_p180 NaPP protocols yielding measured mean D_p values of 24 and 160, respectively.

3.4.3 Calculations

Before beginning production, the quantities of CS, NaPP, copper, and acetic acid required for each specific material formulation must be calculated. The material formulation defines what CS solution concentration, PP solution concentration, copper concentration and which PP Dp are used to make the material. Eq. (1) and (2) are used to determine the mass of dry CS and NaPP required for the solutions (PPM is equivalent to mg/L and constituent solution volumes remain constant at 0.05 L for every material formulation). Eq. (3) is used to determine the volume of copper stock solution that must be added to the CS solution and Eq. (4) calculates the starting volume of acetic acid required for the CS solution. An example of the required quantities for a material formulation of 15000 PPM CS, 25000 PPM PP and 2000 PPM copper can be seen in Table 2.

$$mass_{cs} = concentration_{cs} * volume \qquad (1)$$

$$mass_{PP} = concentration_{PP} * volume \qquad (2)$$

$$volume_{Cu} = volume \times \frac{concentration_{Cu}}{stock\ concentration_{Cu}} \qquad (3)$$

$$volume_{AA} = volume - volume_{cu} \qquad\qquad (4)$$

Table 2 - Required quantities for an example material formulation.

Material Formulation			Required Quantities			
CS Concentration (PPM)	PP Concentration (PPM)	Copper Concentration (PPM)	Mass of CS (mg)	Mass of NaPP (mg)	Volume of Copper Stock (L)	Volume of Acetic Acid (L)
15000	25000	2000	750	1250	0.005	0.045

3.4.4 Instructions

Day 1: Solution Preparation

1. Add 50 mL of ultrapure water and the calculated volume of acetic acid to separate beakers along with a magnetic stirrer in each.
2. Weigh out the calculated masses of NaPP and CS on a precision scale then add the NaPP to the ultrapure water beaker and the CS to the acetic acid beaker on magnetic stirrers. (When adding the powders, the stirring should be fast enough to create a controlled vortex to reduce powder clumping)
3. Leave the solutions to stir overnight or until fully dissolved.

Day 2: Mixing

4. Once the CS is fully dissolved, add the calculated volume of copper solution and continue to mix for 1 hour or until the solution is homogeneous.
5. Now that both solutions are prepared, remove the stir bars and first add the PP solution to a 250 mL wide-mouth Nalgene bottle followed by the CS-Cu solution. If the CS is too viscous to pour, use a clean stir stick to scrap the residual solution into the Nalgene.
6. Mix the solutions using a homogenizer with a 2.5 cm diameter impeller attachment on speed level 3 (1400 rpm) for 30 seconds while moving the impeller around the bottom of the Nalgene. Scrap/remove any complex that has built up on the impeller head and return to the Nalgene. Repeat this step 3 times in total.
7. Cap the Nalgene and refrigerate overnight.

8. Pour the contents of the Nalgene into a vacuum filter with fast-drain filter paper and drain the supernatant from the gel complex.

9. Add 100 mL of Tris buffer to the gel complex and gently stir with a clean stir stick before draining the rinse medium. Depending on the sample formulation, draining may be instant or take several minutes. Repeat this step 3 total times and measure the pH on the final rinse.

10. Remove the drained complex and rehydrate with a small amount of Tris buffer to create a paste if necessary.

11. Equally divide the gel complex paste into a 24 well-plate and freeze overnight at ~-4°C. (Wells should be as consistent as possible and no more than half full)

Day 4: Freeze-drying

12. To freeze-dry the complex, add the well-plate without a cover face up to a freeze-drying chamber at -50°C and 0.1 mBar for 24 hours.

13. After 24 hours the sample production is complete. Store in a vacuum desiccator until use to avoid sample degradation due to humidity.

3.5 Protocol Consistency

3.5.1 Methods

With a standard operating procedure in place, the final step required before moving on to the DoE is to test the production protocol consistency. Three samples were made from the same sample formulation following the standard operating procedure. Samples 1 and 2 were made by the primary experimenter on separate days, while sample 3 was made by a secondary experimenter. The samples were then characterized for their handling properties, absorption capacity, chemical composition and elution profile to compare consistency. Handling properties were measured subjectively based on the appearance of the samples and by sample manipulation. Absorption capacity was measured by weighing the samples before and after soaking them in water to determine the percentage of weight increase. Chemical composition was determined by dissolving the samples and measuring the concentration of phosphorous

and copper using ICP-OES analysis, then calculating the percentage of phosphorous and copper in the sample. For the elution profile, 5 mg samples were left in 2 mL of a 0.1mg/mL lysozyme tris buffer for 10 minutes, 30 minutes, 90 minutes and 24 hours. The amount of phosphorous and copper in the degradation media was then measured using ICP-OES.

3.5.2 Results and Discussion

The three samples were white and spongy materials that were practically indistinguishable from one another in appearance. When manipulated, all samples behaved the same with respect to compressibility and resistance to stretching. Each sample earned the same score of 3 on a subjective handling property rating system described in the following chapter. The results for the absorption capacity, copper content and phosphorous content can be seen in Table 3 with the standard deviation between the sample groups shown as well. The mean elution profiles for each of the samples can be seen Figure 6. A single factor analysis of variance was run for the absorption capacity, copper content, phosphorous content, copper elution profile and phosphorous elution profile that returned P-values of 0.0666, 0.2131, 0.0977, 0.5406 and 0.9192.

Based on appearance and handling properties there was no discernible difference between the three samples, so the protocol is qualitatively consistent. Since none of the P-values were <0.05 the analysis of variance confirms there is no statistical difference between the mean sample characteristics with 95% certainty. Furthermore, the standard deviations were relatively low when compared to the desired detection and prediction sensitivity for the DoE. This indicates that the standard operating procedure is consistent and reproducible enough to move forward with the DoE.

Table 3 - Protocol consistency results and standard deviation between the sample groups.

	Absorption Capacity (%)	Copper (%)	Phosphorous (%)
Sample 1	1639 (SD=±50)	2.465 (SD=±0.195)	11.746 (SD=±0.865)
Sample 2	1810 (SD=±83)	2.437 (SD=±0.135)	12.235 (SD=±0.837)
Sample 3	1449 (SD=±193)	2.212 (SD=±0.030)	10.432 (SD=±0.190)
Standard Deviation Between samples	±147	±0.113	±0.762
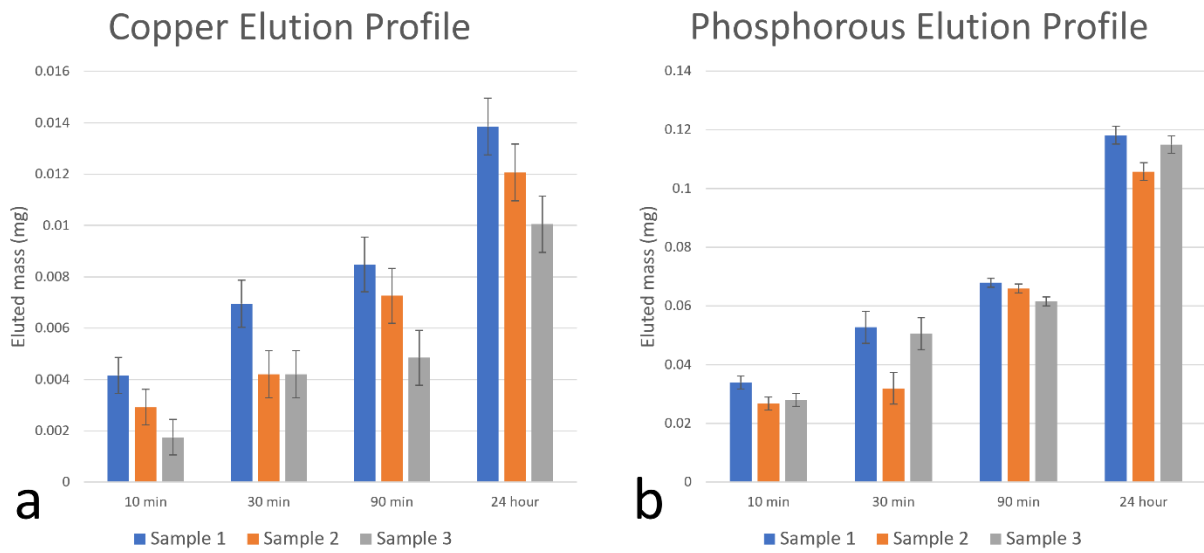
Figure 6 - Copper elution profile (a) and phosphorous elution profile (b) for protocol consistency samples.

33

Chapter 4: Design of Experiments

4.1 Introduction

DoE is a systematic research method to efficiently study the relationship between multiple input variables known as factors and key output variables known as responses. In a DoE approach, models are generated to predict resulting responses for specific factor levels, allowing experimenters to optimize the factors for target response levels [85]. The traditional scientific method takes one factor and adjusts that factor only, while holding all other factors constant. The problem with this method is it becomes very inefficient as more factors are included and does not account for the potential interaction effects between factors that could impact a response. In a DoE approach, the factors are altered in parallel to reduce the number of experimental runs while still revealing their effect on responses. This approach also considers multi-factor interactions, addressing the challenge of factors that are dependent on one another [85].

A DoE approach can be executed manually without the use of any specific tools. However, utilizing specialized software makes the DoE setup and statistical analysis much more accessible. The statistical software package Design-Expert (version 13) from Stat-Ease Inc. was used in this research project. Design-Expert is specifically dedicated to performing DoE and offers a variety of tools for statistical analysis, graphing and optimization. To set up a DoE using Design-Expert, first the design template must be selected based on the type of process that is being optimized in the DoE. The factors and their ranges are then defined, and the number of runs is determined. The last step is to define the responses that will be included in the DoE so that the software can generate the design space [86].

The design space is a table of sample runs with columns for the factors and responses. Upon generation, only the factor columns are pre-determined, indicating what levels must be used to produce the samples. The samples must then be made and characterized for all the responses to complete rest of the table. With the design space defined, the software can be used to generate predictive models for each of the responses[85]. The predictive models are equations that compute a predicted value for the responses, where the factors are the model

terms of the equations. For this study, term A represents CS concentration, B represents PP concentration, C represents copper concentration and D represents PP D_p. Terms that are combined represent factor interactions; for example, AB denotes the two-factor interaction between CS and PP concentration. To make the equation coefficients easier to interpret, the equations are reported in coded factor terms such that the factor level range is transformed so the lower limit is -1 and the upper limit is +1. This normalizes the factor coefficients for differences in ranges and units so the relative significance of the factors can still be compared by looking at the coefficients [87]. The models are also represented graphically as 3D response surfaces to visualize the impact each factor has on the predicted response levels. Since there are four factors, various response surfaces with different factors as axes can be generated for each response. For the purpose of reporting results in this thesis, the factors with the highest coefficients were selected as the axes as this produces the most informative graphs.

The order of the model is determined by the model terms that are included in the equation, which are selected by an algorithm that seeks to improve the analysis of variance. Before accepting a model, the analysis of variance and diagnostic plots should be examined to ensure the model with the most predictive power is generated. For a model to pass the analysis of variance the model P-value must be <0.05 and significant model terms must be included. The R^2 value is a measure of how well a model fits by looking at how much variance is explained by the model. The difference in adjusted and predicted R^2 values should be <0.2, otherwise there may be a problem with the predictive power of the model. Adequate precision is the signal to noise ratio associated with the model and should be >4. In the diagnostic plots, the Box-Cox plot should be checked to determine what transform, if any, are recommended. Transforms are useful in cases where model error scales with the magnitude of the response. A transform takes the response data and converts it using a specified mathematical operation before generating the predictive model. After the model makes the prediction, the predicted values are transformed back to the responses original scale. The remaining diagnostic plots include the residual plots and influence plots which are used to identify outliers. If specific data points are significant outliers, they should be ignored to improve the predictive power of the model as they may be wrong and overinfluencing the model.

After generating predictive models for each of the responses and verifying their significance, an optimal sample formulation can be generated. This is done by defining the optimization criteria for each response and using Design-Expert's algorithm to find the best possible combination of response levels based on their defined importance.

4.2 Design Space Preparation

4.2.1 Design Template

When choosing a design template there are three categories of design spaces to consider. The first and most basic category of design spaces are factorial designs. These are used primarily for screening purposes to understand if certain factors are important to the process. Factorial designs can reveal which factors are important out of many possibilities or the effect a known factor individually has on a process. Factorial designs work by taking response data from runs with the factors set at a low or high level, then using interpolation to predict the responses for factor levels in between the set points. This assumes linear relationships between the factors and responses, which is often not the case [85]. The next category of design spaces are the more complex response surface designs. These are more robust design spaces that enable full modelling and optimization of responses with multiple factors considered. Response surface designs use the same principles as factorial designs but include additional design points beyond a low and high level to allow quadratic or even higher order modelling. This is the type of design space necessary for this research project as the end goal is to optimize the factors in parallel [87]. The final category of design spaces are mixture designs which accomplish the same results as response surface designs but are specifically designed for processes where the factors are relative proportions of the components. In a mixture design all factors must be entered in the same units and each run must sum to the same total of components. This is not the case for the process in this research project, so mixture design spaces were avoided.

Of the response surface designs Central Composite and Box-Behnken are the most recommended and most popular choices [86]. Central Composite designs are essentially 2-level factorial designs that have been augmented with additional center and axial points to fit quadratic models. Each factor will have five different levels and center points are replicated to

enhance prediction capability near the center of the factor space. Box-Behnken designs are similar to a Central Composite approach, however, they only have three levels and do not have runs at the extreme combinations for each factor. Although this reduces prediction capability at the extremes, it has much better precision in the center of the factor space [86, 87]. For both design templates, adding categoric factors duplicates the design space for each categoric treatment, doubling the number of runs. A third design template recommended by Design-Expert is the Optimal RSM design. Optimal designs avoid duplicating the design space for categoric factors and allow for additional model points, center points, lack-of-fit points and replicate points to be added to the design space. The design points in Optimal designs are not a specific pattern but, rather, are selected by an algorithm [86]. This means that each time the design space is generated the runs are slightly different as there are many statistically equivalent sets of design points.

Because the process in this research project includes numeric and categoric factors, the Optimal RSM design template was selected. I-optimal optimality was selected for the design space as it produces models with lower average prediction variance and is recommended when the goal is to optimize factor levels [86]. 4 lack-of-fit points, 3 replicate points and 2 additional center points were included resulting in a total of 23 runs within the design space.

4.2.2 Factors

After selecting the design template, the next step was to define the factors and their ranges. While refining the production protocol, it was concluded that the factors to include in the DoE would be CS solution concentration, PP solution concentration, copper solution concentration and PP D_p. CS, PP and copper concentration were numeric factors since they could be accurately adjusted to any level within the defined range, while PP D_p was a 2 level categoric factor because the D_p could not be accurately adjusted. The lower and upper limits were 5000-25000 PPM, 5000-100000 PPM, and 0-2000 PPM for CS, PP, and copper concentration, respectively. These limits were decided based on information that was gained during preliminary work. The lower limits for CS and PP were set at 5000 PPM because polyelectrolyte complexes did not form reliably when the concentrations were below 5000 PPM. The CS upper limit was fixed at 25000 PPM, as any concentration above this resulted in a

solution that was too viscous to properly mix. Although samples could be made using PP solutions with higher concentrations, the PP upper limit was set at 100000 PPM since increasing the concentration beyond 100000 PPM did not significantly affect the sample's appearance, handling properties or absorption capacity. The copper lower limit was set at 0, as it was not clear whether including copper at all would have a positive effect on the material. A corresponding upper limit of 2000 PPM was set, as concentrations of copper higher than 2000 PPM would likely induce copper levels well beyond what is reported as cytotoxic, around 10 PPM [50]. PP D_p values of approximately 20 and 180 were selected as the categoric levels to represent shorter and longer chain PP; additionally, there were established lab protocols to reliably make NaPP of these approximate chain lengths.

4.2.3 Responses

The final step in the design space preparation was to define the responses. Each response should in some way measure how well the samples meet the design criteria for an ideal trauma wound dressing. This includes the material physical properties, hemostatic effect, antibacterial effect and biocompatibility. To be an effective response, the response must be consistently and accurately characterized for all the samples within the design space. If there is great variation in accuracy between measurements of samples then the resulting models will have inadequate prediction capabilities. The best responses are measured numeric responses; however, if there is no feasible objective measure for a property then subjective rating systems can be used [86]. The responses that were selected for this design space and a brief description justifying their inclusion are as follows.

CS to PP Ratio

The CS to PP ratio was included as a response so that the effect this ratio has on other responses could be investigated using the Design-Expert tools. It is not a true response as it is predetermined by the CS and PP solution concentrations and not a measured characteristic.

Copper and Phosphorous Content

Copper and phosphorous content are measures of the percentage by mass of copper or phosphorus in each sample. Knowing these percentages makes it possible to estimate the

compositional breakdown of PP and copper for each material and allows for an indirect estimate of CS content. This response ensures there are consequential amounts of PP and copper included in the material so that the hemostatic and antibacterial benefits of each component can be extracted. It is also useful for understanding how different copper and phosphorous contents correlate to other responses. This response uses units of %.

Ease of Production

The ease of production score is a subjective rating system response that represents how easy the production method was for each sample run. A rating system was used for this response as no objective measure could feasibly represent how easy it was to create samples of a given formulation. The samples were rated on a scale of 1-3 and their score was determined based on how easy it was to mix the solutions and rinse/cast the complex. Samples where the solutions were so viscous that they were difficult to work with or required significant amounts of scraping/picking while mixing received worse scores. Samples also received worse scores if they took a long time or did not drain fully during rinsing or were difficult to spread evenly in the molds. If a sample displayed both issues it received a score of 1, if it displayed only one of the issues it received a score of 2 and if it displayed neither issue it received a score of 3. A scoring rubric for this response can be seen in Table 4. This response is unitless.

Handling Properties Score

The handling properties score is a subjective rating system response that represents how suitable the material handling properties are for trauma wound dressing. Objective measures such as tensile and compressive strength were attempted as handling property responses but ultimately could not be used do to technical challenges and overall feasibility. Measuring tensile and compressive strength required that samples be cast in specific moulds and used more sample material than could be allotted to a single response. Instead, the samples were rated on a scale of 1 to 3 and their score was determined by thoroughly handling, stretching, compressing and bending the samples. If the sample immediately started to fall apart when being handled it received a score of 1. Samples that remained intact while handling but could not endure much manipulation (stretching, compression or bending) received a score of 2. Otherwise, a score of 3 was assigned if the sample remained intact and functional while being

39

stretched, compressed and bent to a level that is reasonably expected during application. A scoring rubric for this response can be seen in Table 4. This response is unitless.

Table 4 - Scoring rubric for ease of production score and handling properties score.

Score	1	2	3
Ease of Production	Sample was difficult to work with in the mixing and rinsing stages.	Sample was difficult to work with in either the mixing or rinsing stage but not both.	Sample was easy to work with in the mixing and rinsing stages.
Handling Properties	Sample began to disintegrate upon handling without additional manipulation.	Sample remained intact when handled but lost integrity if stretching, compression or bending was applied.	Sample maintained functionality throughout extensive handling involving stretching, compression and bending.

Apparent Density

Apparent Density (also referred to as bulk density) is a measure of density that includes the interparticle space in the volume. Initially this response was supposed to be a measure of surface area, given that increased surface area in contact with media could result in more robust biological effects. However, due to the extremely low density of the samples, characterization methods such as BET nitrogen adsorption and pycnometer analysis were not feasible. Here, apparent density was used as a proxy for surface area of the material that would be in contact with wound exudate/blood. This response uses units of g/cm^3.

Absorption Capacity

Absorption capacity is a measure of how much water by percentage of sample mass a material can absorb. This response addresses both physical properties and hemostatic design criteria. In order to effectively apply a dressing to a wound with profuse bleeding, the material must be absorbent, otherwise the dressing will fail to adhere to the wound. Absorption capacity is also important for hemostasis because as the material swells, it creates a plug in the defect to

control bleeding and also concentrates coagulation factors at the wound site as the water is absorbed from the blood [16]. Including absorption capacity as a response was critical so that it could be maximized in the optimized material. This response uses units of %.

Copper and Phosphorous Elution

Copper and phosphorous elution are measures of how much copper and phosphorous, as a percentage of the mass of the sample, are being released as the material is left in degradation media for extended periods of time. Because the materials are CS based, the degradation media contained lysozyme, the enzyme that would be responsible for CS degradation *in vivo*. To mimic the levels of lysozyme found in serum, a concentration of 0.1 mg/mL was used for the degradation media [88, 89]. This response was included because the purpose of incorporating copper and PP in the material is to improve antibacterial and hemostatic effects, respectively. To realize these effects the copper and PP must be able to come out of the material to interact with the wound site. Copper and phosphorous elution was measured at 10 minutes, 30 minutes, 90 minutes and 24 hours to establish a profile that would capture immediate elution levels and elution after the maximum intended application duration. This response uses units of %.

Blood Clotting Index

Blood clotting Index is a measure of the percentage of hemoglobin that was incorporated into a clot after the material was left in sheep's blood for 10 minutes. It was included as a response to address the design criteria for hemostatic potential by determining how extensive the clotting reaction was for each sample. This response was originally intended to be a measure of blood clotting time to determine how quickly each sample induces a clot. However, this approach proved infeasible for this type of material. This response uses units of %.

Cytotoxic Concentration

Cytotoxic concentration is an *in vitro* measure of the concentration of sample in cell media required to induce a cytotoxic response. The conditions are considered cytotoxic if less than 70% cell viability is observed after 24 hours. This is included as a response to address the

biocompatibility design criteria by ensuring the sample is not cytotoxic at expected concentrations. Because it is unclear what the exact dosage of this material would be due to the unknown nature of trauma wounds, the goal should be to minimize the cytotoxicity as much as possible. This response uses units of mg/mL.

4.2.4 Design Space

With the design template selected and the factor ranges and desired responses defined, the design space was generated as shown in Figure 7. Referencing this design space, samples for each run were fabricated and subsequently characterized for each response using the methods detailed in the following section.

Run	Factor 1 A:CS Concentration PPM	Factor 2 B:PP Concentration PPM	Factor 3 C:Cu Concentration PPM	Factor 4 D:Polyphosphate Degree of Polymerization Dp	Response 1 CS to PP Ratio Unitless	Response 2 Copper Content %	Response 3 Phosphorous Content %	Response 4 Ease of Production Unitless	Response 5 Handling Properties Score Unitless	Response 6 Apparent Density g/cm^3
1	5000	24000	1120	180						
2	25000	5000	600	180						
3	5000	100000	1390	180						
4	15000	52500	1000	20						
5	15000	52500	1000	180						
6	23400	100000	1049.71	180						
7	19000	100000	0	180						
8	5000	50600	2000	20						
9	5000	33500	0	180						
10	11000	5000	2000	180						
11	15000	52500	970	20						
12	25000	96200	510	20						
13	25000	71500	2000	180						
14	15000	52500	1000	180						
15	25000	5000	600	180						
16	15000	52500	970	20						
17	25000	5000	2000	20						
18	5000	100000	0	20						
19	16200	100000	2000	20						
20	9500	100000	1050	20						
21	14300	5000	1550.51	20						
22	21600	14500	0	20						
23	5000	5000	700	20						

Response 7 Absorption Capacity %	Response 8 Copper elution 10 min %	Response 9 Copper el... %	Response 10 Copper el... %	Response 11 Copper el... %	Response 12 Phosphorous elution 10 min %	Response 13 Phosphoro... %	Response 14 Phosphoro... %	Response 15 Phosphoro... %	Response 16 Blood Clotting Index %	Response 17 Cytotoxic Concentration mg/mL

Figure 7 - Generated design space detailing the sample formulations for each run and the responses to be characterized.

4.3 Methods

4.3.1 Sample Production

Samples for each run were made following the standard operating procedure as described in section 3.4. Freeze-dryer capacity limited production of samples to 3 runs per day so all 23 runs were completed over an 8-day period. Samples were freeze-dried in 24 well-plates for convenience when characterizing the samples for each response.

4.3.2 Copper and Phosphorous Content

Copper and phosphorous content of each sample run was analyzed using ICP-OES. To prepare the ICP-OES samples, three 10 mg pieces from each sample run were dissolved in 6 mL of 70% HNO_3 + 3 mL of 38% HCL inside a 50 mL Falcon tube. The samples were left loosely capped for one hour or until fully dissolved before being topped up to the 50 mL line with ultrapure water and vortexed. 2 mL of the digestion was then added to 15 mL Falcon tubes with 8 mL of ultrapure water and vortexed. The samples were then analyzed using ICP-OES. The copper and phosphorous content by percentage of the sample mass was calculated using Eq. (5), where C is the concentration of copper or phosphorous measured by ICP-OES in mg/L, d_f is a dilution factor of 0.25, and m is the mass of the original sample in mg.

$$\% \ Copper/phosphorous = \frac{C \times df}{m} \times 100\% \tag{5}$$

4.3.3 Apparent Density

To determine the apparent density, the diameter and thickness of three pucks from each sample run were measured using calipers prior to weighing the pucks on a precision scale. The apparent density of each puck was then calculated using Eq. (6) and the average was recorded as the apparent density.

$$Apparent \ Density = \frac{m}{\left(\frac{D}{2}\right)^2 \times T \times \pi} \tag{6}$$

4.3.4 Absorption Capacity

To determine the absorption capacity, the dry mass of three pucks from each sample run was measured using a precision scale. The pucks were then submerged for 1 minute in a vacuum filter filled with water. After draining the filter, the pucks remained for an additional

minute to allow for the removal of any excess water. The pucks were subsequently re-weighed to determine the wet mass. The absorption capacity of each puck was calculated using Eq. (7) and the average was recorded as the absorption capacity.

$$Absorption\ capacity = \frac{m_{wet} - m_{dry}}{m_{wet}} \times 100\% \qquad (7)$$

4.3.5 Elution Assay

The amount of copper and phosphorous eluted by the samples when submerged in degradation media for 10 minutes, 30 minutes, 90 minutes and 24 hours was measured using ICP-OES. Three 10 mg pieces from each sample run were weighed on a precision scale then added to a 15 mL Falcon tube. 10 mL of Tris buffer with 0.1 mg/mL of lysozyme was added and the samples left on a shaker table at 37 °C and speed level 120 for the intended duration. After the intended duration, the samples were centrifuged at 4400 rpm for 5 minutes before 2 mL was drawn off and added to 8 mL of 2% HNO_3 in a 15 mL Falcon tube. The samples were then analyzed using ICP-OES. The eluted copper and phosphorous relative to percentage of the sample mass was calculated using Eq. (5), where C is the concentration of copper or phosphorous measured by ICP-OES in mg/L, d_f is a dilution factor of 0.05 and m is the mass of the original sample in mg.

4.3.6 Blood Clotting Assay

The blood clotting Assay was adapted from Ong et al. and Shih et al. [78, 90]. Three replicates were done for each sample run. In a 37 °C water bath, 0.2 mL of citrated whole sheep's blood (CL2581, Cedarlane) was added to a 50 mL Falcon tube with 20 µL of 0.2 M $CaCl_2$ to reactivate coagulation. Approximately ¼ of the sample puck (~ 1.25 cm^2) was added to the blood and left for 10 minutes to allow a clot to form on the sample. After 10 minutes the sample along with the clot was removed and 25 mL of water was added to hemolyze the remaining red blood cells. The absorbance of the resulting hemoglobin solution was measured at 540 nm using a Varioskan LUX plate reader. The blood clotting index was then calculated using Eq. (8), where Abs_s is the absorbance of the solution, Abs_w is the absorbance of water and Abs_b is the absorbance of whole blood.

$$Blood\ clotting\ index = \frac{(Abs_s - Abs_w)}{(Abs_b - Abs_w)} \times 100 \qquad (8)$$

4.3.7 Cytotoxicity Assay

An alamarBlue^{TM} assay adapted from the ISO 10993-5 standards was used to assess cell cytotoxicity as a result of exposure to sample elution media [91]. Three technical replicates were done for each sample run. NIH 3T3 cells (provided by the Leung lab) were seeded in 96 well plates with 0.2 mL of cell media at a density of 25000 cells/mL. The cells were then left to incubate for 24 hours before being treated with the elution media. To prepare the elution media, 40 mg of sample was added to 1 mL of fresh media and left on a shaker table at 37 °C for 24 hours. The elution media was then removed and diluted with fresh media to concentrations of 20 mg/mL, 17.5 mg/mL, 15 mg/mL, 12.5 mg/mL, 10 mg/mL, 7.5 mg/mL, 5 mg/mL, 2.5 mg/mL, and 1 mg/mL. 0.2 mL of each elution media concentration was added to the cells then left to incubate for 24 hours prior to adding 0.02 mL of alamarBlue, followed by an additional 4 hours of incubation. The negative control group was treated the same way using only fresh media and the positive control group was media with 10% Dimethyl sulfoxide. Subsequently, a 0.1 mL volume was removed from each well and added to an opaque-walled 96 well plate for fluorescence measurements using a Varioskan LUX plate reader with excitation at 570 nm and emission at 600 nm. The fluorescence of AlamarBlue in Fresh media with no cells was also measured as a calibration standard and AlamarBlue in media followed by autoclaving was used to ensure the resazurin was reducing properly. Increased fluorescence was interpreted as an indication of viable cells and the percentage cell viability was calculated using Eq. (9), where F, $F_{control}$, and $F_{standard}$ correspond to the measured fluorescence of the test samples, the negative control, and the internal standard. The non-cytotoxic concentration was then determined by finding the highest elution media concentration where >70% cell viability was maintained for each sample.

$$\% \; Cell \; Viability = \frac{F - F_{standard}}{(F_{control} - F_{standard})} \times 100\% \tag{9}$$

4.4 Results

4.4.1 Completed Design Space

After characterizing all the runs for each response, the design space was completed as shown in Figure 8. Using this data, Design-Expert generated the correlation table seen in Figure

9 by plotting the factors and responses against one another and determining how well the data fits a linear relationship to calculate the correlation coefficients. These correlations were represented visually in the table where blue squares and red squares denote negative and positive correlations, respectively, with darker shading being representative of stronger correlations.

Run	Factor 1 A:CS Concentration PPM	Factor 2 B:PP Concentration PPM	Factor 3 C:Cu Concentration PPM	Factor 4 D:Polyphosphate Degree of Polymerizati... Dp	Response 1 CS to PP Ratio Unitless	Response 2 Copper Content %	Response 3 Phosphorous Content %	Response 4 Ease of Production Unitless	Response 5 Handling Properties Score Unitless	Response 6 Apparent Density g/cm^3
1	5000	24000	1120	180	0.208	1.714	9.287	1	1	0.0249
2	25000	5000	600	180	5	3.678	7.806	1	3	0.0194
3	5000	100000	1390	180	0.05	0.601	10.815	2	1	0.0386
4	15000	52500	1000	20	0.286	0.714	11.848	3	2	0.0662
5	15000	52500	1000	180	0.286	0.837	13.464	3	2	0.0631
6	23400	100000	1049.71	180	0.234	0.391	11.346	3	2	0.1022
7	19000	100000	0	180	0.19	0.023	12.345	3	2	0.0826
8	5000	50600	2000	20	0.099	1.391	9.747	2	3	0.0228
9	5000	33500	0	180	0.149	0.007	10.654	2	1	0.0317
10	11000	5000	2000	180	2.2	5.938	9.559	1	3	0.0356
11	15000	52500	970	20	0.286	0.659	11.532	3	2	0.0798
12	25000	96200	510	20	0.26	0.316	12.398	2	1	0.136
13	25000	71500	2000	180	0.35	1.145	12.899	2	2	0.133
14	15000	52500	1000	180	0.286	0.758	11.988	3	2	0.0848
15	25000	5000	600	180	5	3.757	9.074	1	3	0.0241
16	15000	52500	970	20	0.286	0.638	11.252	3	2	0.077
17	25000	5000	2000	20	5	6.61	6.543	1	3	0.0171
18	5000	100000	0	20	0.05	0.007	9.27	2	2	0.0377
19	16200	100000	2000	20	0.162	0.834	11.964	3	1	0.0809
20	9500	100000	1050	20	0.095	0.371	10.024	3	1	0.0548
21	14300	5000	1550.51	20	2.86	5.418	8.359	1	2	0.0261
22	21600	14500	0	20	1.49	0.014	9.594	2	2	0.0553
23	5000	5000	700	20	1	5.095	10.448	2	2	0.0424

Response 7 Absorption Capacity %	Response 8 Copper el... %	Response 9 Copper el... %	Response 10 Copper el... %	Response 11 Copper elution 24 hour %	Response 12 Phosphoro... %	Response 13 Phosphoro... %	Response 14 Phosphoro... %	Response 15 Phosphorous elution 24 hour %	Response 16 Blood Clotting Index %	Response 17 Cytotoxic Concentration mg/mL
3848	0.05	0.068	0.094	0.536	0.632	0.817	0.825	2.263	61.6	0
4334	0.008	0.01	0.007	0.122	0.1	0.115	0.043	0.537	55.42	2.5
2455	0.022	0.026	0.033	0.285	0.962	1.032	1.315	2.712	53.5	0
969	0.04	0.039	0.06	0.144	0.96	0.91	1.442	2.491	61.1	15
888	0.019	0.022	0.036	0.129	0.792	0.865	1.356	2.714	69.83	12.5
710	0.008	0.012	0.016	0.054	0.762	1.004	1.313	2.562	39.8	2.5
761	0	0	0	0.02	0.829	1.084	1.45	2.411	78.14	17.5
1921	0.023	0.042	0.05	0.188	0.341	0.588	0.554	1.174	80.17	10
2576	0	0	0	0.069	0.522	1.047	1.426	2.106	56.19	17.5
2802	0.012	0.036	0.04	0.236	0.145	0.194	0.247	1.468	68.27	0
1205	0.038	0.046	0.063	0.112	0.913	1.131	1.521	2.202	60.87	0
565	0.012	0.015	0.016	0.055	0.678	0.895	1.058	2.296	111.17	15
684	0.028	0.038	0.088	0.109	0.782	1.108	1.394	2.415	55.11	10
1050	0.018	0.023	0.075	0.108	0.653	0.959	1.447	2.734	69.79	10
4805	0.052	0.01	0.049	0.074	0.123	0.063	0.08	0.601	61.23	2.5
1227	0.092	0.047	0.075	0.1	0.778	1.145	1.491	2.249	45.19	10
5673	0.122	0.125	0.151	0.234	0.232	0.134	0.231	1.16	54.25	2.5
2736	0.046	0.001	0.061	0.037	0.289	0.264	0.317	0.639	54.29	20
1017	0.068	0.059	0.091	0.123	1.267	1.48	1.879	2.57	66.72	7.5
1447	0.03	0.014	0.044	0.053	0.463	0.739	0.709	1.286	49.99	20
3875	1.043	0.071	0.106	0.095	0.392	0.237	0.373	1.597	59.94	0
1667	0.116	0	0.016	0.013	0.227	0.257	0.483	0.627	72.11	20
1634	0.414	0.285	0.425	0.567	0.568	0.658	1.05	2.639	69.08	0

Figure 8 - Completed design space table.

Figure 9 - Table of correlation coefficients between the factors and responses.

4.4.2 Copper and Phosphorous Content

Copper and phosphorous content across all runs ranged from 0.007-6.610%, with a mean of 1.77% for copper and 6.543-13.464%, with a mean of 10.531% for phosphorous. Using these results, estimates of the material compositions ranged from 16.675-33.312% PP, 64.180-76.363% CS, and 0.012-11.915% copper. A reduced quadratic model with a square root transform was generated to predict copper content. The coded equation can be seen in Eq. (10)

and the corresponding 3D response surface displayed in Figure 10. Looking at the response surface it is very clear that copper content increases significantly with lower PP concentration. The model was statistically significant with a model F-value of 39.36, model P-value of <0.0001 and P-values that indicate model terms B, C, AD, BC, B^2 and C^2 were significant. Adjusted R^2 and predicted R^2 were within reasonable agreement at 0.9331 and 0.8510, and the signal to noise ratio was 20.3466, indicating adequate precision. Although outliers were identified in the residual plots, they were not ignored as ignoring them resulted in a non-significant model. Similarly, a reduced quadratic model was generated to predict phosphorous content. The coded equation can be seen in Eq. (11) and the corresponding 3D response surface is displayed in Figure 11. This graph suggests that the highest phosphorous content, and thus PP inclusion, occurs when CS and PP concentration are maximized. The model was statistically significant with a model F-value of 13.77, model P-value of <0.0001 and P-values that indicated model terms B, AB and B^2 are significant. Adjusted R^2 and predicted R^2 were within reasonable agreement at 0.6990 and 0.5666, and the signal to noise ratio was 10.5607, indicating adequate precision. The diagnostic plots showed no obvious outliers, so all runs were included in the phosphorous content analysis.

$$\sqrt{Copper\ Content} = 0.8433 + 0.0156A - 0.6711B + 0.6258C + 0.0110D + 0.1297AD - 0.2326BC + 0.5942B^2 - 0.3688C^2 \tag{10}$$

$$Phosphorous\ Content = 11.60 + 0.3940A + 1.26B + 1.04AB - 1.62B^2 \tag{11}$$
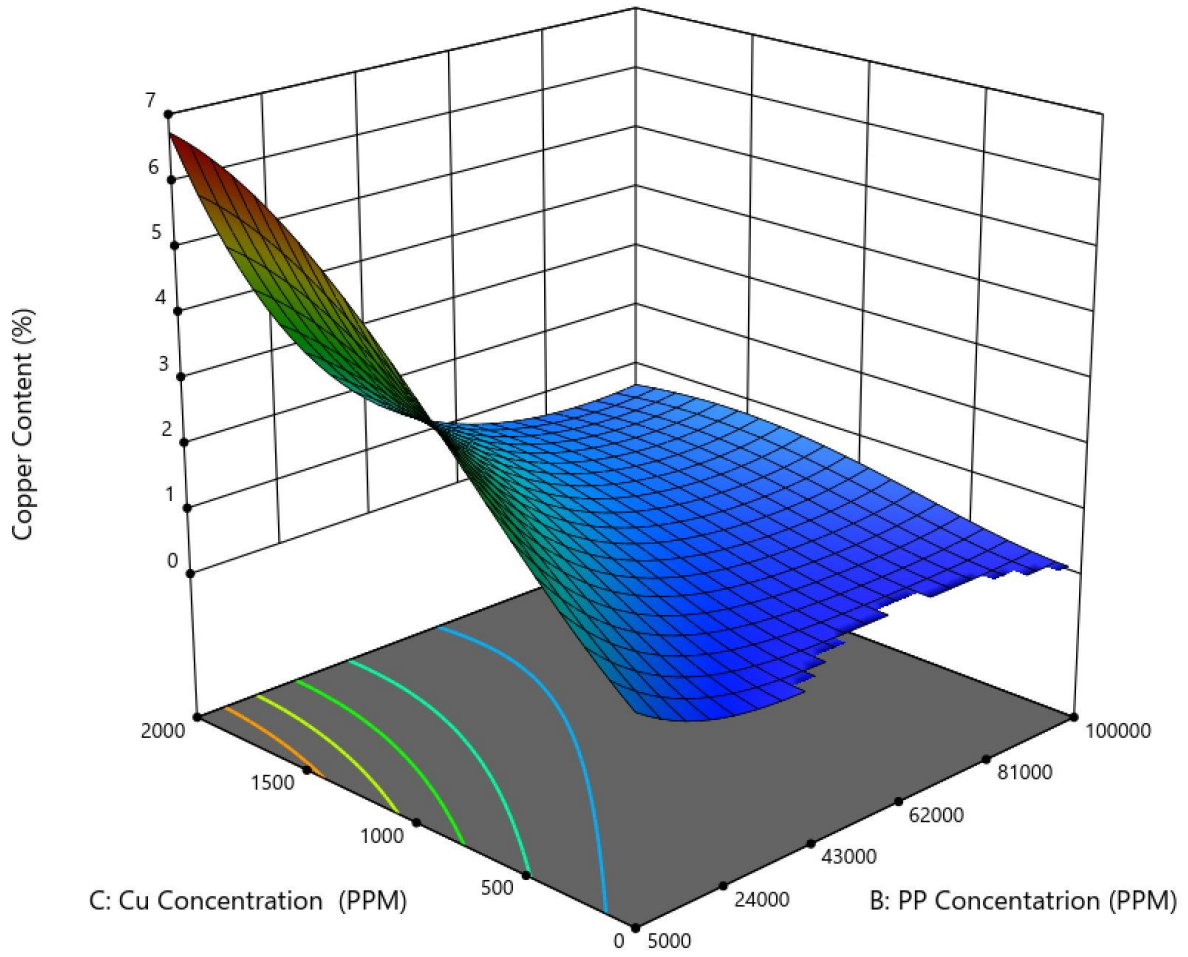
Figure 10 - 3D response surface for copper content.
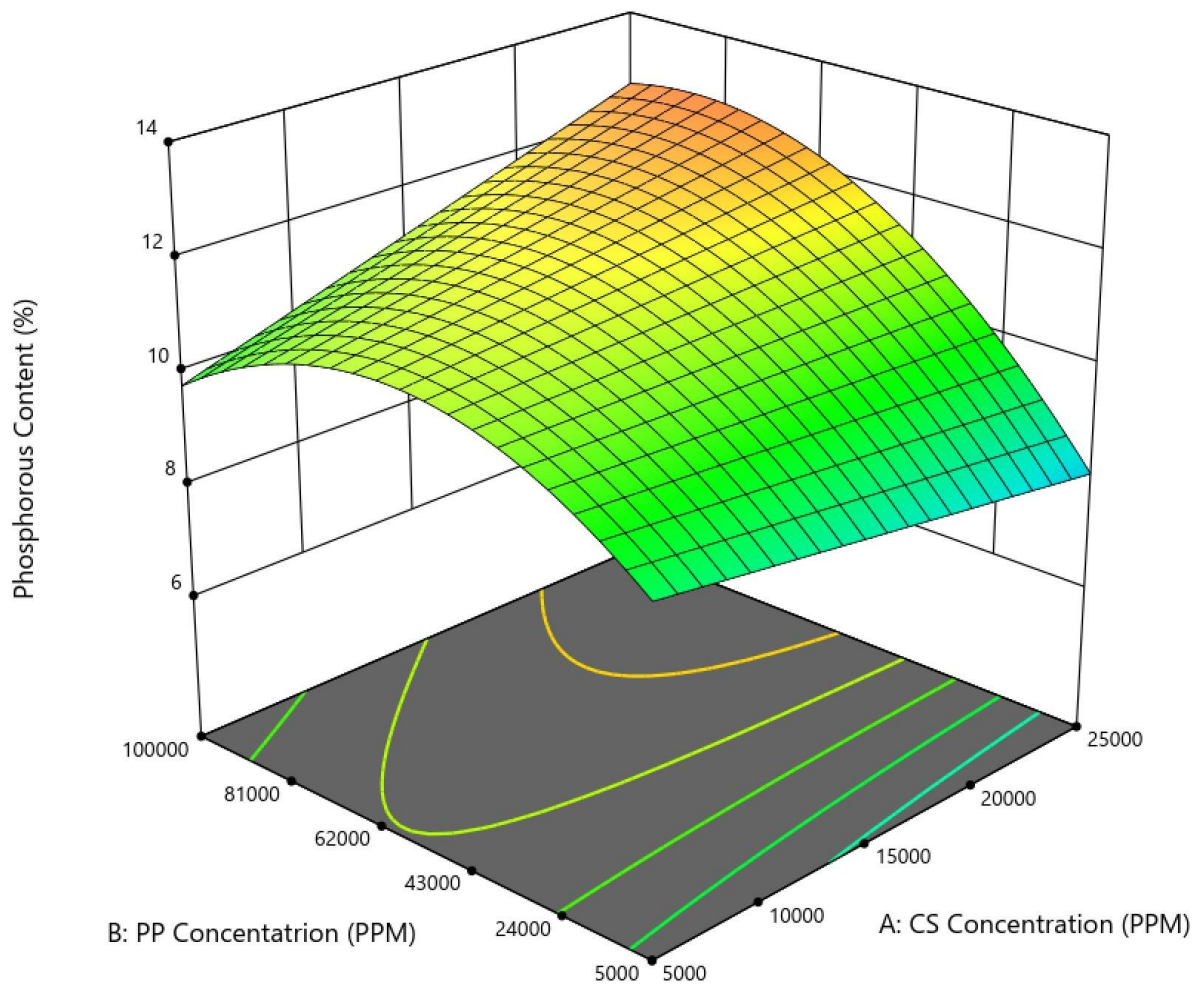
Figure 11 - 3D response surface for phosphorous content.

4.4.3 Ease of Production

For ease of production, 6 runs had a score of 1, 8 runs had a score of 2 and 9 runs had a score of 3. A reduced quadratic model was generated to predict ease of production. The coded equation can be seen in Eq. (12), with the corresponding 3D response surface shown in Figure 12. Interestingly, it appears ease of production plummets when PP concentration is low and CS concentration is either too low or too high. The model was statistically significant with a model F-value of 34.83, model P-value of <0.0001 and P-values that indicate model terms B, A^2 and B^2 were significant. Adjusted R^2 and predicted R^2 were within reasonable agreement at 0.8896 and 0.8237, and the signal to noise ratio was 16.7748, again indicating adequate precision. Run 23

was an outlier in the residual plots so to improve fit statistics it was ignored in the ease of production analysis.

$$Ease\ of\ Production = 2.98 + 0.1590A + 0.7543B - 0.1629C - 0.8187A^2 - 0.7080B^2 \tag{12}$$
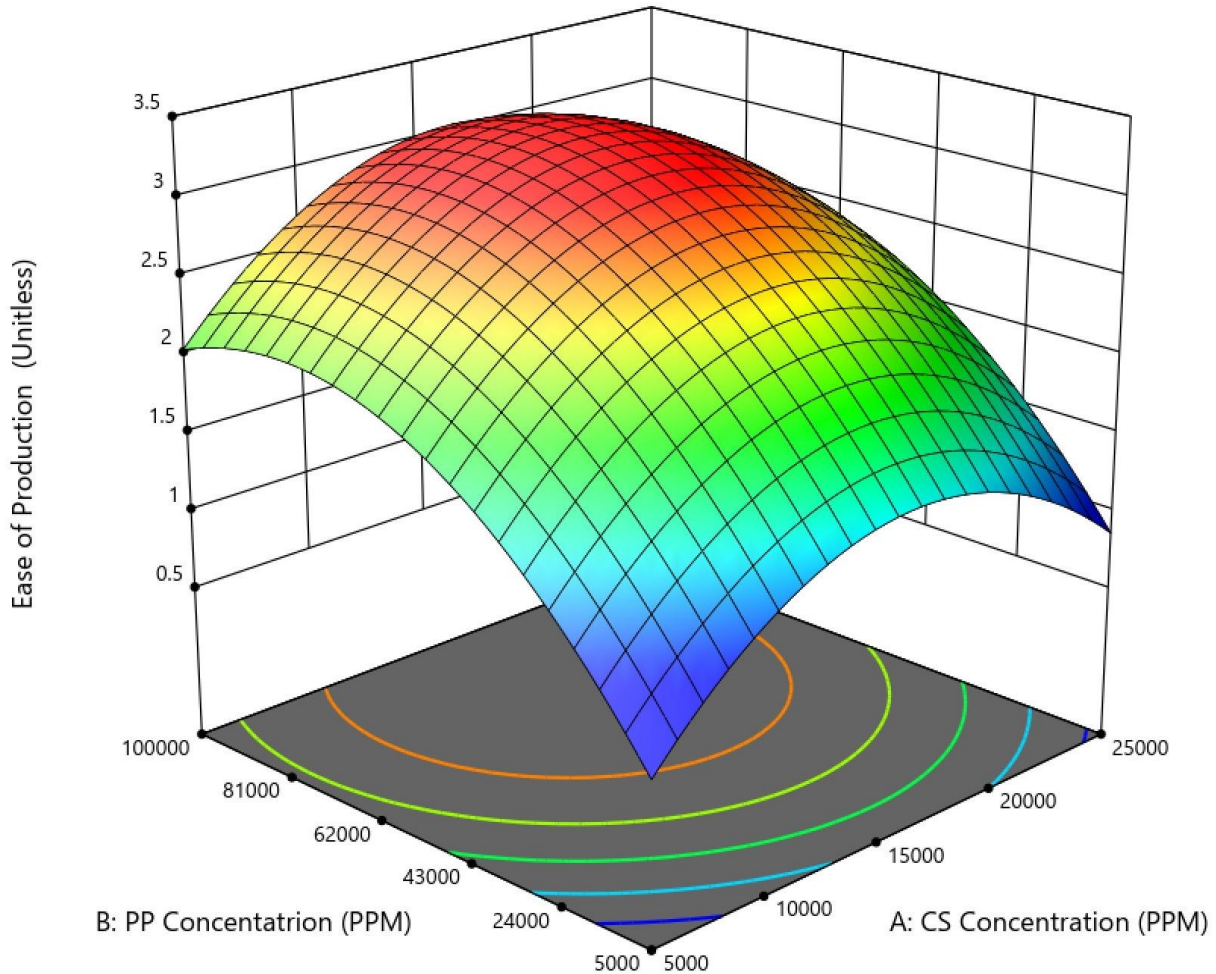
Figure 12 - 3D response surface for ease of production.

4.4.4 Handling Properties Score

For the handling properties score, 6 runs had a score of 1, 12 runs had a score of 2 and 5 runs had a score of 3. A reduced 2 factor interaction model was generated to predict handling properties score. The coded equation can be seen in Eq. (13) and the corresponding 3D response surface displayed in Figure 13. From the graph it is clear that using a PP concentration that is too high results in samples with poor handling properties. The model was statistically

significant with a model F-value of 9.32, model P-value of 0.0002 and P-values that indicate model terms A, B, AD and BC were significant. Adjusted R^2 and predicted R^2 were within reasonable agreement at 0.0.7259 and 0.6054, and the signal to noise ratio was 9.8394 indicating adequate precision. The diagnostic plots showed no obvious outliers.

$Handling\ Properties\ Score = 1.88 + 0.2271A - 0.4783B + 0.1887C + 0.0423D - 0.2392AB + 0.4434AD - 0.4402BC$

(13)
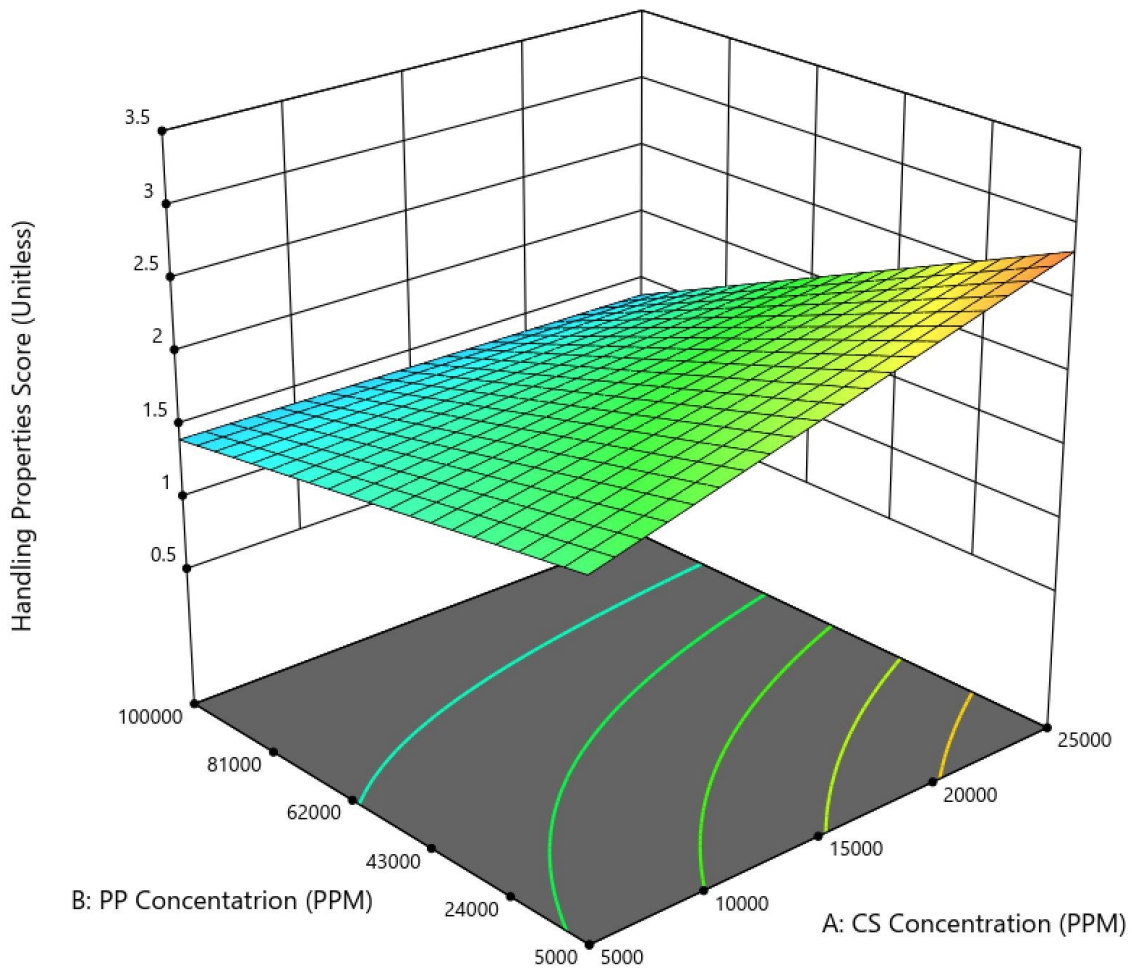
Figure 13 - 3D response surface for handling properties score.

4.4.5 Apparent Density

Apparent density across all runs ranged from 0.0171 to 0.1360 g/cm³, with a mean of 0.0581 g/cm³. A reduced quadratic model was generated to predict apparent density. The coded

equation can be seen in Eq. (14), with the corresponding 3D response surface displayed in Figure 14. From this graph it appears increasing CS or PP concentration each on their own will not increase density; however, if both are increased simultaneously apparent density increases drastically. The model was statistically significant with a model F-value of 40.15, model P-value of <0.0001 and P-values that indicate model terms A, B, AB, CD and B^2 were significant. Adjusted R^2 and predicted R^2 were within reasonable agreement at 0.9257 and 0.8786, and the signal to noise ratio was 20.7262 indicating adequate precision. The diagnostic plots showed no obvious outliers.

$$Apparent\ Density = 0.0715 + 0.0257A + 0.0252B + 0.0004C - 0.0024D + 0.0235AB + 0.0131CD - 0.0186B^2 \ (14)$$
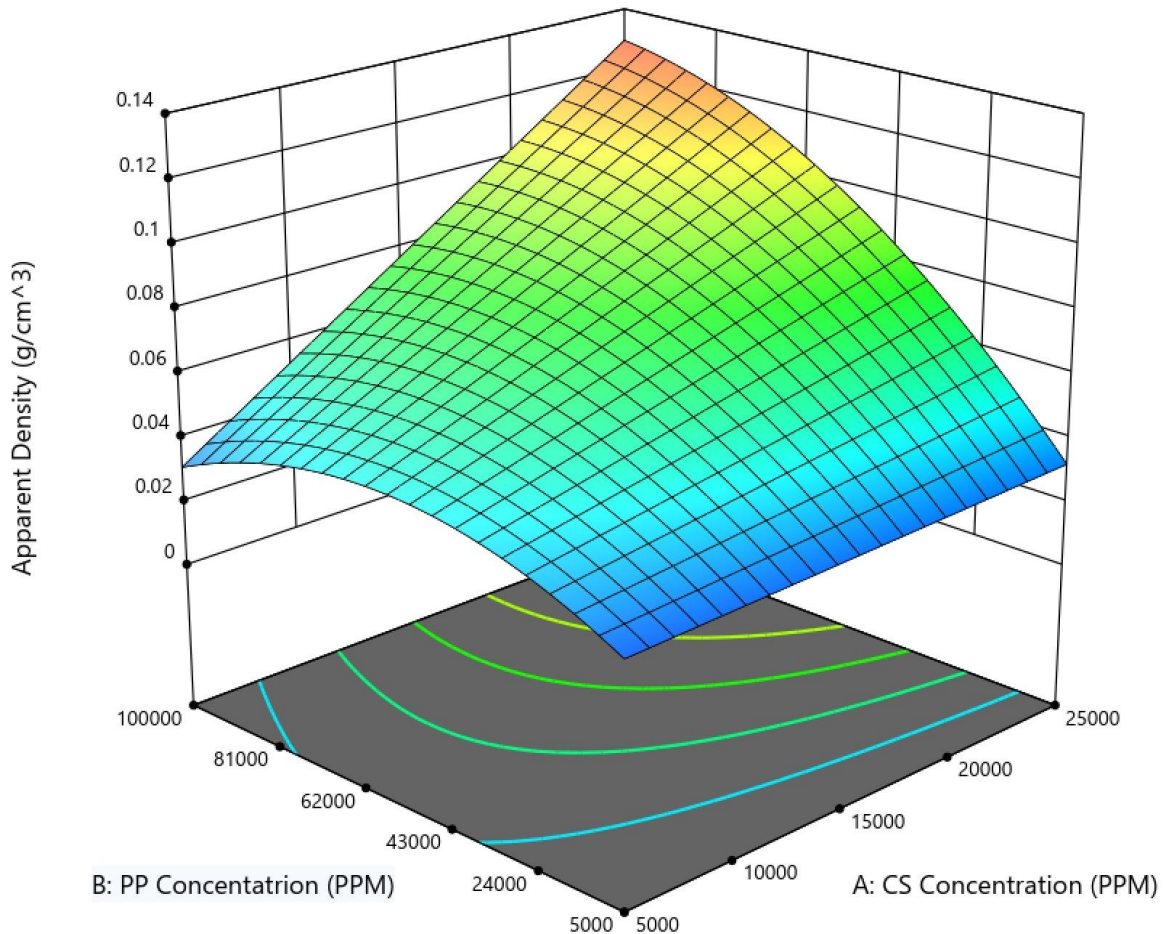
Figure 14 - 3D response surface for apparent density.

53

4.4.6 Absorption Capacity

Absorption capacity across all runs ranged from 565 to 5673%, with a mean of 2124%. A reduced quadratic model with an inverse square root transform was generated to predict absorption capacity. The coded equation can be seen in Eq. (15); the corresponding 3D response surface is shown in Figure 15. The absorption capacity appears to be greater when PP concentration is minimized and has peaks when CS concentration is at its lowest or highest. The model was statistically significant with a model F-value of 55.34, model P-value of <0.0001 and P-values that indicate model terms A, B, AB, A^2 and B^2 were significant. Adjusted R^2 and predicted R^2 were within reasonable agreement at 0.9539 and 0.9142, and the signal to noise ratio was 22.2843 indicating adequate precision. Run 23 was an outlier in the Cook's distance plot so, to improve fit statistics, it was ignored in the absorption capacity analysis.

$$\frac{1}{\sqrt{Absorption\ Capacity}} = 0.0311 + 0.0057A + 0.0075B - 0.0004C + 0.0001D + 0.0047AB + 0.0012CD - 0.0032A^2 -$$
$$0.0061B^2 \hspace{10cm} (15)$$
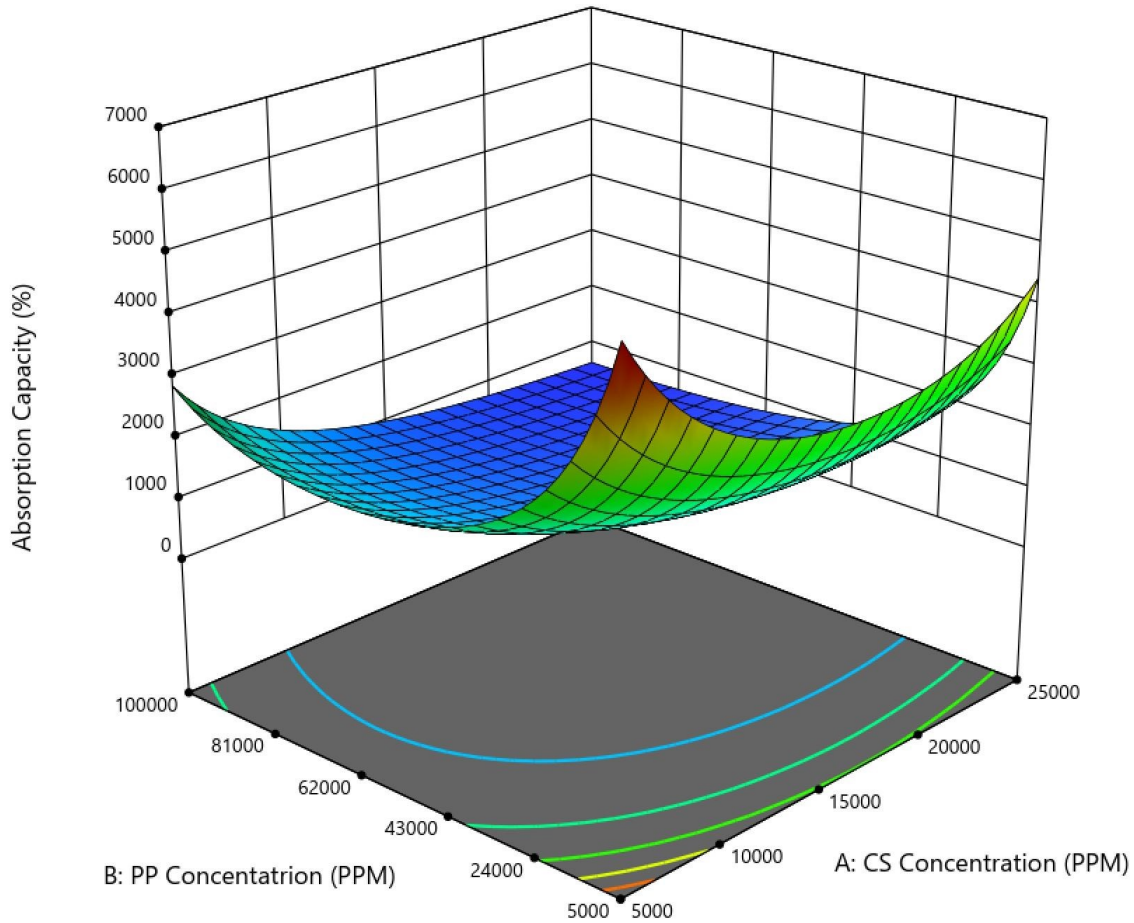
Figure 15 - 3D response surface for absorption capacity.

4.4.7 Elution Profiles

Elution profiles for both copper and phosphorous were relatively consistent for all runs with varying magnitudes. The mean elution profiles across all runs can be seen in Figure 16. The elution data for the 10-, 30- and 90-minute responses were not conducive to statistically significant models so predictive models were only made for the 24-hour elution responses. Because the intended application is a 24-hour period and the elution media used for other responses is 24-hour elution media, it was deemed that only the 24-hour responses were truly necessary for optimization. A reduced quadratic model with a natural log transform was generated to predict 24-hour copper elution. The coded equation can be seen in Eq. (16), with the corresponding 3D response surface shown in Figure 17. The model was statistically

55

significant with a model F-value of 15.03, model P-value of <0.0001 and P-values that indicate model terms A, B, C, A^2 and D^2 were significant. Adjusted R^2 and predicted R^2 were within reasonable agreement at 0.7612 and 0.6528, and the signal to noise ratio was 15.2803, indicating adequate precision. The diagnostic plots showed no obvious outliers. A reduced quadratic model was also generated to predict 24-hour phosphorous elution. The coded equation can be seen in Eq. (17), with the corresponding 3D response surface displayed in Figure 18. The model was statistically significant with a model F-value of 22.42, model P-value of <0.0001 and P-values that indicate model terms B, D, AB, AC, BD and C2 were significant. Adjusted R^2 and predicted R^2 were within reasonable agreement at 0.0.9146 and 0.7599, and the signal to noise ratio was 12.5919 indicating adequate precision. To achieve a model with adequate R^2 agreement, runs 6 and 19 were ignored in the 24-hour phosphorous elution analysis.
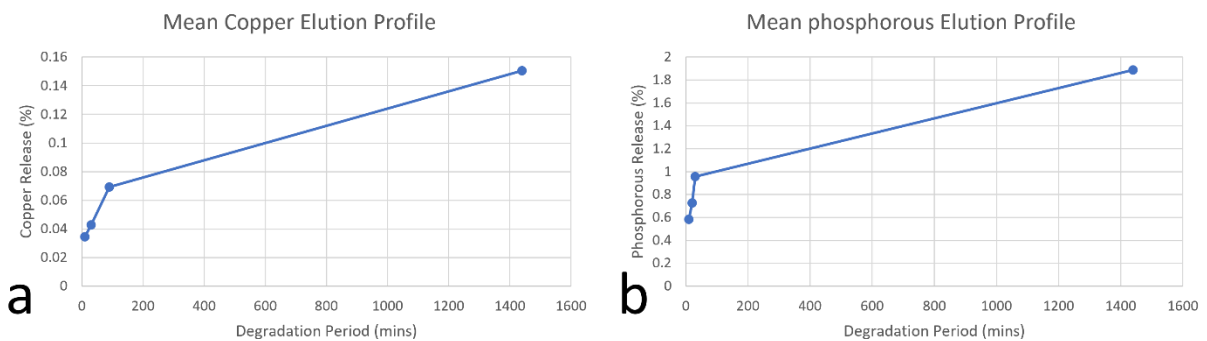
Figure 16 - Mean copper elution profile (a) and mean phosphorous elution profile (b) across all runs.

$$ln(Copper\ Elution\ 24h) = -2.28 - 0.4820A - 0.3381B + 0.8632C + 0.6000A^2 - 0.7905C\verb|^|2 \qquad (16)$$
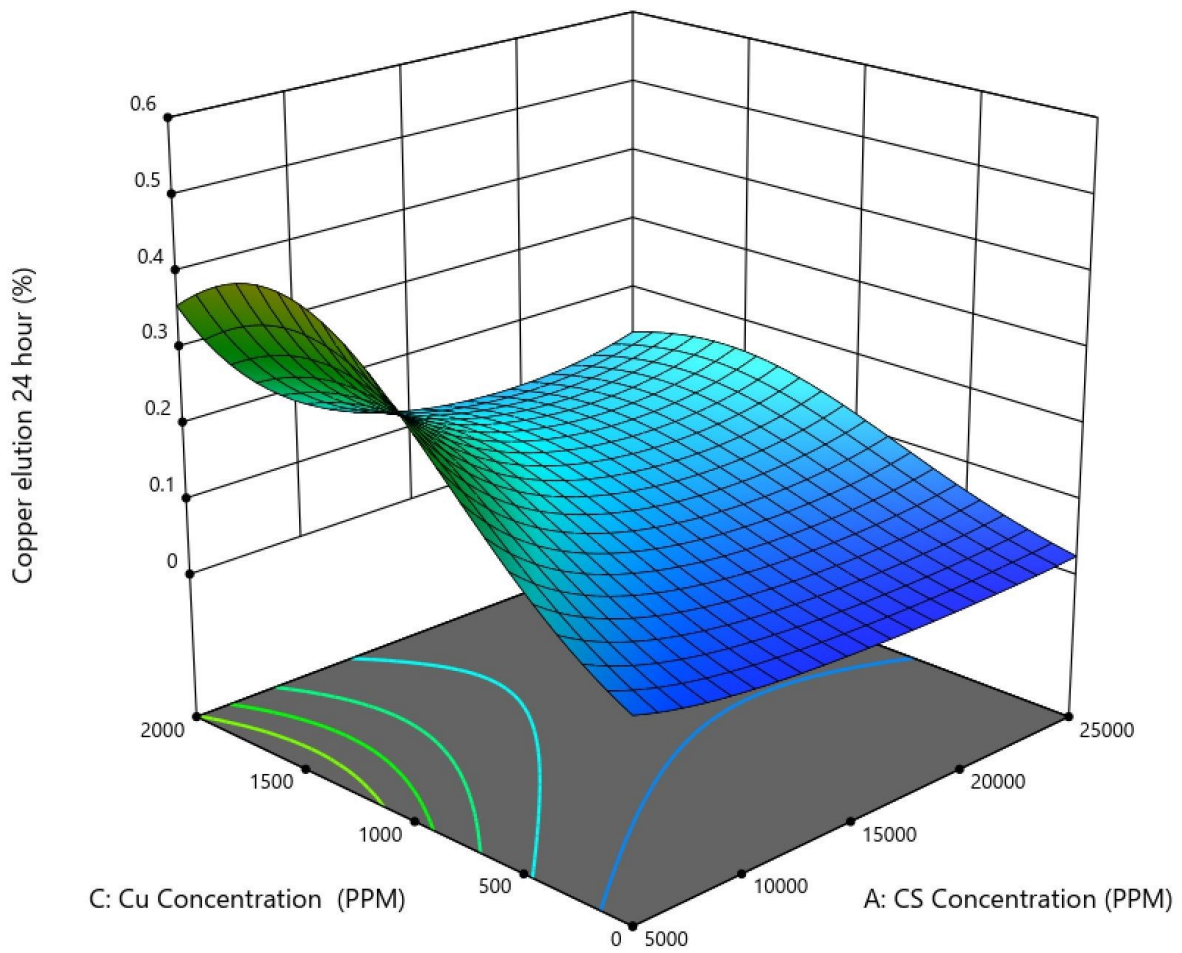
Figure 17 - 3D response surface for 24-hour copper elution.

$Phosphorous\ Elution\ 24h = -2.43 - 0.0454A - 0.3708B + 0.1089C + 0.2293D + 0.6046AB + 0.2546AC - 0.1437AD + 0.4123BD - 0.2486B^2 - 0.7622C\textasciicircum 2$ (17)
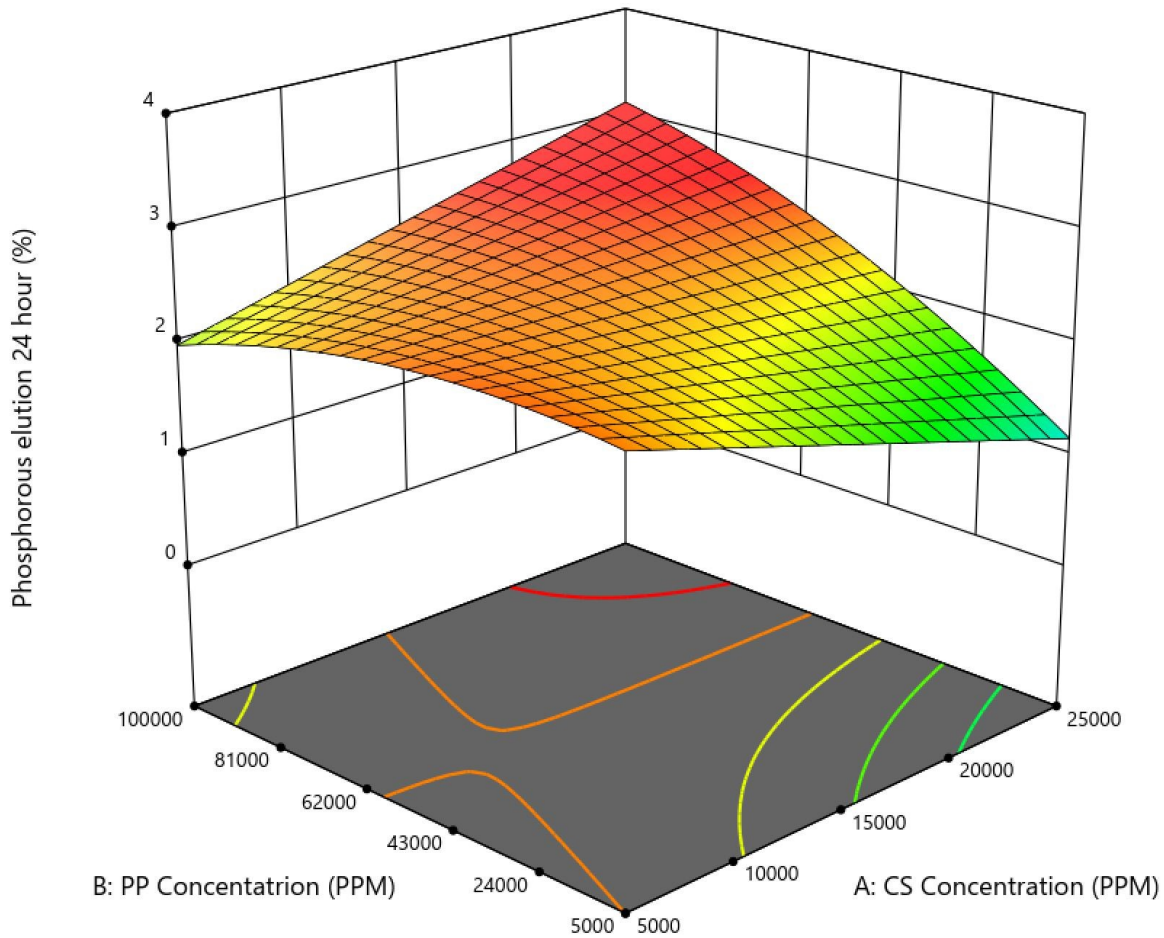
Figure 18 - 3D response surface for 24-hour phosphorous elution.

4.4.8 Blood Clotting Index

Blood clotting index across all runs ranged from 39.80 to 80.17%, with a mean of 63.21%. A reduced quadratic model was generated to predict blood clotting index. The coded equation can be seen in Eq. (18), with the corresponding 3D response surface displayed in Figure 19. The model was statistically significant with a model F-value of 3.41, model P-value of 0.0321 and P-values that indicate model terms AC and C^2 were significant. Adjusted R^2 and predicted R^2 were within reasonable agreement at 0.3143 and 0.2036, and the signal to noise ratio was 6.3408 indicating adequate precision. Run 12 was an outlier in the residual and Cook's distance plots so, to improve fit statistics, it was ignored in the blood clotting index analysis.

$$Blood\ Clotting\ Index = 56.70 - 2.38A - 0.9057C - 10.28AC + 10.13C^2 \tag{18}$$

58
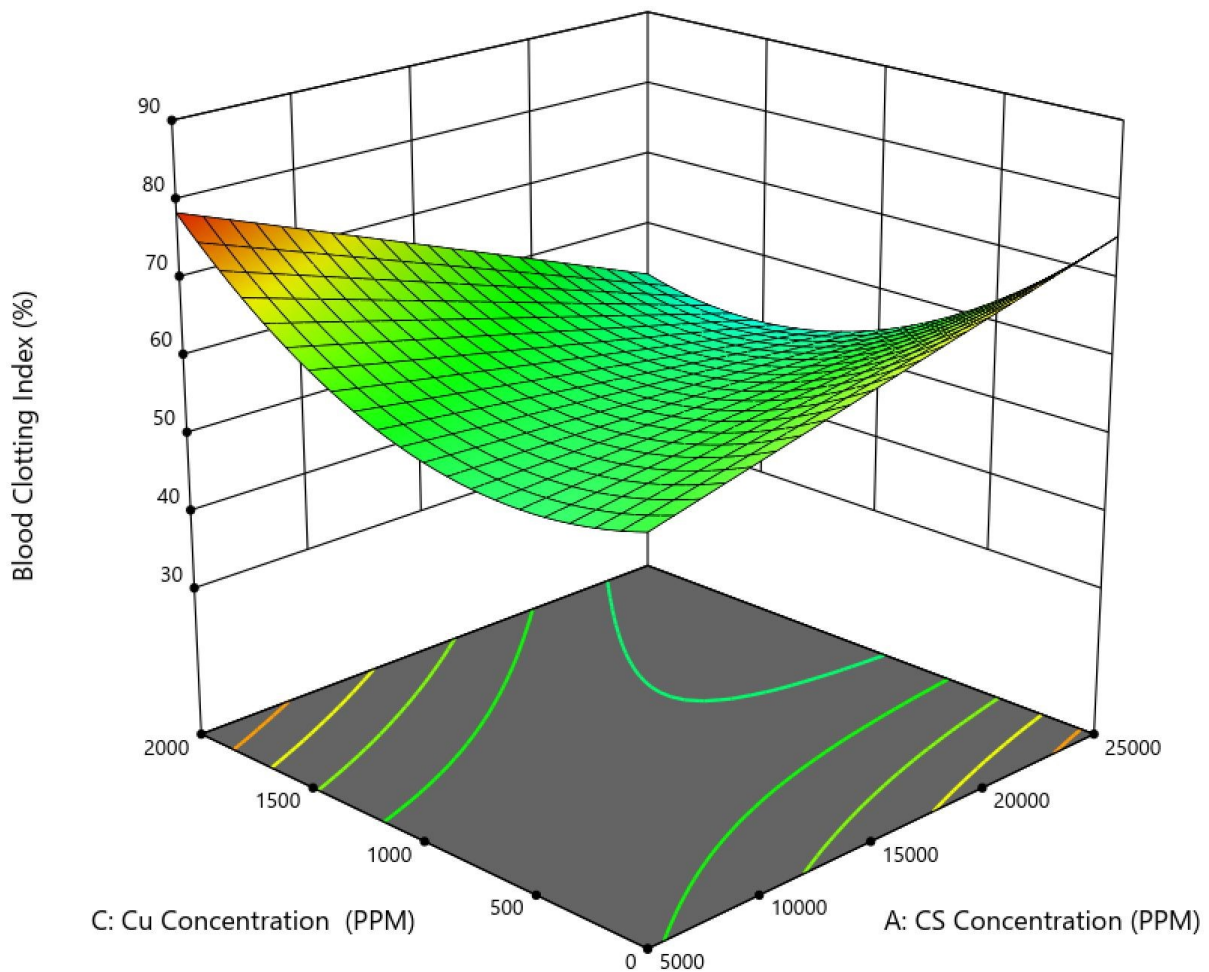
Figure 19 - 3D response surface for blood clotting index.

4.4.9 Cytotoxic Concentration

Cytotoxic concentration across all runs ranged from 0 to 20 mg/mL, with a mean of 8.5 mg/mL. A reduced quadratic model with a square root transform was generated to predict cytotoxic concentration. The coded equation can be seen in Eq. (19), and the corresponding 3D response surface is displayed in Figure 20. The graph makes it clear that higher copper and lower PP concentrations result in cytotoxicity, which aligns with the copper content trend. The model was statistically significant with a model F-value of 6.55, model P-value of 0.002 and P-values that indicate model terms B, C, B^2 and C^2 were significant. Adjusted R^2 and predicted R^2 were within reasonable agreement at 0.5022 and 0.3832, and the signal to noise ratio was 8.2297 indicating adequate precision. The diagnostic plots showed no obvious outliers.

59

$$\sqrt{Cytotoxic\ Concentration} = 2.60 + 0.9027B - 1.15C - 1.36B^2 + 1.50C^2 \qquad\qquad (19)$$
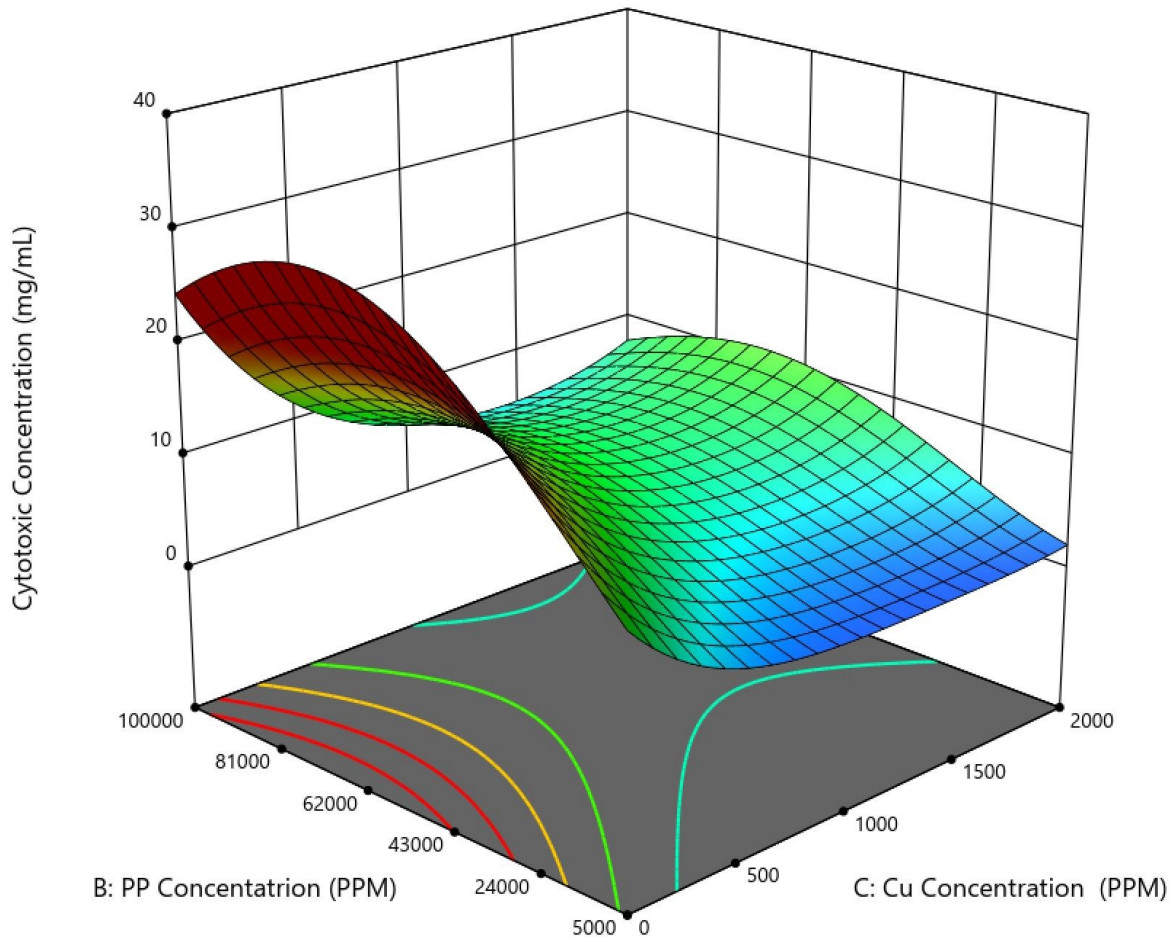
Figure 20 - 3D response surface for cytotoxic concentration.

4.5 Discussion

4.5.1 Correlations

Perhaps one of the best tools for analysis provided by Design-Expert is the correlations table. Using this tool many correlations that help to better understand the material and CS-PP interactions were revealed. Foremost was the observation that PP concentration was the factor with the strongest correlation to the responses measured. This is further supported by the fact that almost every predictive model includes PP concentration as a model term. Perhaps even more interesting to see is that the CS to PP ratio has stronger correlations with the responses

60

than any of the singular factors. This aligns with what was seen during preliminary work and is why CS to PP ratio was included as a response. These correlations are especially strong with the physical property responses, suggesting that having high levels of PP occupying interaction sites on the CS may be contributing to more dense, brittle and fragile material with reduced absorption capacities.

Another interesting correlation is the strong negative correlation between copper and phosphorous content. This makes it very clear that copper being incorporated into the material is doing so through interactions with the CS rather than PP. As the phosphorous content increases copper content falls significantly, suggesting there is competition between copper and PP for interaction sites on the CS. Furthermore, a strong negative correlation is seen between copper content and PP concentration while no significant correlation is seen between phosphorous content and copper concentration, suggesting that PP interactions take priority over copper interactions even though the copper is added to the CS before PP. The most obvious explanation for this strong negative correlation is that, with more PP present, more of the CS amino groups become occupied by PP, displacing the copper and reducing potential interaction sites. Another possibility could be that the increased CS-PP interaction alters the structure of the CS, making interactions between copper and CS less favourable. A final consideration is that an excess of PP may be chelating the copper and keeping it in the supernatant, thus preventing the copper from incorporating into the freeze-dried material. Although it is not entirely clear which of these explanations, if any, are valid, revealing this correlation does offer some insight into CS-PP-copper interactions.

Another important observation from the correlation table was that the only significant correlations with cytotoxic concentration were related to copper levels. Not surprisingly, negative correlations were seen with copper concentration, content, and 24-hour elution. In contrast, a positive correlation was seen with PP concentration, consistent with increased PP content corresponding to lower Cu levels in the material. These correlations support the idea proposed in previous chapters that copper would be the only source of cytotoxicity, since both CS and PP are expected to be biocompatible under these conditions. Unclear is why the correlation with 24-hour elution is not stronger given that the cytotoxicity assay used 24-hour

61

elution media as the treatment media. This suggests there are more variables than just the presence of copper affecting cytotoxicity in this system. One such variable is the polyphosphate that is eluted along with the copper that could be increasing cell metabolic activity or chelating copper which might affect AlamarBlue fluorescence readings.

4.5.2 Predictive models

Analysis of variance tables that report the statistical significances for each predictive model can be seen in Appendix A. One way to interpret the results from the predictive models is to look at the model terms with the most significant effect to understand which factors are influencing any given response the most. This is best done by looking at the significant model terms that have the highest equation coefficients.

For copper content the two highest coefficients were attached to terms B and C (PP and copper concentration). This supports the conclusion drawn from the correlation table that PP and copper are competing for interaction. The fact that term B has a higher negative coefficient than C also supports the notion that PP interactions take priority over copper interactions. For phosphorous content the highest coefficient is attached to term B, not surprising given that one would expect a higher PP concentration to result in more PP inclusion in the material.

Terms A and B (CS and PP concentration) were associated with the highest coefficients for the physical property responses. The CS to PP ratio can be thought of as the ratio of these two terms and thus makes sense that they would be the most significant. Interestingly, Term B coefficient was much higher than A for ease of production, handling properties score and absorption capacity. This indicates that for these responses, PP concentration has a more significant impact than CS concentration suggesting that, even if the CS to PP ratio is the same, higher concentrations of PP can be a detriment to the physical properties of the material. The coefficients associated with terms A and B as they relate to apparent density, on the other hand, are almost identical. The conclusion here is that the CS to PP ratio is what really determines density, regardless of the specific concentrations.

Both copper and phosphorous elution profiles appear to mimic the shape of a radical function. Although only 4 time points were included, it is clear there is an initial burst release

that then appears to taper off the longer the sample remains in degradation media. This burst release is likely due to copper and PP that has been physically incorporated during processing rather than through direct interactions with the CS, with subsequent release associated with material degradation that continues to slow down as the weaker bonds are broken down, leaving behind increasingly stable bonds. The model equations for copper and phosphorous 24-hour elution also revealed some interesting results. Term A (CS concentration) was a significant model term with a relatively high coefficient for copper elution even though it was not a significant term for copper content. This suggests the CS concentration is somehow influencing the degradation characteristics of the material as this change in copper elution is not a result of a change in copper content. Similarly, Term C (copper concentration) was a significant model term for phosphorous elution even though it was not significant for phosphorous content. So again, it is possible that copper concentration is also influencing degradation characteristics.

It is difficult to draw many specific conclusions from the blood clotting index and cytotoxic concentration model equations as they have inferior statistical power when compared to the other models. This outcome was not unexpected since biological responses can have inherently sharp response curves and high variability even when meticulously controlled. For example, cells can be treated with effectively the exact same conditions and yet still behave differently [92]. Regardless, some interesting information could still be drawn from these models. The model equation for blood clotting index does not include term B (PP concentration), somewhat surprising given that PP was included to enhance hemostatic effects. One possible explanation is that the PP levels required to achieve any benefit have already been met and exceeded, noting that for all runs phosphorous levels between 6.543 and 13.464% were measured. For cytotoxic concentration, only terms that are related to the copper content are significant and the highest coefficient is attached to copper concentration. This further validates that any cytotoxicity associated with these materials is due to the copper.

Chapter 5: Optimization, Validation and Verification

5.1 Introduction

Having successfully generated statistically significant predictive models for all the key responses, the next objective was to optimize the material for the intended application. Using Design-Expert, optimization criteria that includes response goal, acceptable lower and upper limit, and importance level must be defined for each of the responses. These criteria were selected based on the design inputs for an ideal trauma wound dressing. Design inputs include adequate physical properties, high absorbency, low cytotoxicity, enhanced hemostatic and antibacterial effects as defined in section 1.5.4. The criteria were then combined to create a desirability function which Design-Expert seeks to maximize to determine the best possible combination of factor levels. The desirability function produces a score from 0-1 for each optimized formulation, 0 being a formulation that does not meet any of the criteria, and 1 being a formulation that perfectly achieves all criteria. Because antibacterial effects were not a response in the DoE, and copper was only included in the material to improve antibacterial effects, three optimized material formulations were generated with different optimization criteria for copper related responses. The first was optimized to maximize cell viability while still including copper, the second was optimized to maximize copper content and elution and the third was optimized without including copper. This made it possible to investigate the impact of copper on the material's antibacterial effects using the results from the antibacterial assay in the verification stage.

The added benefit of optimizing three sample formulations was that each could be used to validate the predictive models. Each optimized sample was synthesized following the standard operating procedure defined for the DoE and characterized for the same responses using the same methods as previously described. The results were then compared to the predicted response levels to ensure the values fell within the prediction tolerance for each response; having three samples available greatly increased the confidence of the validation. With the predictive models validated, the final goal of the research project was to verify the effectiveness of the material as a trauma wound dressing. To achieve this goal, the three

optimized materials were compared to a commercial trauma wound dressing (Celox™) and a CS-only freeze-dried material. Absorption capacity, cytotoxicity, hemostatic potential and antibacterial effects were all evaluated *in vitro* as an indication of how the material would perform in a trauma wound dressing application relative to Celox™ and the CS-only mesh.

5.2 Generating Optimized Materials

5.2.1 Optimization Criteria

To generate the three optimized materials, three sets of optimization criteria had to be defined with the objective for copper-related responses in mind. These criteria were identical for all the responses other than copper content, 24-hour copper elution and cytotoxic concentration and can be seen in Table 5, Table 6 and Table 7, respectively. Phosphorous content and 24-hour P elution were not given an optimization goal because none of the design inputs relate to a specific level of PP, only that PP is included. For ease of production, the goal was to maximize this response since an easier production protocol is always desired. However, this does not directly affect the performance of the material, so the importance level was set at the minimum of 1. Handling properties were also maximized and the importance level left neutral at 3; a minimum score of 1.75 was set because a score of 1 would not provide adequate physical properties. Apparent Density was minimized since a lower density should correlate to higher surface area, increasing interaction with the material. The importance level was left neutral because apparent density only indirectly correlates to the design inputs. The most important response for optimization is to maximize the absorption capacity since it directly effects the physical and hemostatic properties of the material; the importance level was therefore assigned the highest value of 5. With respect to hemostasis, the blood clotting index was minimized since this is indicative of more extensive clot formation. However, its importance was left neutral despite the obvious desire for enhanced hemostasis as a design input because the predictive power for this response was low and increasing importance could overly influence the resulting material formulation.

Margin of safety is a response that was introduced at this stage to ensure the expected exposure from the optimized material would not exceed the permitted daily parenteral

exposure of 340 µg/day as defined in the European Medicines Agency guideline on elemental impurities [93]. This permitted daily exposure was determined based on data from rat studies with modification factors F1, F2 and F3 applied to relate the data to humans. F1 was a factor of 5 to extrapolate from rat to human, F2 was 10 to account for variability between individuals and F3 was 5 to account for short-term study effects [93]. Expected exposure was calculated assuming a 5 cm^3 "dose" of material and using the apparent density and 24-hour copper elution data. Margin of safety was calculated by dividing the expected exposure by the permitted daily exposure, which should always remain greater than 1 [94]. To ensure the margin of safety remains greater than 1, the acceptable lower limit was set at 1 and the goal was set to remain within range.

The optimization criteria for the first optimized material can be seen in Table 5. The aim was to maximize cytotoxic concentration first and foremost while still attempting to maximize copper content and 24-hour Cu elution to enhance antibacterial properties. To reflect this bias, the importance levels for copper content and copper elution were set very low at 2 (accounting for the fact that there were two responses concerned with increase Cu), while that for cytotoxic concentration was set at the maximum level of 5 since it was the only response limiting copper inclusion and release.

The second optimized material (Table 6) aimed to maximize copper content and elution while maintaining a minimum cytotoxic concentration of 5 mg/mL. The intent here was to investigate if increased copper would greatly improve the antibacterial response of these CS-PP wound dressing. Adding the lower limit of 5 mg/mL ensured the material would have acceptable minimum cytocompatibility for trauma wound applications. Accordingly, the importance levels for copper content and 24-hour Cu elution were increased to 4 (but not 5, since once again there would be two responses contributing to higher Cu levels).

The third optimized material (Table 7) excluded copper entirely, allowing cytotoxic concentration to be maximized without any trade-offs from trying to maximize copper simultaneously. This material formulation effectively served as an internal control to determine whether including copper had any significant benefits, specifically surrounding antibacterial

effects, since this had not been confirmed to this point. To do this, copper solution

concentration was set to 0 so no goal was needed for copper content or 24-hour Cu elution.

Table 5 - Optimized sample number 1 with criteria selected to maximize cell viability while still including copper.

Sample 1 - Optimized for maximum cell viability with copper included						
Response	Goal	Lower limit	Upper limit	Lower Weight	Upper Weight	Importance
A:CS Concentration	is in range	5000	25000	1	1	N/A
B:PP Concentatrion	is in range	5000	100000	1	1	N/A
C:Cu Concentration	is in range	0	2000	1	1	N/A
D:Polyphosphate Degree of Polymerization	is in range	20	180	1	1	N/A
Copper Content	maximize	0.007	6.61	1	1	2
Phosphorous Content	none	6.543	13.464	1	1	N/A
Ease of Production	maximize	1	3	1	1	1
Handling Properties Score	maximize	1.75	3	1	1	3
Apparent Density	minimize	0.0171	0.136	1	1	3
Percent Water Absorption	maximize	565	5673	1	1	5
Copper elution 24 hour	maximize	0.013	0.567	1	1	2
Phosphorous elution 24 hour	none	0.537	2.734	1	1	N/A
Blood Clotting Index	minimize	39.8	80.17	1	1	3
Cytotoxic Concentration	maximize	5	20	1	1	5
Margin of Safety	is in range	1	4.84	1	1	N/A

Table 6 - Optimized sample number 2 with criteria selected to maximize copper content and elution.

Sample 2 - Optimized for maximum copper						
Response	Goal	Lower limit	Upper limit	Lower Weight	Upper Weight	Importance
A:CS Concentration	is in range	5000	25000	1	1	N/A
B:PP Concentatrion	is in range	5000	100000	1	1	N/A
C:Cu Concentration	is in range	0	2000	1	1	N/A
D:Polyphosphate Degree of Polymerization	is in range	20	180	1	1	N/A
Copper Content	maximize	0.007	6.61	1	1	4
Phosphorous Content	none	6.543	13.464	1	1	N/A
Ease of Production	maximize	1	3	1	1	1
Handling Properties Score	maximize	1.75	3	1	1	3
Apparent Density	minimize	0.0171	0.136	1	1	3
Percent Water Absorption	maximize	565	5673	1	1	5
Copper elution 24 hour	maximize	0.013	0.567	1	1	4
Phosphorous elution 24 hour	none	0.537	2.734	1	1	N/A
Blood Clotting Index	minimize	39.8	80.17	1	1	3
Cytotoxic Concentration	is in range	5	20	1	1	N/A
Margin of Safety	is in range	1	4.84	1	1	N/A

Table 7 - Optimized sample number 3 with criteria selected to optimize the material without including copper.

Sample 3 - Optimized with no copper						
Response	Goal	Lower limit	Upper limit	Lower Weight	Upper Weight	Importance
A:CS Concentration	is in range	5000	25000	1	1	N/A
B:PP Concentratrion	is in range	5000	100000	1	1	N/A
C:Cu Concentration	is equal to 0	0	2000	1	1	N/A
D:Polyphosphate Degree of Polymerization	is in range	20	180	1	1	N/A
Copper Content	none	0.007	6.61	1	1	N/A
Phosphorous Content	none	6.543	13.464	1	1	N/A
Ease of Production	maximize	1	3	1	1	1
Handling Properties Score	maximize	1.75	3	1	1	3
Apparent Density	minimize	0.0171	0.136	1	1	3
Percent Water Absorption	maximize	565	5673	1	1	5
Copper elution 24 hour	none	0.013	0.567	1	1	N/A
Phosphorous elution 24 hour	none	0.537	2.734	1	1	N/A
Blood Clotting Index	minimize	39.8	80.17	1	1	3
Cytotoxic Concentration	maximize	5	20	1	1	5
Margin of Safety	none	1	4.84	1	1	N/A

5.2.2 Optimized Material Formulations

With the optimization criteria defined for each sample, the three optimized material formulations were generated. The formulations with the highest desirability score for each optimization criteria were selected and are defined in Table 8, with the corresponding predicted response levels shown in Table 9. Samples for the three optimized material formulations were then synthesized following the standard operating procedure described in Section 3.4 (Figure 21).

Table 8 - Factor levels and desirability score for the three optimized materials.

Optimized Material	CS Concentration (PPM)	PP Concentration (PPM)	Cu Concentration (PPM)	Polyphosphate Degree of Polymerization	Desirability
1	23713.034	5000.177	211.614	180	0.482
2	21553.973	5000.029	976.88	180	0.581
3	5000	100000	0	20	0.567

Table 9 - Predicted response levels for the three optimized materials.

Optimized Material	Copper Content (%)	Phosphorous Content (%)	Ease of Production Score	Handling Properties Score	Apparent Density (g/cm³)	Absorption Capacity (%)	Copper Elution 24 hour (%)	Phosphorous Elution 24 hour (%)	Blood Clotting Index	Cytotoxic Concentration (mg/mL)	Desirability
1	1.645	8.162	1.360	2.701	0.016	4101.616	0.102	0.371	68.403	9.114	0.482
2	4.837	8.301	1.328	2.986	0.026	3881.568	0.167	1.075	59.646	5.000	0.581
3	0.057	9.806	2.152	2.070	0.044	2469.366	0.103	0.686	45.480	17.867	0.567
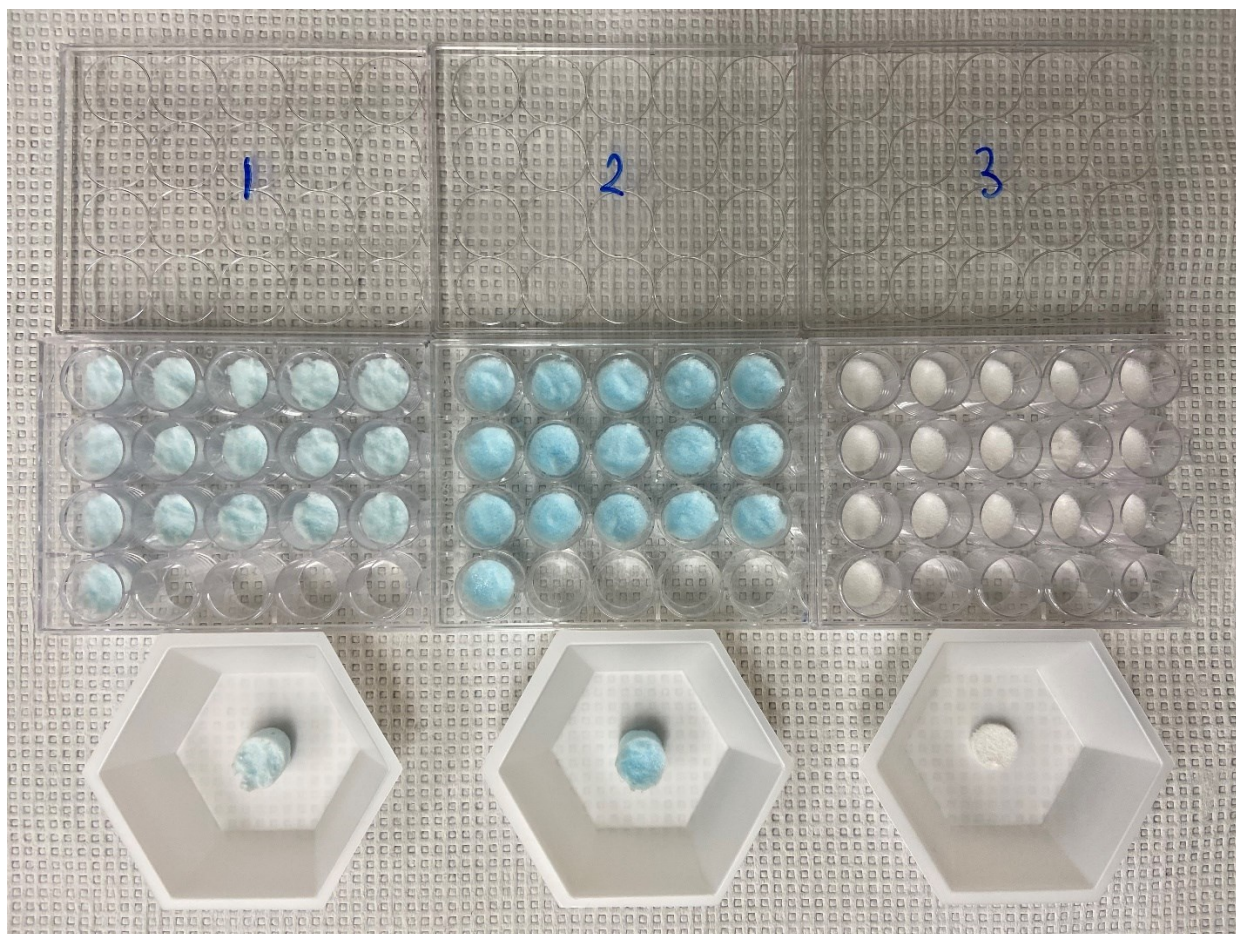
Figure 21 - Synthesized sample batches for the three optimized materials.

5.3 Validating Predictive Models

After successfully synthesizing the three optimized materials, the samples were characterized for each of the DoE responses using the same methods described in section 4.3. The measured response levels were then compared to the predicted levels and their tolerance ranges described in Table 10, Table 11 and Table 12 for the three formulations. All the measured response levels fell within the prediction tolerance ranges apart from blood clotting index for formulation 2, indicating that all predictive models other than the blood clotting index can be considered valid. This was not entirely unexpected, as the blood clotting index model displayed the worst results with respect to analysis of variance of any of the models.

Table 10 - Predicted level, tolerance range and measured levels of the responses for the first optimized material.

Responses	Copper Content ($)	Phosphorous Content (%)	Ease of Production Score	Handling Properties Score	Apparent Density (g/cm³)	Absorption Capacity (%)	Copper Elution 24 hour (%)	Phosphorous Elution 24 hour (%)	Blood Clotting Index	Cytotoxic Concentration (mg/mL)
					Optimized Material 1					
Predicted level	1.838	8.162	1.164	2.702	0.0165	4374	0.051	0.202	68.69	6.22
Tolerance range	0.672-3.468	5.964-10.360	0.501-1.827	1.759-3.644	0-0.0402	2446-8768	0.016-0.132	0-0.830	48.47-88.92	0-24.92
Measured level	1.254	9.494	1	3	0.0219	4474	0.031	0.476	54.63	13.75

Table 11 - Predicted level, tolerance range and measured levels of the responses for the second optimized material.

Responses	Copper Content ($)	Phosphorous Content (%)	Ease of Production Score	Handling Properties Score	Apparent Density (g/cm³)	Absorption Capacity (%)	Copper Elution 24 hour (%)	Phosphorous Elution 24 hour (%)	Blood Clotting Index	Cytotoxic Concentration (mg/mL)
					Optimized Material 2					
Predicted level	4.858	8.301	1.275	2.986	0.0264	3611	0.147	1.1	55.32	1.6
Tolerance range	2.913-7.199	6.142-10.459	0.633-1.917	2.112-3.861	0.0041-0.0487	2165-6508	0.048-0.368	0.502-1.699	36.50-74.14	0-9.95
Measured level	3.861	8.247	1	3	0.0172	5961	0.073	0.789	31.64	3.75

Table 12 - Predicted level, tolerance range and measured levels of the responses for the third optimized material.

Responses	Copper Content ($)	Phosphorous Content (%)	Ease of Production Score	Handling Properties Score	Apparent Density (g/cm³)	Absorption Capacity (%)	Copper Elution 24 hour (%)	Phosphorous Elution 24 hour (%)	Blood Clotting Index	Cytotoxic Concentration (mg/mL)
					Optimized Material 3					
Predicted level	0.052	9.806	2.212	2.07	0.0439	2438	0.046	0.591	59.83	24.51
Tolerance range	0-0.421	7.504-12.108	1.527-2.898	1.067-3.073	0.0191-0.0688	1531-4191	0.014-0.124	0-1.264	38.82-80.84	3.63-59.26
Measured level	0.052	11.209	2	2	0.0282	2784	0.063	0.892	56.76	20

5.4 Verifying Effectiveness

5.4.1 Methods

To verify the potential effectiveness of the optimized materials as trauma wound dressings, the three formulations, designated as Sample Group 1, 2 and 3, were compared to a commercial trauma wound dressing (Celox™) and a freeze-dried material made of only CS. The responses used for comparison included absorption capacity, cytotoxic concentration and the blood clotting index considered for the DoE and described in Section 4.3. Additionally, an activated partial thromboplastin time (aPTT) and antibacterial suspension assay were conducted to further investigate the hemostatic and antibacterial potential of the optimized materials. aPTT was chosen as an additional means to characterize hemostasis as it is a well-established assay that measures clotting activity through the contact pathway, which PP is purported to accelerate [95]. The antibacterial suspension assay used was meant to be included in the DoE; however, the results were not suitable for modelling due incorrect sample concentrations. Instead, only *S. aureus* was used and the methodology was refined based on what was learned

from the DoE tests and applied during the verification stage. All assays included three replicates for each sample group (technical replicates), however, the cytotoxicity and antibacterial assay, also included two biological replicates, meaning the tests were repeated on separate days with distinct cell and bacteria samples. The methodology used for these additional assays are described below. To determine whether the differences between groups were significant for each response, paired two tailed T-tests were used.

Activated Partial Thromboplastin Time

The aPTT assay was adapted from Buriuli et al., Momeni et al. and Weber et al. [36, 73, 96]. In a 15 mL Falcon tube, an approximately 0.125 cm^3 piece of sample was added to 0.3 mL of platelet poor plasma (CCN-10, PrecisionBiologic) and held in a 37 °C water bath for 10 minutes. Subsequently, 0.1 mL of the treated plasma was removed and added to a new 15 mL falcon tube along with 0.1 mL of QuikCoag^{TM} aPTT-EA reagent (C.BMD.APTT, BioMedica Diagnostics) and incubated in a 37 °C water bath for another 3 minutes. 0.1 mL of 0.02 M calcium chloride solution at 37 °C was then added to the tube and the timer was started immediately. The mixture was visually monitored for liquid flow while gently rolling the falcon tube. Once liquid flow was no longer detected the timer was stopped and the time was recorded as the clotting time in seconds. The negative control group was untreated platelet poor plasma.

Antibacterial Assay

A colony forming unit (CFU) direct contact antibacterial suspension assay adapted from the ASTM E2149-13a standards was used to measure the antibacterial potential [97]. To prepare the bacterial suspension a tryptic soy broth agar plate was streaked with a frozen stock of *S. Aureus* (SA 5121, ATCC) and left to incubate at 37 °C for 24 hours. Three colonies were then isolated and scraped using a dip stick, then dipped into separate 10 mL culture tubes containing 5 mL of tryptic soy broth stock followed by another 24-hour incubation period. Subsequently, the bacteria stocks were combined in a 50 mL Falcon tube and vortexed. Three 0.2 mL aliquots of the stock were then added to a 96-well plate and the optical density (OD) at 600 nm was measured using a Varioskan LUX plate reader. The stock was then diluted to achieve a desired volume (V_{stock}) of bacteria stock with an OD of 0.1 by adding a volume of fresh tryptic soy broth that was calculated using Eq. (20). This diluted bacteria stock represented the prepared

bacterial suspension. 1 mL of the suspension was then added to a culture tube and treated with 2.5 mg/mL of sample. This concentration was selected as it represents a realistic dosage on the lower end for the intended application. Pilot tests also showed that concentrations above 2.5 mg/mL would result in >99.99% kill percentages with no discernible differences between the groups. To prepare the samples, approximately 2.5 ± 0.5 mg of each material were weighed and stored in a 24-well plate. The plate was then put in a UV sterilizer 1 hour prior to use to sterilize the samples and prevent contamination. The culture tubes containing the suspension and the samples were then left to incubate on a shaker table for 24 hours at 37 °C. After this incubation period 0.2 mL of the treated bacteria suspension was pipetted into a 96-well plate. It was then serial diluted by a factor of ten by adding 0.02 mL of the previous dilution to 0.18 mL of phosphate-buffered saline until a dilution of 10^{-7} was reached. 0.02 mL of each dilution from 10^{-2} to 10^{-7} was spot plated on a tryptic soy broth agar plate and left for a final overnight incubation period at 37 °C. The agar plates were then photographed and the CFU of the least diluted spot plate with 30-300 countable colonies were counted. The negative control group was bacteria suspension without sample addition and the positive control group was bacteria suspension with 5 μL of Ciprofloxacin added. The CFU/mL of each group was calculated using Eq. (21) and the bacteria kill percentage relative to the negative control was calculated using Eq. (22).

$$V_{TSB} = \frac{0.1 \times V_{stock}}{OD} \tag{20}$$

$$\frac{CFU}{mL} = \frac{CFU}{dilution\ factor \times V_{spotted}} \tag{21}$$

$$Kill\ Percentage = \frac{\left(\frac{CFU}{mL}\right)_{neg} - \left(\frac{CFU}{ml}\right)}{\left(\frac{CFU}{mL}\right)_{neg}} \times 100\% \tag{22}$$

5.4.2 Results

Absorption Capacity

The absorption capacity was a measure of how much water by percentage weight the samples could absorb. The measured absorption capacity values for each sample group can be seen in Figure 22. The CS-PP materials all had higher absorption capacities than the Celox™ and CS-only controls.
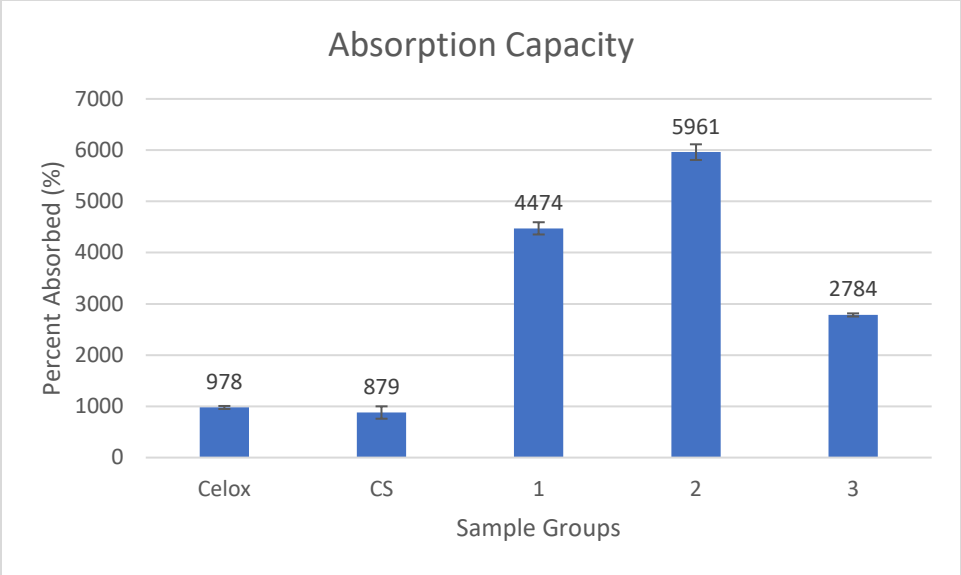
Figure 22 - Bar graph showing the absorption capacity by percentage weight of the samples.

Cytotoxic Concentration

The cytotoxicity assay that was used measured the maximum concentration of sample elution media where >70% cell viability was maintained. The maximum concentration tested was 20 mg/mL because the material formulations were too absorbent to obtain an elution media if more that 40 mg/mL was added. The cytotoxic concentrations for each group can be seen in Figure 23. Material formulation 3 had a cytotoxic concentration similar to Celox™ and CS while material formulations 2 and 3 were lower. A further line plot showing the cell viability at each of the measured elution media concentrations is provided in Figure 24.
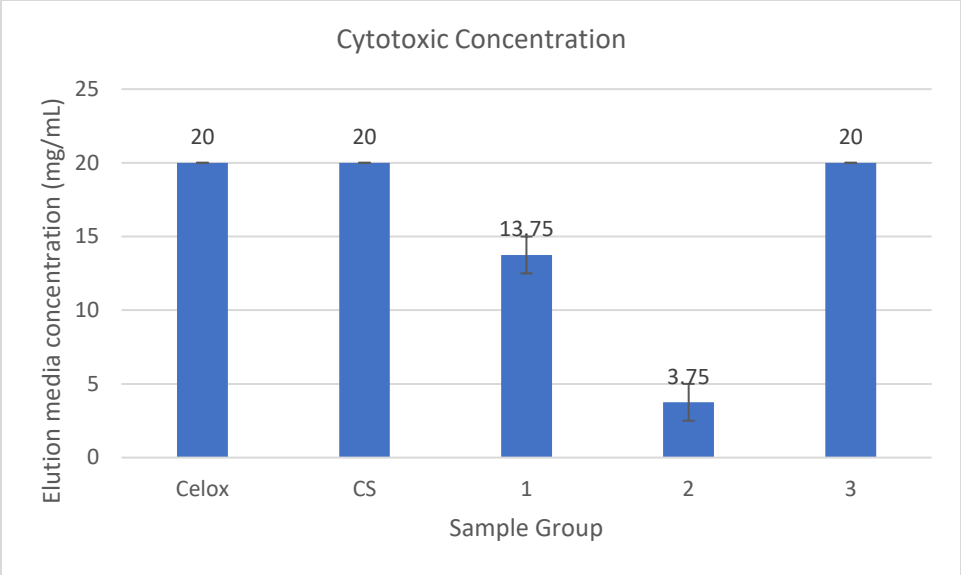
Figure 23 - Bar graph showing the maximum measured elution media concentration where >70% cell viability was maintained.
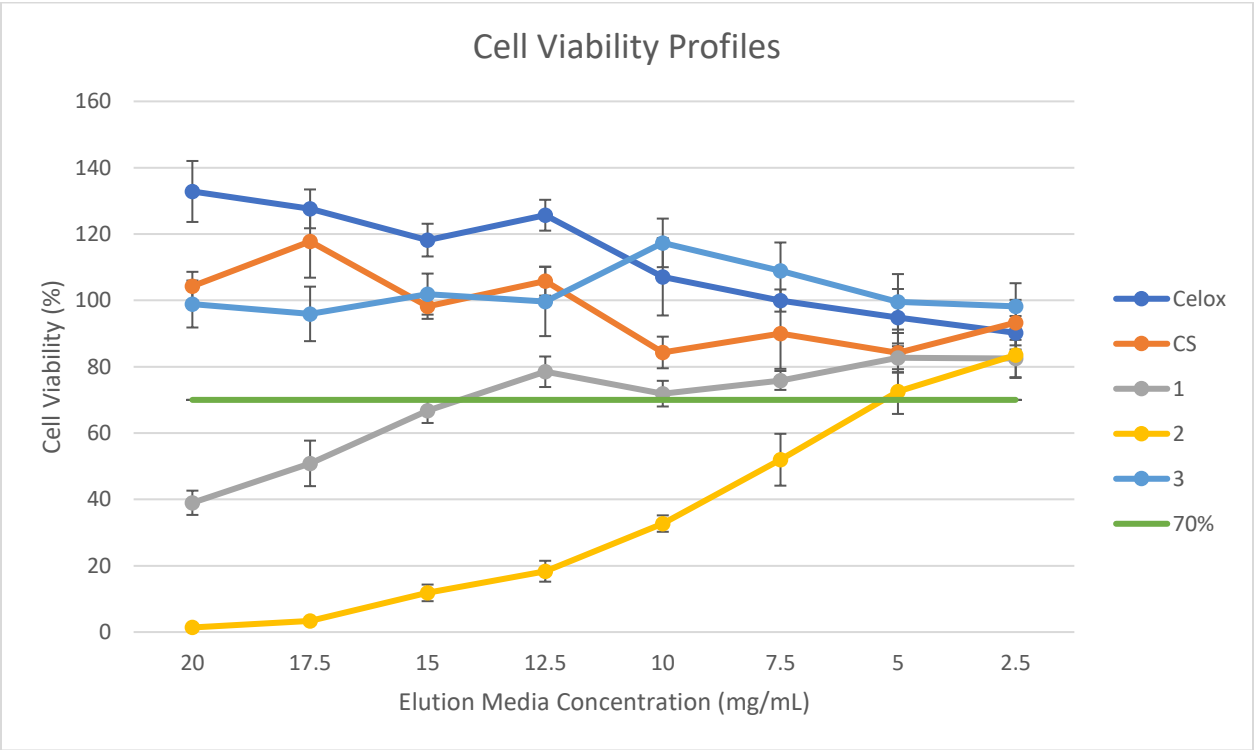
Figure 24 - Line plot showing the cell viability at each of the measured elution media concentrations. The green line denotes the threshold where the elution media is no longer considered cytotoxic.

The whole blood clotting assay measured how much hemoglobin was incorporated into a clot when a sample was added to sheep's blood. The blood clotting index was determined by removing the clot and measuring the remaining hemoglobin relative to whole blood using absorbance readings. An index of 100 would mean no blood clot formation, with a lower blood clotting index indicative of a more developed clot suggesting greater hemostatic effects. The blood clotting indices for each of the groups can be seen in Figure 25. The aPTT assay measured how long it took for a clot to form in platelet poor plasma that had been treated with the sample groups. The times can then be compared to the negative control of untreated platelet poor plasma to determine if the samples improved clotting time. The clotting times for this assay can be seen in Figure 26.
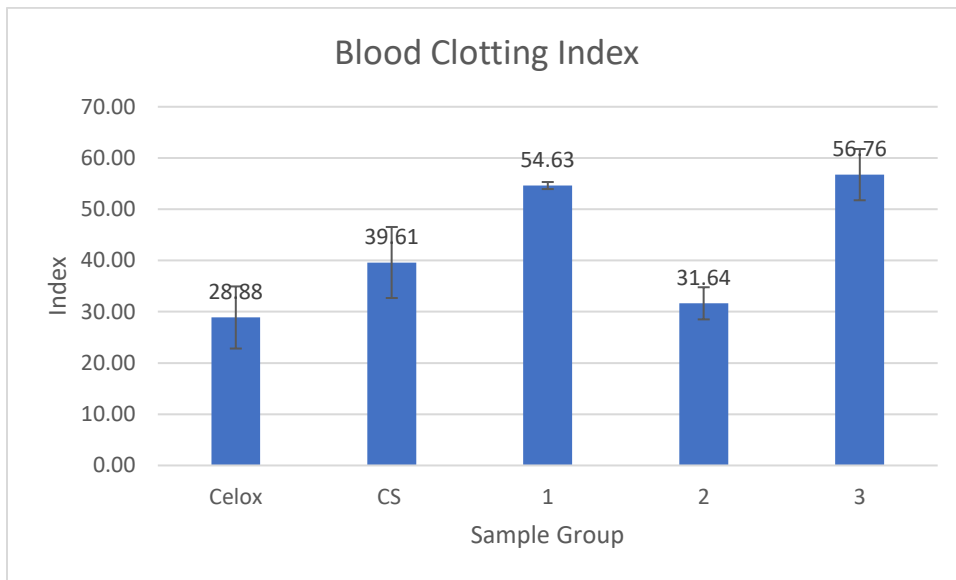
Figure 25 – Bar graph showing the blood clotting indexes for each of the sample groups.
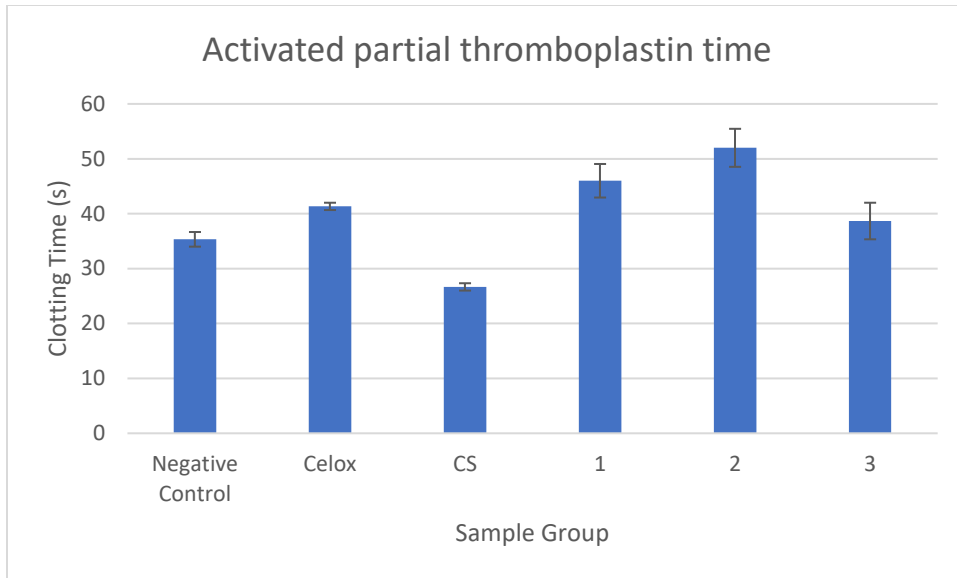
Figure 26 - Bar graph showing the aPTT for each of the sample groups.

Antibacterial Assay

The antibacterial assay measured what percentage of bacteria was killed by submerging the sample in a bacterial suspension. This percentage was determined by how much bacteria remained in suspension after the treatment, relative to how much bacteria remained if the suspension was left untreated. The positive control was 5 µg/mL Ciprofloxacin, which was within the reported peak serum level range after a clinically relevant dosage [98, 99]. Ciprofloxacin had a kill percentage of 99.99%, while all the sample groups exceeded a 95% kill rate (Figure 27).
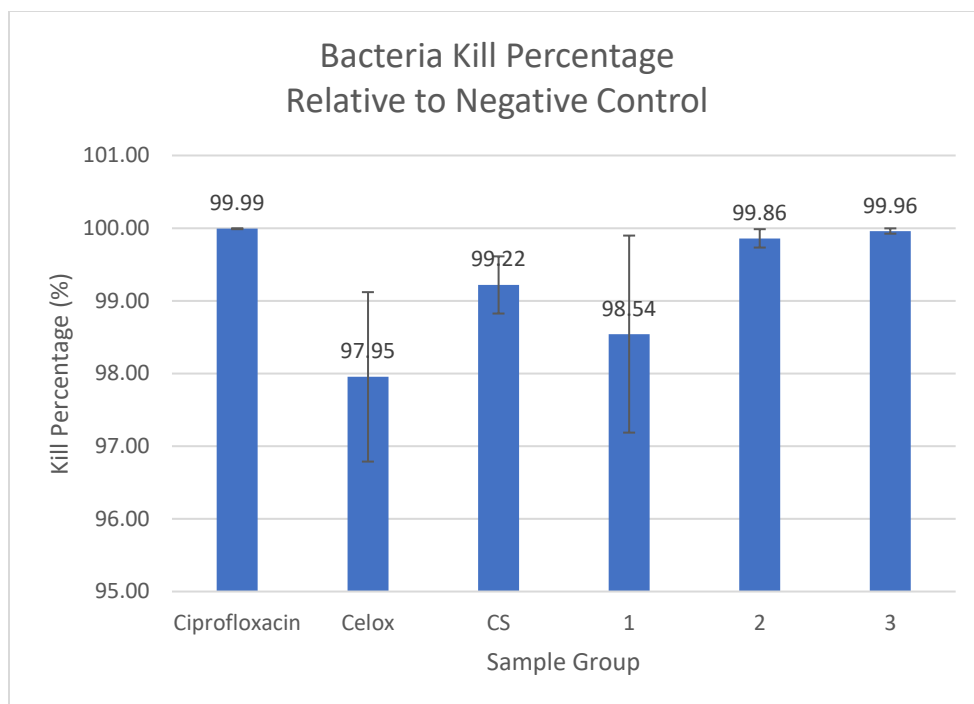
Figure 27 - Bar graph showing the bacteria kill percentage relative to the negative control for each group.

5.4.3 Discussion

Of the properties tested in the verification stage, absorption capacity was the only property where the optimized CS-PP materials clearly and significantly outperformed the Celox™ and CS-only material. All three CS-PP materials had significantly higher absorption capacity than not only the Celox™, but the CS only material as well. The latter result was unexpected since, in the DoE, it was found that higher CS to PP ratios led to materials with higher absorption capacities. This indicates that including PP to some degree enables the CS to absorb more water, possibly by reducing the hydrophobicity of the outer layer of the material and allowing water to absorb throughout the bulk of the material. That being said, formulations 1 and 2 using lower PP concentration still significantly outperformed formulation 3 with respect to absorption capacity, consistent with the results of the DoE.

CS-PP formulations 1 and 2 were cytotoxic at higher concentrations while formulation 3 (no Cu), Celox™ and CS maintained cell viability values above 70% to the maximum sample concentration of 20 mg/mL. It is evident that the copper is responsible for the loss of cell viability since only the materials with copper exhibit any cytotoxicity. Formulation 2 with the

highest Cu content was the most cytotoxic. Because it is unclear how much of the material might be used to pack various wounds in trauma situations, it is important for the material to maintain cytocompatibility at as high a concentration as possible. It should be noted that AlamarBlue is an assay that measures metabolic activity as a marker of cell viability. Thus, cell viability readings greater than 100% do not necessarily mean the material has greater cytocompatibility but could rather just be encouraging more metabolic activity.

None of the CS-PP formulations performed significantly better than Celox™ or CS overall on the coagulation assays. Celox™ and Formulation 2 performed the best on the blood clotting index assay. However, the improved response seen with formulation 2 over the other CS-PP formulations could be mainly due to it having a higher absorption capacity. The CS-only material performed significantly better than the other materials on the aPTT assay and was the only material to induce a clot faster than the untreated platelet poor plasma. This result was unexpected, as PP is thought to accelerate contact pathway initiation and reduce clotting time. Although unexpected, these results were consistent with what was found in literature that performed this assay on similar materials [36, 73]. One explanation for this could be that the PP D_p used in the materials is too low for activation of the contact pathway. Literature suggests that only very long chain PP (many hundreds of phosphate units long) is effective at accelerating contact pathway initiation, while medium chain length PP similar to what is released by platelets (60-100 units) and slightly longer is effective at accelerating Factor V activation [100-102]. The PP used in the CS-PP formulations had mean D_p of either ~160 or ~24, meaning this PP likely would not be effective at accelerating aPTT since it is contact pathway driven. Another explanation could be due to phospholipids in the aPTT agent interacting with the negative charges on the PP. This absence of phospholipids would considerably hinder thrombin formation. In whole blood or *in vivo* this likely would not affect clotting time as phospholipids are abundant on platelets and other blood cells [36]. It is also worth mentioning the potential impact copper cations may have on clotting was not accounted for in these studies. While there have been a few isolated reports of excess Cu interfering with coagulation, no definitive consensus on its impact in this regard was found [103, 104].

The CS-PP materials did appear slightly more effective at killing *S. Aureus* than Celox™ or the CS only material. However, with all materials achieving a >95% kill rate, it is unclear how clinically meaningful this would be in the intended application. Although the copper was included to improve antibacterial effects, it was the optimized formulation with no copper that was most effective at 99.9% effectiveness when compared to the clinically relevant dose of ciprofloxacin. This could be because CS on its own is highly effective at killing *S. Aureus*, so additional copper may not have any effect [105]. Although the results from this assay suggest there is no antibacterial benefits to including copper, it could have major benefits against other bacteria strains. More comprehensive antibacterial testing using various bacteria strains should be conducted before any conclusion about whether copper is worth including is made.

Although the optimized CS-PP formulations did not clearly outperform the commercial competitor Celox™ or CS-only control in the verification stage, they did exhibit potential as an effective trauma wound dressing. Of the three optimized materials, formulation 3 demonstrated the most potential overall. Further testing around hemostatic and antibacterial effects should be conducted to determine whether this material has the potential to greatly improve trauma wound patient outcomes if used in place of the current standard of care.

Chapter 6: Summary and Concluding Remarks

6.1 Study Summary

The overall objective of this thesis was to develop a wound dressing material that would improve the treatment of traumatic hemorrhaging injuries. To achieve this, CS, PP and copper were combined using polyelectrolyte complexation followed by freeze drying to create an absorbent mesh-like material with proposed enhanced hemostatic and antibacterial effects. During preliminary work CS, PP and copper solution concentrations, and PP D_p were identified as the key variable factors for optimization, and a standard operating procedure that yielded consistent and reproducible samples was defined.

A DoE approach was taken to investigate the impact factor levels (processing variables) had on key responses relating to the design inputs of an ideal trauma wound dressing. The relationships between the factors and responses were identified using predictive response surface models enabling optimization of the factor levels to achieve the intended response criteria. Three optimized material formulations were generated under slightly different optimization criteria for copper-related responses so the benefit of copper could be investigated. The predictive power of the DoE was validated for all but one response by confirming that the measured response values of the resulting optimized formulations fell within prediction tolerances. Their potential effectiveness as trauma wound dressings was assessed by comparing the optimized materials to Celox™, a commercial wound dressing, and a CS-only mesh. Although it was not clear that the CS-PP materials were superior to Celox™ or CS based on the tests that were run, they did clearly exhibit potential for the foundation of a superior trauma wound dressing.

6.2 Hypotheses Revisited

Hypothesis 1: CS, PP and Copper solution concentrations will have the biggest impact on material properties while other process variables will have little to no impact.

CS, PP and copper solution concentrations had the biggest impact on material properties of any process variable tested. As such, these variables along with PP D_p were used as the factors for the DoE.

Hypothesis 2: **The product arising from the standard operating procedure will display consistent appearance, handling properties, absorption capacity, chemical composition and elution profiles for samples produced using the same formulation, independent of the operator.**

Samples made following the standard operating procedure with the same material formulation showed no statistical differences in appearance, handling properties, absorption capacity, chemical composition and elution profiles, irrespective of the operator tasked with synthesizing.

Hypothesis 3: **Predictive models will be statistically robust enough to allow for optimization of response levels within the design space.**

Predictive models capable of optimization were successfully generated for copper and phosphorous content, ease of production, handling properties, apparent density, absorption capacity, 24-hour Cu and P elution, blood clotting index and cytotoxic concentration.

Hypothesis 4: **The measured response levels for the optimized material formulations will fall within the accepted prediction tolerances thereby validating the predictive models.**

Of the measured response levels for the three optimized materials, all values fell within prediction tolerances apart from blood clotting index for material formulation 2. This validated all responses other than blood clotting index as effective predictive models.

Hypothesis 5: **Due to the inclusion of CS and copper for antibacterial effects and PP and CS for hemostatic effects, an optimized material formulation comprised of CS, PP and Cu will demonstrate greater antibacterial and hemostatic capacity when compared to a commercial trauma wound dressing in vitro. This material formulation will also demonstrate comparable cytotoxicity.**

When compared to Celox™ and a CS-only mesh, the optimized CS-PP formulations demonstrated increased antibacterial effects. However, it is unclear how impactful this would be for the intended application. The CS-PP materials did not demonstrate significantly greater hemostatic capacity, and only formulation 3 demonstrated comparable cytotoxicity. As anticipated, formulations that included copper had greater cytotoxicity.

6.3 Study Limitations

6.3.1 Factors

In order to keep the design space to a manageable size and not exceed time constraints for this project, various limitations were involved in the factor selection. One such limitation was the use of only 3 continuous factors and a categoric factor. Including more process variables as factors could have resulted in better optimization results. However, in doing so the number of sample runs would have increased beyond what was feasible to complete within the time frame for this thesis project. This limitation was mitigated by thoroughly testing the production protocol during preliminary work to determine which process variables demonstrated the most impact and thus were best suited as factors for the DoE. Treating PP D_p as a categoric factor limited the value of this factor as there weren't any significant findings related to PP D_p while still increasing the number of samples significantly. Unfortunately, it was not possible to include PP D_p as a continuous factor because the D_p cannot be precisely and reliably controlled to the degree that is necessary for a DoE. Had PP D_p been a continuous factor, it is likely that much more could have been revealed about its polyelectrolyte interactions as well as information on what D_p may have been most effective with respect to hemostasis. Additionally, PP with a D_p between 60-100 units and a D_p in the many hundreds of units could have been used as the two categoric levels to better reflect the ranges that are reported as effective for hemostasis in literature [100-102]. In retrospect it would have been better to exclude PP D_p as a factor altogether in the DoE and instead run pilot experiments to determine the most effective D_p for hemostasis.

6.3.2 Responses

Similar limitations relating to time constraints and maintaining a feasible design space can be said regarding the responses included in the DoE. Using objective measurements for mechanical properties such as tensile strength and toughness rather than a handling properties score likely would have revealed more about the CS-PP interactions and allowed more specific optimization. This was attempted, although mounting samples of this material type on the tensiometer and obtaining meaningful results consumed too much sample mass and would have required much more time as the samples had to be specially made to fit the instrument.

Although not ideal, the handling properties score was sufficient as a response since the design input around mechanical properties did not require specific values but rather just that the material could be appropriately manipulated for the application.

Explicitly including surface area as a response would have improved the design space since it was hypothesized that a greater surface area would result in greater biological effects, as more of the material would be in contact with the environment. Two methods were attempted to measure surface area including Brunauer-Emmett-Teller nitrogen adsorption and pycnometer analysis; however, the samples were not dense enough to produce reliable surface area measurements using either method. To address this limitation apparent density was included as a response as a proxy for surface area since, in theory, materials that are made of the same components and less dense should have greater relative surface area.

The use of blood clotting index as the only hemostasis response in the DoE was another limitation. This response was intended to be a whole blood clotting time assay. However, visually determining what time the blood was fully clotted was highly inconsistent with a solid absorbent material in the blood. A blood clotting index was adopted instead although it does not directly measure how quickly a clot forms but rather how extensive the clot formation is. Adding more hemostasis related responses such as the aPTT assay to the DoE could have revealed more information around the hemostatic effects of the CS-PP-Cu material.

Limitations surrounding the elution profile responses involved the assay methodology and representation of the results. The assay was carried out in a lysozyme buffer solution rather than a more accurate simulated environment such as blood or a simulated body fluid due to ICP-OES not being able to handle biological serum. It is likely that this impacted both the degradation of the material and the observed elution, with a blood clot having the potential to encapsulate the material and limit elution. The results were reported in the DoE as the percentage of phosphorous or copper that was eluted at each time point. This created 8 responses while only extracting significant benefit from the 24-hour time points. Rather than including all the time points as separate responses, a function could have been fit to the elution profile so the results could be reported as the slope or decay time constant. This would reduce

the number of responses and allow the burst release portion of the elution profiles to be considered in the optimization as well.

The AlamarBlue assay that was used works by measuring the amount of resazurin that is converted to resorufin by viable cells using fluorescence readings as resorufin produces a bright red fluorescence. Although this is a standard way of measuring cytotoxicity, the assay more specifically measures rates of cell viability, metabolic activity, and proliferation [106]. Because this was the only cytotoxicity response it is possible that other aspects of the elution media, such as the PP, could be influencing metabolic activity or proliferation which would interfere with the cell viability results. Combining AlamarBlue results with a more objective measure of cell viability, such as live dead staining would alleviate this concern. The *in vitro* assay used here was also not a very representative model of an actual wound bed as it uses a static environment, while in a wound bed a more dynamic environment is expected. Therefore, copper release and concentration would be different in a real wound which may yield different cytotoxicity readings. To address this a more accurate simulated wound bed could be used to better mimic the expected environment.

A major limitation was that the DoE completely lacked a response for antibacterial effects. An antibacterial suspensions assay on *S. Aureus* and *E. Coli* was conducted for all the samples in the design space but it did not yield results that were usable in the DoE. It was confirmed during pilot tests that several sample runs were effective against both *S. Aureus* and *E. Coli* at reasonably expected concentrations. However, the effective concentration range for each bacteria strain was completely different with *S. Aureus* being susceptible to CS at much lower concentrations [107]. In these initial studies the sample concentration that was used for both bacteria strains was the same. Unfortunately, all the samples were close to 100% effective in killing *S. Aureus* at this concentration while none had any effect on *E. Coli*. These results had no value to the DoE as there was no difference between any of the samples. Given more time, these tests could have been rerun with the correct sample concentrations to reveal the differences in antibacterial effectiveness between the sample runs. Since rerunning these tests on all the sample runs with various sample concentrations would have consumed far more time than was remaining in the project timeline, antibacterial effects were not included as a response

in the DoE. To mitigate this limitation, three sample formulations were optimized with different copper levels so that the impact copper had on antibacterial effects could still be investigated.

6.3.3 Predictive models

Although all the included predictive models showed statistical significance, some of the responses could not be modeled and others were limited in their predictive power. When generating predictive models for the copper elution time points that corresponded to the burst release, statistical significance could not be achieved and therefore burst release of copper was not considered in the optimization. This was likely due to the concentration of copper being so low at the shorter time points that the ICP-OES could not measure the copper elution reliably enough to model. Additionally, the ICP-OES instrument used to measure the 24-hour copper and phosphorous elution in the validation stage had an inferior quantifiable limit than the instrument used in the DoE. This resulted in the 24-hour elution measurements being very close to the non-quantifiable range, limiting the reliability of this validation. The blood clotting index specifically was limited as it failed the validation, leaving no valid hemostasis response as part of the optimization. Even the other responses that were accurately validated had very wide prediction tolerances, further highlighting the limitations of the predictive models. That being said, many of the predicted values were very close to the measured values regardless of the wide tolerance ranges. Despite less-than-ideal predictive power and tolerances, this DoE still enabled some optimization while revealing more about these CS-PP-Cu interactions for this polyelectrolyte system.

6.3.4 Verification

The thoroughness of the verification stage was limited by time in part due to the size of the DoE and how much time it consumed. The coagulation assays that were used were not an ideal representation of the conditions that would be expected, as the blood clotting index assay did not measure clotting time and the aPTT assay used platelet poor plasma rather than whole blood. Including an assay that looked at clotting time in whole blood in addition to the aPTT assay would increase the confidence of the conclusions made surrounding clotting time. There was also no measure of clot stability, which could be an important characteristic as rebleed can cause problems in trauma situations. In addition, the antibacterial assay only examined

effectiveness against *S. Aureus*. Although this is the most common bacterial strain found in infections following traumatic wounds, there are many other bacterial strains that may be susceptible to these materials [108]. With the current antibacterial results there does not appear to be any benefit to including copper; however, tests against other prominent strains of bacteria could reveal some benefit. With an extended timeline more extensive hemostatic and antibacterial testing could have been conducted to determine if the CS-PP-Cu materials were superior to Celox™ or CS only.

6.4 Recommendations for Future Work

6.4.3 Improving the DoE and CS-PP Material

To address some of the mentioned limitations, enhancements to the DoE could be made to improve the optimized materials. In order to fix or remove the PP D_p factor, the DoE would have to be repeated using different categoric levels or with PP D_p removed as a factor entirely. Without completely redoing the DoE, the design space could be augmented by adding more runs to improve predictive power and more responses could be included to further characterize the materials and improve the optimization. The antibacterial assay used in the verification stage could be reintegrated into the DoE using the correct sample concentrations and various relevant bacterial strains to allow direct optimization of antibacterial effect. Further hemostatic testing such as the aPTT assay and rheometry studies to investigate clot stability would strengthen predictive power around hemostatic effects. A response that measures CS content directly would allow confirmation of the material composition estimates that were made from the copper and phosphorous content data.

6.4.1 Further *in vitro* testing

As mentioned in the limitations, continuation of *in vitro* testing to verify effectiveness as a trauma wound dressing is recommended. Expansion of the verification should focus mainly on hemostatic and antibacterial effects to hopefully demonstrate the potential benefit of a CS-PP-Cu formulation over other materials available for trauma wound dressings. Some additional hemostasis-related assays that could prove beneficial include prothrombin time, platelet adhesion and appropriate whole blood clotting time assays. Prothrombin time would

complement the aPTT assay as it uses similar methodology but measures activation of the extrinsic pathway rather than the intrinsic pathway [36]. Measures of platelet adhesion would be useful as it is proposed that CS promotes coagulation via platelet aggregation [30]. A whole blood clotting time assay that is effective with absorbent materials would be a better representation of *in vivo* conditions. Finally, a rheometry study could be pursued as a measure of clot stability.

With respect to antibacterial testing, the main priority should be investigating the effectiveness of the CS-PP-Cu material against other prominent bacteria strains found in infected trauma wounds. These are mainly gram-negative bacteria including *P. aeruginosa*, *E. coli*, *P. mirabilis* and *A. baumannii* [108]. Other types of antibacterial assays could also be included such as agar zone of inhibition methods (ISO 20645:2004), to confirm the suspension assay results, or adhesion methods to specifically assess the material as an antibacterial barrier [109].

6.4.2 *In vivo* testing

After adequate *in vitro* testing has been completed the next logical step would be *in vivo* testing of the CS-PP-Cu material using an appropriate pre-clinical animal model. Many similar medical devices use rats as the animal model for this type of testing, though it is suggested that porcine models are the best for evaluating medical devices applied to the skin [110, 111]. This testing should address cytocompatibility, a hemostasis study and an antibacterial study to quantify effectiveness of the materials.

6.5 Concluding Remarks

This thesis not only produced a material demonstrating promising characteristics for trauma wound dressing, but also contributed significantly to the greater understanding of CS, PP and copper polyelectrolyte complexation interactions. After further product development and testing, a highly effective trauma wound dressing with enhanced hemostatic and antibacterial effects could be implemented based on the material and work defined in this thesis. Findings within this thesis could also help contribute to the development of various novel CS-PP devices with alternative biomedical applications.

References

[1]   J. E. Tintinalli *et al.*, *Tintinalli's emergency medicine: a comprehensive study guide*, 9th ed. (McGraw-Hill's AccessMedicine). New York, N.Y: McGraw-Hill Education LLC, 2020.

[2]   A. Sood, M. S. Granick, and N. L. Tomaselli, "Wound Dressings and Comparative Effectiveness Data," (in eng), *Adv Wound Care (New Rochelle),* vol. 3, no. 8, pp. 511-529, 2014, doi: 10.1089/wound.2012.0401.

[3]   J. H. Morrissey, S. H. Choi, and S. A. Smith, "Polyphosphate: an ancient molecule that links platelets, coagulation, and inflammation," *Blood,* vol. 119, no. 25, pp. 5972-5979, 2012, doi: 10.1182/blood-2012-03-306605.

[4]   S. A. Smith, N. J. Mutch, D. Baskar, P. Rohloff, R. Docampo, and J. H. Morrissey, "Polyphosphate modulates blood coagulation and fibrinolysis," (in eng), *Proc Natl Acad Sci U S A,* vol. 103, no. 4, pp. 903-908, 2006, doi: 10.1073/pnas.0507195103.

[5]   P. S. Bakshi, D. Selvakumar, K. Kadirvelu, and N. S. Kumar, "Chitosan as an environment friendly biomaterial – a review on recent modifications and applications," *Int J Biol Macromol,* vol. 150, pp. 1072-1083, 2020, doi: 10.1016/j.ijbiomac.2019.10.113.

[6]   M. Dash, F. Chiellini, R. M. Ottenbrite, and E. Chiellini, "Chitosan—A versatile semi-synthetic polymer in biomedical applications," *Progress in polymer science,* vol. 36, no. 8, pp. 981-1014, 2011, doi: 10.1016/j.progpolymsci.2011.02.001.

[7]   L. Gritsch, C. Lovell, W. H. Goldmann, and A. R. Boccaccini, "Fabrication and characterization of copper(II)-chitosan complexes as antibiotic-free antibacterial biomaterial," *Carbohydrate Polymers,* vol. 179, pp. 370-378, 2018/01/01/ 2018.

[8]   K. Williamson, R. Ramesh, and A. Grabinsky, "Advances in prehospital trauma care," (in eng), *Int J Crit Illn Inj Sci,* vol. 1, no. 1, pp. 44-50, Jan 2011, doi: 10.4103/2229-5151.79281.

[9]   B. B. Michael Kostiuk, *Trauma Assessment*, I. S. [Internet], ed., Treasure Island (FL): StatPearls Publishing, 2023. [Online]. Available: https://www.ncbi.nlm.nih.gov/books/NBK555913/.

[10]   H. C. Tien, F. Spencer, L. N. Tremblay, S. B. Rizoli, and F. D. Brenneman, "Preventable Deaths From Hemorrhage at a Level I Canadian Trauma Center," *The journal of trauma,* vol. 62, no. 1, pp. 142-146, 2007, doi: 10.1097/01.ta.0000251558.38388.47.

[11]   S. E. van Oostendorp, E. C. T. H. Tan, and L. M. Geeraedts, "Prehospital control of life-threatening truncal and junctional haemorrhage is the ultimate challenge in optimizing trauma care; a review of treatment options and their applicability in the civilian trauma setting," *Scandinavian journal of trauma, resuscitation and emergency medicine,* vol. 24, no. 1, pp. 110-110, 2016, doi: 10.1186/s13049-016-0301-9.

[12]   A. Komori, H. Iriyama, T. Kainoh, M. Aoki, T. Naito, and T. Abe, "The impact of infection complications after trauma differs according to trauma severity," *Scientific Reports,* vol. 11, no. 1, p. 13803, 2021/07/05 2021, doi: 10.1038/s41598-021-93314-5.

[13]   P. Agarwal, R. Kukrele, and D. Sharma, "Vacuum assisted closure (VAC)/negative pressure wound therapy (NPWT) for difficult wounds: A review," (in eng), *J Clin Orthop Trauma,* vol. 10, no. 5, pp. 845-848, Sep-Oct 2019, doi: 10.1016/j.jcot.2019.06.015.

[14]   R. J. Alharbi, V. Lewis, and C. Miller, "International Perspectives of Prehospital and Hospital Trauma Services: A Literature Review," *Trauma Care*, vol. 2, no. 3*,* pp. 445-462doi: 10.3390/traumacare2030037.

[15]   E. M. Bulger *et al.*, "An Evidence-based Prehospital Guideline for External Hemorrhage Control: American College of Surgeons Committee on Trauma," *Prehospital emergency care,* vol. 18, no. 2, pp. 163-173, 2014, doi: 10.3109/10903127.2014.896962.

[16]   P. Yu and W. Zhong, "Hemostatic materials in wound care," (in eng), *Burns Trauma,* vol. 9, pp. tkab019-tkab019, 2021, doi: 10.1093/burnst/tkab019.

[17]   S. Palta, R. Saroa, and A. Palta, "Overview of the coagulation system," *Indian journal of anaesthesia,* vol. 58, no. 5, pp. 515-523, 2014, doi: 10.4103/0019-5049.144643.

[18]   D. M. Monroe and M. Hoffman, "The clotting system - a major player in wound healing," *Haemophilia : the official journal of the World Federation of Hemophilia,* vol. 18, no. s5, pp. 11-16, 2012, doi: 10.1111/j.1365-2516.2012.02889.x.

[19]   V. J. Marder, *Hemostasis and thrombosis basic principles and clinical practice*, 6th ed. Philadelphia: Wolters Kluwer/Lippincott Williams & Wilkins Health, 2013.

[20]   F. Pérez-Gómez and R. Bover, "The New Coagulation Cascade and Its Possible Influence on the Delicate Balance Between Thrombosis and Hemorrhage," *Revista Española de Cardiología (English Edition),* vol. 60, no. 12, pp. 1217-1219, 2007.

[21]   S. M. Joseph, S. Krishnamoorthy, R. Paranthaman, J. A. Moses, and C. Anandharamakrishnan, "A review on source-specific chemistry, functionality, and applications of chitin and chitosan," *Carbohydrate polymer technologies and applications,* vol. 2, p. 100036, 2021, doi: 10.1016/j.carpta.2021.100036.

[22]   S. Kou, L. M. Peters, and M. R. Mucalo, "Chitosan: A review of sources and preparation methods," *Int J Biol Macromol,* vol. 169, pp. 85-94, 2021, doi: 10.1016/j.ijbiomac.2020.12.005.

[23]   R. S. C. M. de Queiroz Antonino *et al.*, "Preparation and Characterization of Chitosan Obtained from Shells of Shrimp (Litopenaeus vannamei Boone)," *Mar Drugs,* vol. 15, no. 5, p. 141, 2017, doi: 10.3390/md15050141.

[24]   N. D. Arnold, W. M. Brück, D. Garbe, and T. B. Brück, "Enzymatic Modification of Native Chitin and Conversion to Specialty Chemical Products," *Mar Drugs,* vol. 18, no. 2, p. 93, 2020, doi: 10.3390/md18020093.

[25]   M. Khajavian, V. Vatanpour, R. Castro-Muñoz, and G. Boczkaj, "Chitin and derivative chitosan-based structures — Preparation strategies aided by deep eutectic solvents: A review," *Carbohydr Polym,* vol. 275, pp. 118702-118702, 2022, doi: 10.1016/j.carbpol.2021.118702.

[26]   V. Mikušová and P. Mikuš, "Advances in Chitosan-Based Nanoparticles for Drug Delivery," *International Journal of Molecular Sciences,* vol. 22, no. 17, p. 9652, 2021.

[27]   I. Aranaz *et al.*, "Chitosan: An Overview of Its Properties and Applications," *Polymers,* vol. 13, no. 19, 2021, doi: 10.3390/polym13193256.

[28]   E. Y. Garoy *et al.*, "Methicillin-Resistant Staphylococcus aureus (MRSA): Prevalence and Antimicrobial Sensitivity Pattern among Patients—A Multicenter Study in Asmara, Eritrea," *The Canadian journal of infectious diseases & medical microbiology,* vol. 2019, pp. 8321834-9, 2019, doi: 10.1155/2019/8321834.

[29]   C.-L. Ke, F.-S. Deng, C.-Y. Chuang, and C.-H. Lin, "Antimicrobial Actions and Applications of Chitosan," *Polymers (Basel),* vol. 13, no. 6, p. 904, 2021, doi: 10.3390/polym13060904.

[30]   H. S. Whang, W. Kirsch, Y. H. Zhu, C. Z. Yang, and S. M. Hudson, "Hemostatic Agents Derived from Chitin and Chitosan," *Journal of Macromolecular Science, Part C,* vol. 45, no. 4, pp. 309-323, 2005, doi: 10.1080/15321790500304122.

[31]   Y. Xia, R. Yang, H. Wang, Y. Li, and C. Fu, "Application of chitosan-based materials in surgical or postoperative hemostasis," *Frontiers in materials,* vol. 9, 2022, doi: 10.3389/fmats.2022.994265.

[32]   G. Deprés-Tremblay, A. Chevrier, N. Tran-Khanh, M. Nelea, and M. D. Buschmann, "Chitosan inhibits platelet-mediated clot retraction, increases platelet-derived growth factor release, and increases residence time and bioactivity of platelet-rich plasma in vivo," *Biomedical materials (Bristol),* vol. 13, no. 1, p. 015005, 2017.

[33]   Y. W. Wang *et al.*, "Biological Effects of Chitosan-Based Dressing on Hemostasis Mechanism," (in eng), *Polymers (Basel),* vol. 11, no. 11, Nov 19 2019, doi: 10.3390/polym11111906.

[34]   X. Wang, H. C. Schröder, U. Schloßmacher, and W. E. Müller, "Inorganic polyphosphates: biologically active biopolymers for biomedical applications," (in eng), *Prog Mol Subcell Biol,* vol. 54, pp. 261-94, 2013, doi: 10.1007/978-3-642-41004-8_10.

[35]   A. Momeni and M. J. Filiaggi, "Synthesis and characterization of different chain length sodium polyphosphates," *Journal of non-crystalline solids,* vol. 382, pp. 11-17, 2013, doi: 10.1016/j.jnoncrysol.2013.10.003.

[36]   A. Momeni and M. J. Filiaggi, "Degradation and hemostatic properties of polyphosphate coacervates," *Acta biomaterialia,* vol. 41, pp. 328-341, 2016, doi: 10.1016/j.actbio.2016.06.002.

[37]   M. Okawa, M. Sakoda, S. Ohta, K. Hasegawa, Y. Yatomi, and T. Ito, "The Balance between the Hemostatic Effect and Immune Response of Hyaluronan Conjugated with Different Chain Lengths of Inorganic Polyphosphate," *Biomacromolecules,* vol. 21, no. 7, pp. 2695-2704, 2020, doi: 10.1021/acs.biomac.0c00390.

[38]   S. A. Smith *et al.*, "Polyphosphate exerts differential effects on blood clotting, depending on polymer size," *Blood,* vol. 116, no. 20, pp. 4353-4359, 2010, doi: 10.1182/blood-2010-01-266791.

[39]   J. H. Yeon *et al.*, "Localization of Short-Chain Polyphosphate Enhances its Ability to Clot Flowing Blood Plasma," *Scientific reports,* vol. 7, no. 1, pp. 42119-42119, 2017, doi: 10.1038/srep42119.

[40]   J. M. Gajsiewicz, S. A. Smith, and J. H. Morrissey, "Polyphosphate and RNA Differentially Modulate the Contact Pathway of Blood Clotting," *The Journal of biological chemistry,* vol. 292, no. 5, pp. 1808-1814, 2017, doi: 10.1074/jbc.M116.754325.

[41]   F. Müller *et al.*, "Platelet Polyphosphates Are Proinflammatory and Procoagulant Mediators In Vivo," *Cell,* vol. 139, no. 6, pp. 1143-1156, 2009, doi: 10.1016/j.cell.2009.11.001.

[42]   N. J. Mutch, R. Engel, S. Uitte de Willige, H. Philippou, and R. A. S. Ariëns, "Polyphosphate modifies the fibrin network and down-regulates fibrinolysis by attenuating binding of tPA and plasminogen to fibrin," *Blood,* vol. 115, no. 19, pp. 3980-3988, 2010, doi: 10.1182/blood-2009-11-254029.

[43]   S. H. Choi, S. A. Smith, and J. H. Morrissey, "Polyphosphate is a cofactor for the activation of factor XI by thrombin," *Blood,* vol. 118, no. 26, pp. 6963-6970, 2011, doi: 10.1182/blood-2011-07-368811.

[44]   A. D. Kulkarni *et al.*, "Polyelectrolyte complexes: mechanisms, critical experimental aspects, and applications," *Artificial Cells, Nanomedicine, and Biotechnology,* vol. 44, no. 7, pp. 1615-1625, 2016/10/02 2016, doi: 10.3109/21691401.2015.1129624.

[45]   Y. P. Timilsena, T. O. Akanbi, N. Khalid, B. Adhikari, and C. J. Barrow, "Complex coacervation: Principles, mechanisms and applications in microencapsulation," *International journal of biological macromolecules,* vol. 121, pp. 1276-1286, 2019, doi: 10.1016/j.ijbiomac.2018.10.144.

[46]   K. T. Delaney and G. H. Fredrickson, "Theory of polyelectrolyte complexation—Complex coacervates are self-coacervates," *The Journal of chemical physics,* vol. 146, no. 22, pp. 224902-224902, 2017, doi: 10.1063/1.4985568.

[47]   S. Lankalapalli and V. R. Kolapalli, "Polyelectrolyte Complexes: A Review of their Applicability in Drug Delivery Technology," (in eng), *Indian J Pharm Sci,* vol. 71, no. 5, pp. 481-7, Sep 2009, doi: 10.4103/0250-474x.58165.

[48]   S. Fanaee and M. J. Filiaggi, "Macro bead formation based on polyelectrolyte complexation between long-chain polyphosphates and chitosan," *Materials advances,* vol. 4, no. 7, pp. 1678-1686, 2023, doi: 10.1039/d2ma01091g.

[49]   J. H. Hamman, "Chitosan based polyelectrolyte complexes as potential carrier materials in drug delivery systems," (in eng), *Mar Drugs,* vol. 8, no. 4, pp. 1305-22, Apr 19 2010, doi: 10.3390/md8041305.

[50]   L. Fowler, H. Engqvist, and C. Öhman-Mägi, "Effect of Copper Ion Concentration on Bacteria and Cells," *Materials,* vol. 12, no. 22, p. 3798, 2019, doi: 10.3390/ma12223798.

[51]   R. Jastrzab, M. Nowak, M. Zabiszak, A. Odani, and M. T. Kaczmarek, "Significance and properties of the complex formation of phosphate and polyphosphate groups in particles present in living cells," *Coordination Chemistry Reviews,* vol. 435, p. 213810, 2021/05/15/ 2021, doi: https://doi.org/10.1016/j.ccr.2021.213810.

[52]   A. Momeni and M. J. Filiaggi, "Comprehensive Study of the Chelation and Coacervation of Alkaline Earth Metals in the Presence of Sodium Polyphosphate Solution," *Langmuir,* vol. 30, no. 18, pp. 5256-5266, 2014, doi: 10.1021/la500474j.

[53]   A. Momeni and M. J. Filiaggi, "Rheology of polyphosphate coacervates," *Journal of rheology (New York : 1978),* vol. 60, no. 1, pp. 25-34, 2016, doi: 10.1122/1.4935127.

[54]   O. A. C. Monteiro and C. Airoldi, "Some Thermodynamic Data on Copper–Chitin and Copper–Chitosan Biopolymer Interactions," *Journal of Colloid and Interface Science,* vol. 212, no. 2, pp. 212-219, 1999/04/15/ 1999, doi: https://doi.org/10.1006/jcis.1998.6063.

[55]   R. Terreux, M. Domard, C. Viton, and A. Domard, "Interactions Study between the Copper II Ion and Constitutive Elements of Chitosan Structure by DFT Calculation," *Biomacromolecules,* vol. 7, no. 1, pp. 31-37, 2006/01/01 2006, doi: 10.1021/bm0504126.

[56]   I. Salah, I. P. Parkin, and E. Allan, "Copper as an antimicrobial agent: recent advances," *RSC advances,* vol. 11, no. 3, pp. 18179-18186, 2021, doi: 10.1039/d1ra02149d.

[57]   Y. Fu, F.-M. J. Chang, and D. P. Giedroc, "Copper Transport and Trafficking at the Host–Bacterial Pathogen Interface," *Accounts of chemical research,* vol. 47, no. 12, pp. 3605-3613, 2014, doi: 10.1021/ar500300n.

[58]   X. Ma, S. Zhou, X. Xu, and Q. Du, "Copper-containing nanoparticles: Mechanism of antimicrobial effect and application in dentistry-a narrative review," (in eng), *Front Surg,* vol. 9, p. 905892, 2022, doi: 10.3389/fsurg.2022.905892.

[59]   S. Dhivya, V. V. Padma, and E. Santhini, "Wound dressings - a review," (in eng), *Biomedicine (Taipei),* vol. 5, no. 4, p. 22, Dec 2015, doi: 10.7603/s40681-015-0022-9.

[60]   V. Jones, J. E. Grey, and K. G. Harding, "Wound dressings," (in eng), *Bmj,* vol. 332, no. 7544, pp. 777-80, Apr 1 2006, doi: 10.1136/bmj.332.7544.777.

[61]   M. Mir *et al.,* "Synthetic polymeric biomaterials for wound healing: a review," *Progress in biomaterials,* vol. 7, no. 1, pp. 1-21, 2018, doi: 10.1007/s40204-018-0083-4.

[62]   R. Zeng *et al.,* "Approaches to cutaneous wound healing: basics and future directions," *Cell and tissue research,* vol. 374, no. 2, pp. 217-232, 2018, doi: 10.1007/s00441-018-2830-1.

[63]   B. G. Kozen, S. J. Kircher, J. Henao, F. S. Godinez, and A. S. Johnson, "An Alternative Hemostatic Dressing: Comparison of CELOX, HemCon, and QuikClot," *Academic emergency medicine,* vol. 15, no. 1, pp. 74-81, 2008, doi: 10.1111/j.1553-2712.2007.00009.x.

[64]   M. Welch, J. Barratt, A. Peters, and C. Wright, "Systematic review of prehospital haemostatic dressings," *BMJ military health,* vol. 166, no. 3, pp. 194-200, 2020, doi: 10.1136/jramc-2018-001066.

[65]   H. R. Hatamabadi, F. Asayesh Zarchi, H. Kariman, A. Arhami Dolatabadi, A. Tabatabaey, and A. Amini, "Celox-coated gauze for the treatment of civilian penetrating trauma: a randomized clinical trial," (in eng), *Trauma Mon,* vol. 20, no. 1, p. e23862, Feb 2015, doi: 10.5812/traumamon.23862.

[66]   M. A. Khan and M. Mujahid, "A review on recent advances in chitosan based composite for hemostatic dressings," *International journal of biological macromolecules,* vol. 124, pp. 138-147, 2019, doi: 10.1016/j.ijbiomac.2018.11.045.

[67]   L. F. Littlejohn, J. J. Devlin, S. S. Kircher, R. Lueken, M. R. Melia, and A. S. Johnson, "Comparison of Celox-A, ChitoFlex, WoundStat, and Combat Gauze Hemostatic Agents Versus Standard Gauze Dressing in Control of Hemorrhage in a Swine Model of Penetrating Trauma," *Academic emergency medicine,* vol. 18, no. 4, pp. 340-350, 2011, doi: 10.1111/j.1553-2712.2011.01036.x.

[68]   A. K. Singh, S. M. Kotrashetti, A. Kapoor, and T. P. Kale, "Effectiveness of Hemcon Dental Dressing Versus Conventional Method of Haemostasis in 40 Patients on Oral Antiplatelet Drugs," *Sultan Qaboos University medical journal,* vol. 12, no. 3, pp. 330-335, 2012, doi: 10.12816/0003147.

[69]   B. Gegel *et al.*, "The effects of QuikClot Combat Gauze and movement on hemorrhage control in a porcine model," *Military medicine,* vol. 177, no. 12, pp. 1543-1547, 2012, doi: 10.7205/MILMED-D-12-00165.

[70]   (2021). *510(k) Summary -K202830 Axiostat Patch*.

[71]   M. Kabeer, P. P. Venugopalan, and V. C. Subhash, "Pre-hospital Hemorrhagic Control Effectiveness of Axiostat® Dressing Versus Conventional Method in Acute Hemorrhage Due to Trauma," *Curēus (Palo Alto, CA),* vol. 11, no. 8, pp. e5527-e5527, 2019, doi: 10.7759/cureus.5527.

[72]   F. Yousefian *et al.*, "Antimicrobial Wound Dressings: A Concise Review for Clinicians," (in eng), *Antibiotics (Basel),* vol. 12, no. 9, Sep 11 2023, doi: 10.3390/antibiotics12091434.

[73]   M. Buriuli, W. G. Kumari, and D. Verma, "Evaluation of hemostatic effect of polyelectrolyte complex-based dressings," *Journal of biomaterials applications,* vol. 32, no. 5, pp. 638-647, 2017, doi: 10.1177/0885328217735956.

[74]   X. Fan *et al.*, "Morphology-controllable cellulose/chitosan sponge for deep wound hemostasis with surfactant and pore-foaming agent," *Materials Science & Engineering C,* vol. 118, p. 111408, 2021, doi: 10.1016/j.msec.2020.111408.

[75]   X. Fan *et al.*, "One-step fabrication of chitosan sponge and its potential for rapid hemostasis in deep trauma," *Biomedical materials (Bristol),* vol. 16, no. 1, pp. 015010-015010, 2020, doi: 10.1088/1748-605X/aba878.

[76] W. Liu *et al.*, "Polymer Composite Sponges with Inherent Antibacterial, Hemostatic, Inflammation-Modulating and Proregenerative Performances for Methicillin-Resistant Staphylococcus aureus-Infected Wound Healing," *Advanced healthcare materials,* vol. 10, no. 22, pp. 2101247-n/a, 2021, doi: 10.1002/adhm.202101247.

[77] S. S. Biranje, P. V. Madiwale, K. C. Patankar, R. Chhabra, P. Dandekar-Jain, and R. V. Adivarekar, "Hemostasis and anti-necrotic activity of wound-healing dressing containing chitosan nanoparticles," *International journal of biological macromolecules,* vol. 121, pp. 936-946, 2019, doi: 10.1016/j.ijbiomac.2018.10.125.

[78] S.-Y. Ong, J. Wu, S. M. Moochhala, M.-H. Tan, and J. Lu, "Development of a chitosan-based wound dressing with improved hemostatic and antimicrobial properties," *Biomaterials,* vol. 29, no. 32, pp. 4323-4332, 2008, doi: 10.1016/j.biomaterials.2008.07.034.

[79] D. G. Klein, D. E. Fritsch, and S. G. Amin, "Wound Infection Following Trauma and Burn Injuries," *Critical care nursing clinics of North America,* vol. 7, no. 4, pp. 627-642, 1995, doi: 10.1016/S0899-5885(18)30355-1.

[80] A. V. Thanusha and V. Koul, "Biocompatibility evaluation for the developed hydrogel wound dressing – ISO-10993-11 standards – in vitro and in vivo study," *Biomedical physics & engineering express,* vol. 8, no. 1, p. 15010, 2022, doi: 10.1088/2057-1976/ac3b2b.

[81] Z. Yang *et al.*, "Highly Stretchable, Adhesive, Biocompatible, and Antibacterial Hydrogel Dressings for Wound Healing," *Advanced science,* vol. 8, no. 8, pp. 2003627-n/a, 2021, doi: 10.1002/advs.202003627.

[82] M. A. M. D. Brown, M. R. M. D. M. S. Daya, and J. A. E. M. T. P. Worley, "Experience with Chitosan Dressings in a Civilian EMS System," *The Journal of emergency medicine,* vol. 37, no. 1, pp. 1-7, 2009, doi: 10.1016/j.jemermed.2007.05.043.

[83] L. P. Arendsen, R. Thakar, and A. H. Sultan, "The Use of Copper as an Antimicrobial Agent in Health Care, Including Obstetrics and Gynecology," (in eng), *Clin Microbiol Rev,* vol. 32, no. 4, Sep 18 2019, doi: 10.1128/cmr.00125-18.

[84]   K. Azuma *et al.*, "Chitin, chitosan, and its derivatives for wound healing: old and new materials," (in eng), *J Funct Biomater,* vol. 6, no. 1, pp. 104-42, Mar 13 2015, doi: 10.3390/jfb6010104.

[85]   P. J. W. Mark J. Anderson, *DOE Simplified: Practice Tools for Effective Experimentation*, Second ed. Boca Raton, FL: CRC Press, 2007.

[86]   H. Anderson. "Design-Expert v13." StatEase https://www.statease.com/docs/v13 (accessed 2013).

[87]   P. J. W. Mark J. Anderson, *RSM Simplified: Optimizing Processes Using Response Surface Methods for Design of Experiments*. Boca Raton, FL: CRC Press, 2005.

[88]   Y. Hou, J. Hu, H. Park, and M. Lee, "Chitosan-based nanoparticles as a sustained protein release carrier for tissue engineering applications," *Journal of biomedical materials research. Part A,* vol. 100A, no. 4, pp. 939-947, 2012, doi: 10.1002/jbm.a.34031.

[89]   N. Poth, V. Seiffart, G. Gross, H. Menzel, and W. Dempwolf, "Biodegradable chitosan nanoparticle coatings on titanium for the delivery of BMP-2," *Biomolecules (Basel, Switzerland),* vol. 5, no. 1, pp. 3-19, 2015, doi: 10.3390/biom5010003.

[90]   M.-F. Shih, M.-D. Shau, M.-Y. Chang, S.-K. Chiou, J.-K. Chang, and J.-Y. Cherng, "Platelet adsorption and hemolytic properties of liquid crystal/composite polymers," *International journal of pharmaceutics,* vol. 327, no. 1, pp. 117-125, 2006, doi: 10.1016/j.ijpharm.2006.07.043.

[91]   *Biological evaluation of medical devices Part 5: Tests for in vitro cytotoxicity*, I. O. f. Standardization, Switzerland, 2009.

[92]   C. Hirsch and S. Schildknecht, "In Vitro Research Reproducibility: Keeping Up High Standards," (in English), *Frontiers in Pharmacology,* Perspective vol. 10, 2019-December-10 2019, doi: 10.3389/fphar.2019.01484.

[93]   I. H. Guideline, "Guideline for Elemental Inpurities," E. M. Agency Ed. Netherlands: European Medicines Agency, 2019.

[94]   I. O. f. Standardization, *Medical devices - Application of risk management to medical devices. .* Brussels: CEN-CENELEC 2021.

[95]   M. Božič Mijovski, "Chapter Five - Advances in monitoring anticoagulant therapy," in *Advances in Clinical Chemistry*, vol. 90, G. S. Makowski Ed.: Elsevier, 2019, pp. 197-213.

[96]   M. Weber *et al.*, "Blood-Contacting Biomaterials: In Vitro Evaluation of the Hemocompatibility," (in eng), *Front Bioeng Biotechnol,* vol. 6, p. 99, 2018, doi: 10.3389/fbioe.2018.00099.

[97]   *Standard Test Method for Determining the Antimicrobial Activity of Antimicrobial Agents Under Dynamic Contact Conditions.* , A. International, West Conshohocken, PA, USA, 2020.

[98]   M. D'Espine *et al.*, "Serum levels of ciprofloxacin after single oral doses in patients with septicemia," (in eng), *Eur J Clin Microbiol Infect Dis,* vol. 8, no. 12, pp. 1019-23, Dec 1989, doi: 10.1007/bf01975162.

[99]   (2004). *CIPRO (ciprofloxacin hydrochloride) TABLETS*.

[100]   C. J. Baker, S. A. Smith, and J. H. Morrissey, "Polyphosphate in thrombosis, hemostasis, and inflammation," *Research and practice in thrombosis and haemostasis,* vol. 3, no. 1, pp. 18-25, 2019, doi: 10.1002/rth2.12162.

[101]   J. H. Morrissey, "Polyphosphate multi-tasks," *Journal of thrombosis and haemostasis,* vol. 10, no. 11, pp. 2313-2314, 2012, doi: 10.1111/jth.12001.

[102]   R. J. Travers, S. A. Smith, and J. H. Morrissey, "Polyphosphate, platelets, and coagulation," *International journal of laboratory hematology,* vol. 37, no. S1, pp. 31-35, 2015, doi: 10.1111/ijlh.12349.

[103]   E. Jelis, D. Kristol, R. R. Arora, and C. R. Spillert, "The effect of copper ion on blood coagulation," 2004: IEEE, p. 127, doi: 10.1109/NEBC.2004.1300027.

[104]   V. G. Nielsen, T. D. Ward, and P. M. Ford, "Effects of cupric chloride on coagulation in human plasma: role of fibrinogen," *Journal of thrombosis and thrombolysis,* vol. 46, no. 3, pp. 359-364, 2018, doi: 10.1007/s11239-018-1704-4.

[105]   A. Asli *et al.*, "Antibiofilm and antibacterial effects of specific chitosan molecules on Staphylococcus aureus isolates associated with bovine mastitis," (in eng), *PLoS One,* vol. 12, no. 5, p. e0176988, 2017, doi: 10.1371/journal.pone.0176988.

[106]   E. M. Longhin, N. El Yamani, E. Rundén-Pran, and M. Dusinska, "The alamar blue assay in the context of safety testing of nanomaterials," (in eng), *Front Toxicol,* vol. 4, p. 981701, 2022, doi: 10.3389/ftox.2022.981701.

[107]   R. C. Goy, S. T. B. Morais, and O. B. G. Assis, "Evaluation of the antimicrobial activity of chitosan and its quaternized derivative on E. coli and S. aureus growth," *Revista Brasileira de Farmacognosia,* vol. 26, no. 1, pp. 122-127, 2016/01/01/ 2016, doi: https://doi.org/10.1016/j.bjp.2015.09.010.

[108]   V. Puca *et al.*, "Microbial Species Isolated from Infected Wounds and Antimicrobial Resistance Analysis: Data Emerging from a Three-Years Retrospective Study," (in eng), *Antibiotics (Basel),* vol. 10, no. 10, Sep 24 2021, doi: 10.3390/antibiotics10101162.

[109]   A. J. Cunliffe *et al.*, "How Do We Determine the Efficacy of an Antibacterial Surface? A Review of Standardised Antibacterial Material Testing Methods," *Antibiotics,* vol. 10, no. 9, p. 1069, 2021. [Online]. Available: https://www.mdpi.com/2079-6382/10/9/1069.

[110]   A. Omar and P. Nadworny, "Review: Antimicrobial efficacy validation using in vitro and in vivo testing methods," *Advanced drug delivery reviews,* vol. 112, pp. 61-68, 2017, doi: 10.1016/j.addr.2016.09.003.

[111]   Y. T. Shih *et al.*, "Hemostasis Evaluation of Antibacterial and Highly Absorbent Composite Wound Dressings in Animal Hemostasis Models," (in eng), *Polymers (Basel),* vol. 14, no. 9, Apr 26 2022, doi: 10.3390/polym14091764.

Appendix A: Analysis of Variance Tables

Table 13 - Analysis of variance table for copper content predictive model.

Source	Sum of Squares	df	Mean Square	F-value	p-value	
Model	12.80	8	1.60	39.36	< 0.0001	significant
A-CS Concentration	0.0030	1	0.0030	0.0726	0.7915	
B-PP Concentatrion	6.25	1	6.25	153.68	< 0.0001	
C-Cu Concentration	3.86	1	3.86	94.85	< 0.0001	
D-Polyphosphate Degree of Polymerization	0.0027	1	0.0027	0.0671	0.7994	
AD	0.2060	1	0.2060	5.07	0.0410	
BC	0.3487	1	0.3487	8.58	0.0110	
B²	1.45	1	1.45	35.56	< 0.0001	
C²	0.6020	1	0.6020	14.81	0.0018	
Residual	0.5692	14	0.0407			
Lack of Fit	0.5679	11	0.0516	121.60	0.0011	significant
Pure Error	0.0013	3	0.0004			
Cor Total	13.37	22				

Table 14 - Analysis of variance table for phosphorous content predictive model.

Source	Sum of Squares	df	Mean Square	F-value	p-value	
Model	49.14	4	12.28	13.77	< 0.0001	significant
A-CS Concentration	1.91	1	1.91	2.15	0.1601	
B-PP Concentatrion	21.90	1	21.90	24.56	0.0001	
AB	9.15	1	9.15	10.27	0.0049	
B²	11.13	1	11.13	12.48	0.0024	
Residual	16.05	18	0.8918			
Lack of Fit	14.12	15	0.9413	1.46	0.4246	not significant
Pure Error	1.93	3	0.6441			
Cor Total	65.19	22				

Table 15 - Analysis of variance table for ease of production predictive model.

Source	Sum of Squares	df	Mean Square	F-value	p-value	
Model	13.36	5	2.67	34.83	< 0.0001	significant
A-CS Concentration	0.2708	1	0.2708	3.53	0.0786	
B-PP Concentatrion	7.03	1	7.03	91.62	< 0.0001	
C-Cu Concentration	0.2599	1	0.2599	3.39	0.0843	
A²	2.80	1	2.80	36.55	< 0.0001	
B²	1.93	1	1.93	25.11	0.0001	
Residual	1.23	16	0.0767			
Lack of Fit	1.23	13	0.0944			
Pure Error	0.0000	3	0.0000			
Cor Total	14.59	21				

Table 16 - Analysis of variance table for handling properties predictive model.

Source	Sum of Squares	df	Mean Square	F-value	p-value	
Model	8.91	7	1.27	9.32	0.0002	significant
A-CS Concentration	0.6366	1	0.6366	4.66	0.0474	
B-PP Concentatrion	3.14	1	3.14	22.99	0.0002	
C-Cu Concentration	0.3548	1	0.3548	2.60	0.1278	
D-Polyphosphate Degree of Polymerization	0.0401	1	0.0401	0.2938	0.5957	
AB	0.5039	1	0.5039	3.69	0.0739	
AD	2.43	1	2.43	17.78	0.0007	
BC	1.34	1	1.34	9.83	0.0068	
Residual	2.05	15	0.1365			
Lack of Fit	2.05	12	0.1707			
Pure Error	0.0000	3	0.0000			
Cor Total	10.96	22				

Table 17 - Analysis of variance table for apparent density predictive model.

Source	Sum of Squares	df	Mean Square	F-value	p-value	
Model	0.0250	7	0.0036	40.15	< 0.0001	significant
A-CS Concentration	0.0080	1	0.0080	90.29	< 0.0001	
B-PP Concentatrion	0.0087	1	0.0087	97.64	< 0.0001	
C-Cu Concentration	1.940E-06	1	1.940E-06	0.0218	0.8846	
D-Polyphosphate Degree of Polymerization	0.0001	1	0.0001	1.43	0.2511	
AB	0.0047	1	0.0047	52.48	< 0.0001	
CD	0.0017	1	0.0017	19.17	0.0005	
B²	0.0015	1	0.0015	16.52	0.0010	
Residual	0.0013	15	0.0001			
Lack of Fit	0.0011	12	0.0001	1.08	0.5411	not significant
Pure Error	0.0003	3	0.0001			
Cor Total	0.0263	22				

Table 18 - Analysis of variance table for absorption capacity predictive model.

Source	Sum of Squares	df	Mean Square	F-value	p-value	
Model	0.0016	8	0.0002	55.34	< 0.0001	significant
A-CS Concentration	0.0003	1	0.0003	97.22	< 0.0001	
B-PP Concentatrion	0.0006	1	0.0006	174.18	< 0.0001	
C-Cu Concentration	1.271E-06	1	1.271E-06	0.3624	0.5576	
D-Polyphosphate Degree of Polymerization	2.207E-07	1	2.207E-07	0.0629	0.8059	
AB	0.0001	1	0.0001	37.47	< 0.0001	
CD	0.0000	1	0.0000	4.29	0.0587	
A²	0.0000	1	0.0000	10.96	0.0056	
B²	0.0001	1	0.0001	36.22	< 0.0001	
Residual	0.0000	13	3.508E-06			
Lack of Fit	0.0000	10	4.164E-06	3.15	0.1872	not significant
Pure Error	3.963E-06	3	1.321E-06			
Cor Total	0.0016	21				

Table 19 - Analysis of variance table for copper elution 24-hour predictive model.

Source	Sum of Squares	df	Mean Square	F-value	p-value	
Model	14.82	5	2.96	15.03	< 0.0001	significant
A-CS Concentration	2.95	1	2.95	14.96	0.0012	
B-PP Concentatrion	1.58	1	1.58	8.02	0.0115	
C-Cu Concentration	7.27	1	7.27	36.85	< 0.0001	
A^2	1.58	1	1.58	8.02	0.0115	
C^2	2.81	1	2.81	14.24	0.0015	
Residual	3.35	17	0.1972			
Lack of Fit	3.21	14	0.2289	4.67	0.1152	not significant
Pure Error	0.1472	3	0.0491			
Cor Total	18.17	22				

Table 20 - Analysis of variance table for phosphorous elution 24-hour predictive model.

Source	Sum of Squares	df	Mean Square	F-value	p-value	
Model	11.82	10	1.18	22.42	< 0.0001	significant
A-CS Concentration	0.0229	1	0.0229	0.4336	0.5251	
B-PP Concentatrion	1.50	1	1.50	28.52	0.0003	
C-Cu Concentration	0.0986	1	0.0986	1.87	0.2014	
D-Polyphosphate Degree of Polymerization	1.05	1	1.05	19.96	0.0012	
AB	2.60	1	2.60	49.21	< 0.0001	
AC	0.3930	1	0.3930	7.45	0.0212	
AD	0.2368	1	0.2368	4.49	0.0601	
BD	1.83	1	1.83	34.68	0.0002	
B^2	0.2209	1	0.2209	4.19	0.0679	
C^2	2.18	1	2.18	41.38	< 0.0001	
Residual	0.5273	10	0.0527			
Lack of Fit	0.5240	7	0.0749	66.98	0.0027	significant
Pure Error	0.0034	3	0.0011			
Cor Total	12.35	20				

Table 21 - Analysis of variance table for blood clotting index predictive model.

Source	Sum of Squares	df	Mean Square	F-value	p-value	
Model	955.99	4	239.00	3.41	0.0321	significant
A-CS Concentration	66.15	1	66.15	0.9429	0.3452	
C-Cu Concentration	7.96	1	7.96	0.1134	0.7404	
AC	635.41	1	635.41	9.06	0.0079	
C²	456.62	1	456.62	6.51	0.0207	
Residual	1192.76	17	70.16			
Lack of Fit	1052.95	14	75.21	1.61	0.3862	not significant
Pure Error	139.81	3	46.60			
Cor Total	2148.76	21				

Table 22 - Analysis of variance table for cytotoxic concentration predictive model.

Source	Sum of Squares	df	Mean Square	F-value	p-value	
Model	38.26	4	9.56	6.55	0.0020	significant
B-PP Concentatrion	11.45	1	11.45	7.84	0.0118	
C-Cu Concentration	13.08	1	13.08	8.96	0.0078	
B²	8.12	1	8.12	5.56	0.0298	
C²	10.34	1	10.34	7.08	0.0159	
Residual	26.29	18	1.46			
Lack of Fit	21.22	15	1.41	0.8371	0.6546	not significant
Pure Error	5.07	3	1.69			
Cor Total	64.54	22				

Table 23 - Analysis of variance table for margin of safety predictive model.

Source	Sum of Squares	df	Mean Square	F-value	p-value	
Model	33.51	7	4.79	16.68	< 0.0001	significant
A-CS Concentration	0.1200	1	0.1200	0.4180	0.5292	
B-PP Concentatrion	0.0078	1	0.0078	0.0271	0.8719	
C-Cu Concentration	16.86	1	16.86	58.72	< 0.0001	
D-Polyphosphate Degree of Polymerization	0.1301	1	0.1301	0.4534	0.5125	
AB	6.67	1	6.67	23.24	0.0003	
AD	1.52	1	1.52	5.28	0.0388	
C²	8.99	1	8.99	31.31	< 0.0001	
Residual	3.73	13	0.2870			
Lack of Fit	3.25	10	0.3249	2.02	0.3063	not significant
Pure Error	0.4827	3	0.1609			
Cor Total	37.24	20				